Advanced Sensor Research

ADVANCED SENSOR RESEARCH Open Access

www.advsensorres.com

REVIEW OPEN ACCESS

Microfabricated Neural Biosensors for Detection of Neurotransmitters, Biomarkers, and Small Molecules: Emerging Trends on Self-Sustained Systems and Energy Harvesting

Massimo Mariello

Department of Engineering Science, Institute of Biomedical Engineering (IBME), University of Oxford, Headington, Oxford, UK

Correspondence: Massimo Mariello (massimo.mariello@eng.ox.ac.uk)

Received: 17 July 2025 | **Revised:** 24 December 2025 | **Accepted:** 5 January 2026

Keywords: electrochemical | implantable biomedical devices | microfabricated | neurotransmitter detection | plasmonic | small molecule sensing | thin-film biosensors | ultrasound

ABSTRACT

The rapid evolution of neuroscience and bioelectronics has intensified the demand for highly sensitive, selective, and miniaturized biosensors capable of monitoring neurochemical activity with high spatial and temporal resolution. Among these, microfabricated thin-film biosensors have emerged as a powerful platform for the detection of neurotransmitters and small molecules, owing to their ultrathin form factor, mechanical flexibility, and compatibility with implantable systems. Design strategies, material innovations, and functional surface chemistries are now central to enabling real-time, in vivo monitoring with minimal tissue disruption and long-term stability. This review covers the recent progress in microfabricated biosensors, focusing on electrochemical, optical, acoustic, and magnetic modalities for the detection of key neurotransmitters, such as dopamine, serotonin, glutamate, and acetylcholine, as well as biologically relevant small molecules, including glucose, lactate, hydrogen peroxide, and nitric oxide. The integration of thin-film sensors for inflammatory and neurodegenerative disease biomarkers, such as cytokines (e.g., IL-6, TNF-α), amyloid-β, and tau proteins, is also discussed. Key challenges such as drift, biofouling, and signal specificity are critically examined alongside emerging solutions. Finally, current and future applications ranging from fundamental neuroscience and brain-machine interfaces to personalized medicine emphasize the potential of thin-film biosensing technologies in real-world biomedical scenarios.

1 | Introduction

The convergence of electronics with the nervous system has driven a transformative shift in biomedical engineering, enabling sophisticated neural interfaces capable of sensing, stimulation, and dynamic interaction with biological tissues [1, 2]. Historically focused on electrical recording and stimulation, neural interfaces are rapidly evolving toward multifunctional and multimodal systems [3–5], integrating chemical sensing [6, 7], optical modulation [8–10], mechanical feedback [11–13], and wireless communication [14–16], to meet the growing demands of neuroprosthetics [17], brain-machine interfaces (BMIs) [18–20], and closed-loop therapeutic systems [21–24]. These next-generation platforms aspire not only to decode neural activity but also to monitor the surrounding biochemical milieu and respond adaptively in real time, mirroring the complex feedback loops inherent to biological systems.

Central to this evolution is the integration of biosensors [25–27] for neurotransmitters [28, 29], disease-relevant biomarkers [30–32], and other small molecules that offer an expanded window into the dynamic chemical landscape of the nervous system. Neurotransmitters such as dopamine, serotonin, glutamate, and acetylcholine play pivotal roles in neuromodulation and behavior, while small molecules like glucose, lactate, nitric oxide, or water reflect metabolic and inflammatory states [33–38]. Similarly, the detection of biomarkers, including cytokines (e.g., IL-6, TNF-α), amyloid-β, and tau proteins, provides critical insight into neurodegenerative and neuroinflammatory conditions [39–46]. Incorporating sensors for these molecular targets is essential to achieving adaptive, feedback-controlled neural systems with clinical and translational relevance.

To fulfill this vision, sensor technologies must meet strict requirements: high sensitivity, selectivity, biocompatibility, and mechanical compliance with soft, irregular, and often mobile tissue [47–50]. Traditional rigid platforms lack the flexibility and integration capabilities necessary for long-term implantation or conformal interfacing with neural structures. In contrast, microfabricated thin-film biosensors, fabricated using microscale and nanoscale materials and deposition techniques, offer a promising solution [51–53]. Their ultrathin profiles minimize mechanical mismatch and inflammation, while their large surface-area-to-volume ratios enhance electrochemical sensitivity and temporal resolution. Thin films also enable high-density multiplexed sensor arrays and seamless integration with flexible substrates, expanding spatial coverage while preserving tissue health and device fidelity [54–56].

Equally critical is the role of functional materials, from conductive polymers [57, 58] and nanostructured metals [59–62] to biomolecule-functionalized surfaces [63, 64] and hybrid organic-inorganic systems [65–68]. These materials endow thin-film biosensors with specificity for chemical targets and responsiveness to biological environments. For example, enzyme-functionalized electrodes detect neurotransmitters via redox reactions [69], aptamer-based surfaces bind specific biomarkers with high affinity [70], and plasmonic films enable label-free optical detection [62]. Recent advances also incorporate ultrasound-mediated sensing [71], offering deep-tissue, wireless activation and signal enhancement.

This review surveys the emerging trends in thin-film biosensors for detecting neurotransmitters, small molecules, and biomarkers, with a focus on implantable and biointegrated systems, updating and enriching previous reports [72]. These sensors are categorized by their transduction mechanisms: electrochemical, enzymatic, aptameric, plasmonic, and acoustic, and explore their material strategies, biocompatibility considerations, and integration with flexible electronic platforms. In doing so, we emphasize their potential in closed-loop, multimodal neural interfaces and discuss the challenges that remain for chronic implantation, signal stability, and clinical deployment. By mapping this interdisciplinary landscape, we aim to illuminate the role of thin-film biosensors in enabling intelligent, responsive, and adaptive bioelectronic systems for diagnostics, therapeutics, and closed-loop neurotechnology.

2 | Target Analytes and Sensing Strategies

Implantable biosensors targeting neural and systemic biochemical markers are transforming our ability to decode, monitor, and modulate biological activity at molecular resolution. This section explores specific classes of target analytes that hold high relevance for neural interface applications (see Table 1 for a summary list and Figure 1), and outlines the corresponding sensing strategies based on electrochemical, optical, or other modalities. Particular emphasis is placed on neurotransmitters, small signaling molecules, disease-related biomarkers, and the emerging field of multi-analyte and multiplexed detection.

2.1 | Neurotransmitters

Neurotransmitters are the fundamental chemical messengers facilitating neural signal transmission, acting as critical indicators of brain function and dysfunction [28]. The ability to monitor these crucial molecules in real-time and in vivo has emerged as a central objective for advanced BMIs, neuroprostheses, and sophisticated diagnostic devices.

Dopamine (DA), a pivotal catecholamine, governs vital physiological processes including motor control, motivation, and reward pathways [73]. Its electrochemical sensing primarily relies on fast-scan cyclic voltammetry (FSCV) or amperometry. FSCV operates by rapidly sweeping the electrode potential over a defined range (e.g., −0.4 V to +1.3 V vs. Ag/AgCl reference at scan rates typically 300–400 V/s), generating a characteristic "duck-shaped" voltammogram that corresponds to the reversible oxidation and reduction of DA [74]. This technique offers excellent temporal resolution (tens of milliseconds) essential for capturing transient DA fluctuations. The electrodes commonly employed are carbon fiber microelectrodes (5-10 µm diameter) or those modified with poly(3,4-ethylenedioxythiophene) (PEDOT), to enhance electrode conductivity and provide a more stable, biocompatible interface. Recent advancements have focused on thin-film technologies utilizing graphene or carbon nanotube (CNT) composites [75]. These materials offer significantly increased surface area and exploit strong π–π stacking interactions with the aromatic rings present in the DA molecule, leading to enhanced sensitivity and lower detection limits. To overcome interference from co-existing electroactive species such as ascorbic acid and uric acid, enzyme-free detection strategies are predominantly employed. These strategies capitalize on the intrinsic redox activity of DA and incorporate highly selective coatings like Nafion (a perfluorinated ion-exchange polymer that repels anionic interferents) [76] or polyethylene glycol (PEG) [77]. These coatings act as permselective membranes, allowing DA to reach the electrode surface while blocking or retarding the diffusion of common interferents.

Serotonin (5-HT), another crucial monoamine, plays a significant role in mood regulation and sleep cycles [78, 79]. A primary challenge in 5-HT detection stems from its close oxidation potential to DA, making selective differentiation difficult. To address this, differential pulse voltammetry (DPV) is often employed due to its enhanced sensitivity and ability to resolve overlapping electrochemical signals [80]. DPV applies a series of regular potential

TABLE 1 | Several examples of neurochemically relevant species for biosensing applications, i.e., neurotransmitters, biomarkers for neurological disorders, and other small molecules.

Species			Role/Function	Chemical type	Physiological concentration	Altered levels in brain dysfunction	Refs.
Neurotransmitters		Dopamine	Modulates reward, motivation, motor control. Key in basal ganglia.	Catecholamine neurotransmitter	30–50 nM (extracellular); up to μM (at synapse)	↓ in Parkinson's disease; ↑ in schizophrenia, addiction	[73, 145]
		Serotonin (5-HT)	Regulates mood, sleep, appetite, cognition.	Monoamine neurotransmitter	~10–30 nM (extracellular)	↓ in depression, anxiety, OCD; ↑ in serotonin syndrome	[78, 146, 147]
		Glutamate	Primary excitatory neurotransmitter; essential for learning and memory.	Amino acid neurotransmitter	1–10 μM (extracellular); mM range (intracellular)	↑ in epilepsy, stroke, ALS (excitotoxicity)	[148, 149]
		GABA (gamma aminobutyric acid)	Major inhibitory neurotransmitter; stabilizes neural activity.	Amino acid neurotransmitter	200–1000 nM (extracellular)	↓ in epilepsy, anxiety; ↑ in hepatic encephalopathy	[150–152]
		Acetylcholine	Modulates synaptic plasticity, attention, autonomic control.	Ester neurotransmitter	~50–100 nM (extracellular)	↓ in Alzheimer's disease; ↓ in myasthenia gravis	[153, 154]
		Norepinephrine (NE)	Alertness, stress response, sympathetic activity	Catecholamine neurotransmitter	~0.3–1 nM in ECF; ~0.3–5 nM in plasma	↓ in depression, impaired attention, and cognitive decline (e.g., Alzheimer's, Parkinson's). Elevated/dysregulated levels contribute to anxiety disorders and hyperarousal.	[155–157]
Neurological biomarkers	Peptides	IL-6 (Interleukin-6)	Pro-inflammatory cytokine; activates immune response.	Protein (cytokine)	<5 pg/mL (CSF); ~1–10 pg/mL (plasma)	↑ in neuroinflammation, multiple sclerosis, TBI, Alzheimer's	[92, 158]
		TNF-α (Tumor Necrosis Factor-α)	Inflammatory cytokine; modulates apoptosis, synaptic plasticity.	Protein (cytokine)	<10 pg/mL (CSF)	↑ in Alzheimer's, MS, stroke, chronic inflammation	[159, 160]
		Amyloid-β ($A\beta_{42}$, $A\beta_{40}$)	Peptide aggregates associated with neurotoxicity and plaque formation.	Peptide/protein	<500 pg/mL (CSF $A\beta_{42}$)	↑ in Alzheimer's (accumulation in brain); ↓ in CSF	[43, 96, 161]
		Tau protein (total and phosphorylated)	Microtubule-associated protein; hyperphosphorylation leads to neurofibrillary tangles.	Protein	200–400 pg/mL (total tau in CSF); ~80 pg/mL (phospho-tau)	↑ in Alzheimer's, frontotemporal dementia, TBI	[44–46, 162–164]
	Neuroactive steroids	Allopregnanolone	Brain (synthesized from progesterone), Adrenal Glands, Gonads. Positive allosteric modulator of GABA_A receptors, neuroprotective, anxiolytic, antidepressant, anti-inflammatory.	Steroid (Progestin metabolite)	CSF: low nM range (e.g., 0.5-2 nM) Plasma: low nM range (e.g., 0.1-5 nM, varies with sex/cycle)	↓: Major Depressive Disorder, Anxiety Disorders, Alzheimer's Disease (impaired neuroprotection), Post-Traumatic Stress Disorder (PTSD). Altered: Traumatic Brain Injury (TBI).	[101, 102]

(Continues)

TABLE 1 | (Continued)

Species			Role/Function	Chemical type	Physiological concentration	Altered levels in brain dysfunction	Refs.
		Dehydroepiandrosterone sulfate (DHEA-S)	Adrenal Glands (major source), Brain. Neuroprotective, enhances neurogenesis, modulates glutamatergic and GABAergic systems, influences mood and cognition.	Steroid (Androgen precursor)	Plasma: μM range (e.g., 1–10 μM, highly variable by age/sex)	↓: Alzheimer's Disease, Major Depressive Disorder, Age-related cognitive decline.	[100, 103, 165]
		Pregnenolone	Adrenal Glands, Gonads, Brain (precursor to many steroids). Modulates NMDA receptors, neuroprotective, enhances memory, mood regulation.	Steroid	CSF: low nM range (e.g., 1–5 nM) Plasma: low nM range (e.g., 1–10 nM)	↓: Alzheimer's Disease, Schizophrenia (some studies), Depression.	[99, 104, 105]
	Thyroid hormones	Thyroxine (T4)	Thyroid Gland. Prohormone, converted to T3. Essential for brain development, myelination, synaptic plasticity, energy metabolism, cognition.	Amino Acid derivative (Iodothyronine)	Serum Total T4: 5–12 mug/dL Serum Free T4: 0.8-1.8 ng/dL	↓ (Hypothyroidism): Cognitive impairment, memory deficits, "brain fog," depression, psychomotor slowing. ↑(Hyperthyroidism): Anxiety, irritability, agitation, insomnia, concentration difficulties.	[106, 107, 166]
		Triiodothyronine (T3)	Thyroid Gland, peripheral conversion from T4. Active hormone. Direct effects on neuronal gene expression, metabolism, and function.	Amino Acid derivative (Iodothyronine)	Serum Total T3: 80–200 ng/dL Serum Free T3: 2.3-4.2 pg/mL	↓ (Hypothyroidism): Cognitive impairment, depression. ↑(Hyperthyroidism): Anxiety, hyperactivity, mood swings.	[108, 167, 168]
	Hypothalamic-Pituitary-Adrenal (HPA) axis hormones	Cortisol	Adrenal Glands (zona fasciculata). Primary stress hormone, regulates metabolism, immune response, blood pressure, influences mood, memory, and sleep.	Steroid (Glucocorticoid)	Serum: 100–700 nM (diurnal variation) Salivary: 2–20 nM CSF: 1–10 ng/mL; circadian variation	↑ (Chronic): Major Depressive Disorder (MDD), Anxiety Disorders, PTSD, Alzheimer's Disease (exacerbates neurodegeneration), Cushing's syndrome (cognitive deficits). ↓ (Chronic): Adrenal insufficiency, sometimes linked to fatigue and apathy.	[111, 112]
		Adrenocorticotropic Hormone (ACTH)	Anterior Pituitary Gland. Stimulates cortisol release from adrenal cortex.	Peptide	Plasma: 10–60 pg/mL (diurnal variation)	↑: Cushing's Disease (pituitary tumor causing high cortisol), chronic stress. ↓: Adrenal insufficiency (primary).	[169, 170]

(Continues)

TABLE 1 | (Continued)

Species			Role/Function	Chemical type	Physiological concentration	Altered levels in brain dysfunction	Refs.
		Corticotropin-releasing Hormone (CRH)	Hypothalamus. Initiates HPA axis activation, also acts as a neurotransmitter in stress response, anxiety, and depression.	Peptide	CSF: low pM range (e.g., 10–50 pM) Plasma: low pM range (difficult to measure due to binding proteins)	↑: Major Depressive Disorder, Anxiety Disorders, PTSD (often in CSF), Chronic Stress.	[169, 171, 172]
	Other hormones	Melatonin	Pineal Gland. Regulates circadian rhythms, sleep-wake cycle, acts as a powerful antioxidant and anti-inflammatory agent.	Indoleamine	Serum: 10–80 pg/mL (daytime) to 80–200 pg/mL (nighttime peak)	↓: Insomnia, Alzheimer's Disease (impaired sleep, circadian rhythm disruption), Parkinson's Disease (sleep disturbances).	[113, 114]
		Insulin	Pancreas (beta cells). Regulates glucose uptake in peripheral tissues; also crucial for brain glucose metabolism, neuronal survival, synaptic plasticity, and cognition.	Peptide	Serum: 30–180 pM (fasting) CSF: 0.1-0.5 nM (typically 10–20% of plasma)	↓: Alzheimer's Disease ("Type 3 Diabetes"), Impaired glucose utilization in the brain, cognitive decline.	[173, 174]
		Insulin-like Growth Factor 1 (IGF-1)	Liver (primarily), also brain. Promotes neuronal growth, survival, synaptic plasticity, neurogenesis, and myelination.	Peptide	Serum: 100–300 ng/mL (age-dependent) CSF: 1–5 ng/mL	↓: Alzheimer's Disease, Parkinson's Disease, Amyotrophic Lateral Sclerosis (ALS), age-related cognitive decline (impaired neuroprotection/repair).	[175, 176]
		Ghrelin	Stomach (primarily), also hypothalamus. "Hunger hormone." Influences appetite, energy balance, also has neurotrophic effects, modulates mood, reward, and memory circuits.	Peptide	Plasma: 50–500 pg/mL (active form, fluctuates with feeding)	Altered: Eating disorders, obesity-related cognitive dysfunction, potentially neurodegenerative diseases (role in neuroprotection/cognitive function).	[177–179]
		Leptin	Adipose tissue. "Satiety hormone." Regulates energy homeostasis, neurogenesis, synaptic plasticity, influences mood and cognitive function.	Peptide	Plasma: 5–50 ng/mL (variable by body fat)	Altered/Resistance: Obesity-related cognitive impairment, potentially linked to neuroinflammation and neuronal survival in some neurodegenerative contexts.	[180–182]
Small molecules and ions		Glucose	Primary energy substrate for neurons.	Monosaccharide	0.5–2.5 mM (brain interstitial); 4–6 mM (blood)	↓ in hypoglycemia; altered regulation in diabetes and Alzheimer's	[34, 35, 183–186]

(Continues)

TABLE 1 | (Continued)

Species		Role/Function	Chemical type	Physiological concentration	Altered levels in brain dysfunction	Refs.
	Lactate	Metabolic byproduct; alternative neuronal fuel; involved in neuron–glia coupling.	Organic acid	0.5–1.5 mM (extracellular)	↑ in ischemia, TBI, stroke (anaerobic metabolism)	[36, 187, 188]
	Nitric Oxide (NO)	Gaseous signaling molecule; neuromodulator and vasodilator.	Reactive free radical	<100 nM (transient bursts)	↑ in inflammation, neurodegeneration (e.g., Alzheimer's); ↓ in impaired synaptic plasticity	[37, 38, 138, 139, 189]
	Ascorbic Acid (Vitamin C)	Antioxidant; involved in neuromodulation, scavenging ROS	Water-soluble vitamin	~200–400 μM in brain ECF	Depleted levels in conditions of oxidative stress like Alzheimer's, Parkinson's, stroke, and TBI.	[190, 191]
	Uric Acid	Endogenous antioxidant; linked to Parkinson's disease and neuroinflammation	Purine metabolite	~200–400 μM in CSF and plasma	Lowered levels in Parkinson's and Alzheimer's, indicating depleted antioxidant defense. Acutely elevated levels can occur after stroke or TBI, often reflecting cellular damage, but its full role is complex. Chronic high levels (hyperuricemia) are linked to increased risk of vascular dementia and cognitive impairment.	[192, 193]
	Hydrogen Peroxide (H_2O_2)	ROS involved in redox signaling, oxidative stress.	Reactive oxygen species	1–10 μM (transient; tightly regulated)	↑ in neurodegeneration (Parkinson's, ALS); oxidative stress	[194–196]
	Water (H_2O)	Solvent; essential for maintaining ionic gradients, cell volume, intracranial pressure.	Polar molecule	~98% brain tissue mass; ~800 mL/L in CSF	↑ in brain edema, hydrocephalus, TBI; ↓ in dehydration, ischemia	[33, 197–200]
	pH (H^+ ion)	Indicator of metabolic activity; neuronal excitability is pH-sensitive	Proton (H^+ concentration)	Brain ECF pH ~7.3–7.4; slight acidification under stress	Acidosis (lower pH, higher H+) in ischemia, TBI, and seizures contributes to toxicity and neural death. Acute acidosis can impair ATP production, cause excitotoxicity, and disrupt ion channel function. Alkalosis (higher pH, lower H+) can lead to increased neuronal excitability and potentially seizures.	[132, 201]

(Continues)

TABLE 1 | (Continued)

Species		Role/Function	Chemical type	Physiological concentration	Altered levels in brain dysfunction	Refs.
	Oxygen (O_2)	Essential for aerobic metabolism	Small molecule gas	~30–40 mmHg partial pressure in brain tissue	Deficient oxygen (hypoxia/anoxia) is critical in ischemic stroke and hypoxic-ischemic encephalopathy, leading to neuronal cell death. Chronic hypoxia causes inflammation and cognitive decline.	[202, 203]
	Carbon dioxide (CO_2)	Byproduct of respiration; acid-base buffer	Small molecule gas	~45–50 mmHg pCO_2 in CSF	Elevated levels (hypercapnia) lead to cerebral vasodilation, increased intracranial pressure, and respiratory acidosis, causing cognitive impairment, confusion, and drowsiness. Reduced levels (hypocapnia) cause cerebral vasoconstriction and reduced blood flow, potentially leading to ischemia and seizures.	[204, 205]
	Potassium (K^+)	Key ion in action potential and neuronal firing	Electrolyte (cation)	~2.5–3.5 mM in ECF; rises during activity	Excessive extracellular K+ during ischemic stroke, traumatic brain injury, and epileptic seizures leads to neuronal over-excitation and ultimately contributes to neuron death due to energy pump failure. Conversely, low extracellular K+ may also disrupt normal brain function due to neuronal hyperexcitability.	[206, 207]
	Calcium (Ca^{2+})	Synaptic vesicle release, signal transduction	Electrolyte (cation)	~50–100 nM (resting cytosol); ~1.2–1.5 mM in ECF	Excessive influx/overload in ischemia, TBI, and seizures drives neuronal death via excitotoxicity, activating destructive enzymes and causing mitochondrial dysfunction. In neurodegenerative diseases (e.g., Alzheimer's, Parkinson's), chronic dysregulation contributes to synaptic dysfunction and neuronal loss. Low extracellular Ca2+ (hypocalcemia) can increase neuronal excitability, potentially leading to seizures.	[206, 208–210]

(Continues)

TABLE 1 | (Continued)

Species	Role/Function	Chemical type	Physiological concentration	Altered levels in brain dysfunction	Refs.
Zinc (Zn^{2+})	Neuromodulator; associated with synaptic plasticity and Alzheimer's pathology	Trace element cation	~0.1–1 μM in synaptic clefts	Excessive levels in the brain are neurotoxic, contributing to neuronal death in stroke, TBI, and perhaps epilepsy by inducing mitochondrial dysfunction and oxidative stress. Zinc deficiency can impair brain development and lead to cognitive deficits. Dysregulation in neurodegenerative diseases like Alzheimer's is complex, affecting protein aggregation and synaptic function.	[211, 212]

Nomenclature: CSF: cerebrospinal fluid; OCD: obsessive-compulsive disorder; MS: multiple sclerosis.; TBI: traumatic brain injury; ALS: amyotrophic lateral sclerosis.

pulses superimposed on a staircase potential ramp, sampling the current just before and at the end of each pulse, which helps to minimize background current. Integration with molecularly imprinted polymers (MIPs) or highly selective aptamers further refines 5-HT detection. MIPs are synthetic receptors engineered to have specific recognition sites for 5-HT, akin to an antibody-antigen interaction, thereby improving selectivity [81]. Aptamers, on the other hand, are single-stranded nucleic acid molecules that bind to specific target molecules with high affinity and specificity [82]. Recent innovations involve microfluidic sampling integrated with these thin-film sensors [83]. This not only improves temporal resolution by facilitating rapid analyte delivery to the sensor surface but also enables localized neurotransmitter quantification from specific brain regions with high spatial precision.

Glutamate, the principal excitatory neurotransmitter, presents a unique challenge as it is not electroactive itself [84]. Consequently, its detection necessitates an enzyme-mediated transduction pathway. Glutamate oxidase (GluOx) is the enzyme commonly immobilized on electrode surfaces [85]. GluOx catalyzes the oxidation of glutamate into α-ketoglutarate and hydrogen peroxide (H_2O_2). The H_2O_2 produced is then electrochemically detected, typically by oxidation at a positive potential (e.g., +0.6 V vs. Ag/AgCl). To optimize this enzymatic process, thin-film biosensors utilizing materials like ZnO nanorods, gold nanoparticle (AuNP) composites, or conductive polymers are frequently employed [86]. These nanostructured materials provide a high surface area for enhanced enzyme loading, promoting efficient electron transfer and improving diffusion kinetics of the substrate and product. Furthermore, these materials contribute to the stability of the immobilized enzyme, extending the operational lifetime of the biosensor.

Acetylcholine (ACh) is an ester of acetic acid and choline, crucial for both the central and peripheral nervous systems. In the periphery, it's the primary neurotransmitter at neuromuscular junctions, facilitating muscle contraction, and plays a vital role in the autonomic nervous system, regulating heart rate, digestion, and glandular secretions [87]. Within the brain, ACh is implicated in critical cognitive functions such as memory, learning, attention, and arousal. Its excitatory or inhibitory effects depend on the receptor type: nicotinic receptors, which are ion channels, and muscarinic receptors, which are G protein-coupled. The rapid breakdown of ACh by acetylcholinesterase (AChE) ensures precise and fleeting synaptic transmission. ACh detection typically involves a two-step enzymatic reaction [88]. The first step is catalyzed by AChE, which hydrolyzes ACh into choline and acetate. The second step involves choline oxidase (ChOx), which oxidizes choline to betaine and H_2O_2. Similar to glutamate sensing, the H_2O_2 byproduct is then electrochemically detected [89]. Given its pervasive physiological roles, accurately sensing ACh levels is paramount for understanding neurological disorders like Alzheimer's and myasthenia gravis, where cholinergic system dysfunction is evident. Electrochemical sensors, particularly those modified with nanomaterials like WO_3 nanorods or carbon nanotubes [90], offer high sensitivity, rapid response, and miniaturization capabilities. Enzymatic biosensors, leveraging acetylcholinesterase to detect ACh, and even DNA-based fluorescent nanosensors, are emerging as powerful tools for dynamic, spatially resolved monitoring of ACh release in living systems [91].

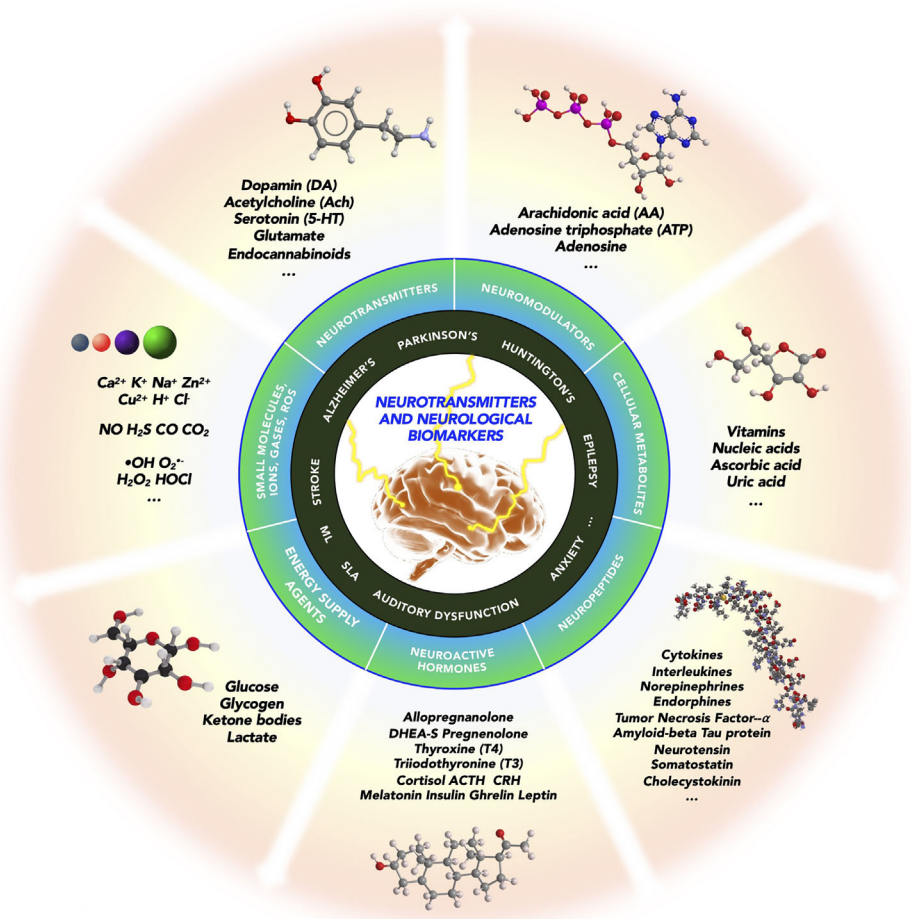

FIGURE 1 | Illustration of the main categories of chemicals relevant to neurological disorders. The black circle lists some of the best-known neurological disorders (ML: multiple sclerosis; SLA: amyotrophic lateral sclerosis). The outer circle classifies the chemicals into several categories: neurotransmitters, neuromodulators, cellular metabolites, neuropeptides, neuroactive hormones, energy supply agents, small molecules, ions, gases, and ROS (reactive oxygen species). Some examples of each category are reported. The chemical structures are for glucose, dopamine, ATP, ascorbic acid, amyloid-beta, and allopregnanolone.

2.2 | Neurological Biomarkers

Biomarkers intricately linked to inflammation and neurodegenerative disease progression are paramount for achieving early diagnosis, accurate prognosis, and effective treatment monitoring. Besides neurotransmitters, other neurological biomarkers include peptides or hormones.

Cytokines, such as Interleukin-6 (IL-6), Tumor Necrosis Factor-α (TNF-α), and Interleukin-1β (IL-1β), are associated with neuroinflammatory processes in brain injuries, neurodegeneration, and psychiatric disorders [39, 92]. Cytokines, once primarily understood as immune system communicators, are now recognized as crucial modulators within neural circuits, profoundly influencing brain development, plasticity, and function in both physiological and pathological states. These pleiotropic signaling proteins, secreted by both immune cells and resident brain cells like microglia and astrocytes, finely tune synaptic transmission, regulate synapse formation and elimination, and impact global neuronal networks. Under healthy conditions, a delicate balance between pro- and anti-inflammatory cytokines is essential for processes such as long-term potentiation (LTP) and long-term depression (LTD), which are fundamental to learning and memory [93, 94]. For instance, low levels of pro-inflammatory cytokines like TNF-α and IL-1β can be beneficial for synaptic plasticity, while their dysregulated or excessive expression during neuroinflammation can lead to synaptic dysfunction, impaired neurogenesis (the birth of new neurons), and neuronal damage [95]. In the context of neurological disorders, this cytokine dysregulation contributes significantly to pathogenesis. Elevated levels of pro-inflammatory cytokines are implicated in neurodegenerative diseases such as Alzheimer's and Parkinson's, where they exacerbate neurotoxicity and contribute to disease progression. Similarly, in psychiatric conditions like major depression and schizophrenia, an altered cytokine profile is increasingly recognized as a contributing factor to symptoms, highlighting the intricate interplay between the immune system and the central nervous system in both health and disease.

Cytokine detection is typically achieved through immunosensors using immobilized antibodies or aptamers on gold or graphene-based thin films. Label-free strategies utilizing electrochemical impedance spectroscopy (EIS), quartz crystal microbalance

(QCM), or surface plasmon resonance (SPR) are increasingly being adapted to soft substrates for in vivo compatibility.

Amyloid-β (Aβ) peptides and Tau proteins are hallmarks of Alzheimer's disease and related tauopathies [45, 96]. Aβ peptides are fragments derived from the amyloid precursor protein (APP), and in AD, they abnormally aggregate into extracellular amyloid plaques within the brain, disrupting neuronal communication and triggering inflammatory responses. Tau proteins, conversely, are crucial for stabilizing microtubules within neurons, which are essential for maintaining cell structure and facilitating intracellular transport. In AD and other tauopathies, Tau undergoes hyperphosphorylation [97], causing it to detach from microtubules, misfold, and aggregate into intracellular neurofibrillary tangles. This leads to a breakdown of the neuronal transport system, impairs synaptic function, and ultimately contributes to widespread neuronal death and the cognitive decline characteristic of these devastating neurodegenerative conditions. The precise interplay between Aβ and Tau pathology, where Aβ accumulation is often considered an early trigger that can promote tau hyperphosphorylation and subsequent tangle formation, is a central focus of current research aimed at understanding and treating these complex disorders.

Thin-film biosensors targeting Aβ or Tau typically employ sandwich immunoassays or aptamer-based recognition [43, 45]. Ultrathin gold or graphene field-effect transistors functionalized with peptide-specific recognition elements enable femtomolar sensitivity [98]. In neural tissue, these sensors must contend with low analyte concentrations and high levels of interferents; thus, antifouling coatings (e.g., PEGylation, zwitterionic layers) and real-time signal processing algorithms are critical.

Beyond neurotransmitters and cytokines, neuroactive hormones represent another critical class of biomarkers for understanding brain function and disease. These signaling molecules, secreted by endocrine glands but often acting directly on the brain, exert profound and long-lasting effects on mood, cognition, behavior, and physiological processes. Hormones like cortisol, estrogen, testosterone, thyroid hormones, and melatonin are recognized for their significant roles in neurodevelopment, neuroprotection, stress response, and the regulation of sleep-wake cycles. Dysregulation in their levels or signaling pathways is frequently implicated in a range of neurological and psychiatric conditions, including chronic stress, depression, anxiety disorders, and even neurodegenerative processes. For instance, chronic elevation of cortisol, a key stress hormone, can lead to hippocampal atrophy and cognitive impairment, while fluctuations in sex hormones are known to influence susceptibility to mood disorders and cognitive decline.

Neuroactive steroids are endogenous or synthetic steroids that rapidly alter neuronal excitability by interacting with membrane-bound receptors, distinct from classical genomic steroid receptors [99, 100]. Their fast, non-genomic actions are crucial for immediate responses in the brain.

A metabolite of progesterone, allopregnanolone (ALLO), is arguably the most well-studied neuroactive steroid [101, 102]. It acts as a potent positive allosteric modulator of the GABA-A receptor, enhancing the effects of GABA. This action leads to anxiolytic (anti-anxiety), sedative, and anticonvulsant effects. Its levels fluctuate with stress, menstrual cycles, and pregnancy, and dysregulation is implicated in conditions like postpartum depression (for which brexanolone, a synthetic ALLO, is FDA-approved) and anxiety disorders.

Dehydroepiandrosterone (DHEA) and DHEA sulfate (DHEAS) are adrenal and gonadal steroids that also function as neuroactive steroids [103]. DHEA and its sulfate ester can act as positive modulators of NMDA receptors (excitatory) and negative modulators of GABA-A receptors, leading to pro-cognitive and mood-elevating effects. They are involved in neurogenesis, neuroprotection, and memory. Declining levels with age are associated with cognitive decline and mood disturbances.

Pregnenolone sulfate (PS) is a precursor to many other steroids [99, 104, 105]: it can act as a potent negative allosteric modulator of GABA-A receptors and a positive modulator of NMDA receptors, contributing to excitatory effects and potentially influencing learning and memory.

Primarily produced by the thyroid gland, thyroxine (T4) and triiodothyronine (T3) are critical for brain development and lifelong neurological function [106–108]. T3 is the more active form, largely converted from T4 within the brain by deiodinase enzymes. These hormones regulate countless genes involved in neurogenesis, neuronal migration, myelination, and synaptogenesis. During development, severe thyroid hormone deficiency can lead to irreversible intellectual disabilities (cretinism) [109]. In adults, imbalances cause significant neurological and psychiatric symptoms. Hypothyroidism often leads to lethargy, cognitive impairment (memory loss, reduced attention), and depression, while hyperthyroidism can manifest as anxiety, irritability, and insomnia [110]. Their actions are mediated through nuclear receptors that influence gene expression, as well as via rapid, non-genomic membrane effects. They are essential for maintaining metabolic rate, influencing neuronal excitability, and supporting overall brain health.

Among other neuroactive hormones, cortisol is a glucocorticoid hormone released by the adrenal glands in response to stress: while essential for acute stress response, chronically elevated cortisol levels can have detrimental effects on the brain, leading to hippocampal atrophy, impaired memory, and increased risk of depression and anxiety. It influences neuroinflammation and neurotransmitter systems [111, 112].

Melatonin is synthesized primarily by the pineal gland, and it is crucial for regulating circadian rhythms and sleep-wake cycles [113, 114]. Its release is inhibited by light and stimulated by darkness, signaling to the brain the appropriate time for rest. It also possesses antioxidant and neuroprotective properties. Dysregulation of melatonin is a hallmark of sleep disorders and is being investigated for its role in neurodegenerative diseases [115].

While traditionally known for reproductive functions, sex hormones (estrogen and testosterone) also exert significant neuroactive effects [116]. Estrogen is neuroprotective, influencing synaptic plasticity, memory, and mood, and plays a role in reducing the risk of neurodegenerative diseases [117]. Testosterone influences cognitive functions, mood, and spatial memory

[118]. Fluctuations or deficiencies in these hormones can impact cognitive health and contribute to mood disorders.

2.3 | Small Molecules and Ions

Small molecules and ions collectively provide invaluable metabolic and inflammatory information, which is absolutely critical for maintaining both systemic and neurophysiological homeostasis [119–121]. Their continuous, real-time monitoring is therefore essential for comprehensively understanding dynamic metabolic states, assessing ischemic stress, and characterizing the intricate processes of neuroinflammation within the central nervous system.

Glucose sensing is a well-established and widely applied technology in clinical settings, particularly for diabetes management [122, 123]. However, its integration into flexible and implantable neural platforms demands significant adaptation. The primary method for in vivo glucose detection remains enzymatic sensing, utilizing glucose oxidase (GOx) [124, 125]. This enzyme is immobilized onto flexible substrates such as Parylene-C or SU-8, chosen for their biocompatibility, mechanical flexibility, and excellent dielectric properties, which facilitate seamless integration into wearable devices or intracranial sensors. Thin films of conducting polymers, like polypyrrole, are frequently employed to robustly entrap the GOx enzyme, critically preserving its catalytic activity while simultaneously ensuring efficient electron transfer to the underlying electrode [126]. Beyond enzymatic approaches, non-enzymatic sensors based on thin films of metals like copper, nickel, or platinum are also being rigorously explored. These offer distinct advantages in terms of enhanced longevity and a reduced dependency on biological cofactors, overcoming limitations associated with enzyme stability and supply in chronic implants. These non-enzymatic sensors typically exploit the direct electrochemical oxidation of glucose on the metal surface. In addition to glucose, crucial ions such as potassium (K^+) and sodium (Na^+) are fundamental to neuronal excitability and osmotic balance. Their real-time monitoring, often achieved using ion-selective electrodes (ISEs) incorporating ionophores within thin polymer membranes (e.g., PVC-based membranes plasticized with appropriate additives), is vital for detecting conditions like spreading depression or acute ischemic events where ion gradients dramatically collapse [127].

Lactate, a pivotal indicator of tissue oxygenation status and metabolic stress, is predominantly detected enzymatically via lactate oxidase (LO_x) [128]. This enzyme catalyzes the conversion of lactate into pyruvate and H_2O_2. Sophisticated thin-film lactate sensors have been engineered using carbon-based electrodes, further modified with nanostructured platinum or gold layers [129, 130]. These noble metal nanostructures serve as highly efficient catalysts for the electrochemical oxidation of the generated H_2O_2, ensuring high sensitivity. The development of stretchable or epidermal electronics with integrated microfluidic channels has enabled skin-mounted lactate monitoring, a capability of immense value not only for sports physiology but also for comprehensive neurometabolic studies, allowing for non-invasive assessment of brain energy metabolism [131].

Beyond lactate, the detection of pH is critical, as changes in proton (H^+) concentration are indicative of metabolic shifts, ischemia, or inflammation [132]. Thin-film pH sensors often leverage materials like iridium oxide (IrO_x) or antimony (Sb) thin films, which exhibit potential changes directly proportional to the H^+ concentration [133–135], or employ ion-sensitive field-effect transistors (ISFETs) where the gate dielectric layer is sensitive to pH variations [136, 137].

Nitric Oxide (NO) is a transient gaseous signaling molecule with diverse roles in synaptic plasticity, vasodilation, and complex immune responses [37, 138, 139]. Its detection presents unique challenges due to its extremely short half-life and highly reactive nature. Consequently, NO sensing necessitates the use of highly selective membranes, such as xerogels or Nafion layers, which provide a permselective barrier to block interferents while allowing NO to reach the electrode surface [140, 141]. High-resolution amperometric detection is then employed to capture the rapid and low-concentration NO transients. Furthermore, thin metal oxide semiconductors, including ZnO or In_2O_3, have been successfully integrated into field-effect transistor (FET)-based sensors for NO detection [142, 143]. These FET sensors offer exceptionally fast response times and remarkably low detection limits, often below 10 nM, which is crucial for capturing physiologically relevant NO dynamics.

Hydrogen Peroxide (H_2O_2), while a reactive oxygen species, also serves as a crucial by-product in a multitude of enzymatic reactions, including those catalyzed by GO_x, $GluO_x$, and LO_x. This makes H_2O_2 a key intermediate for indirect sensing of a wide array of analytes. Thin platinum films or Prussian blue-modified electrodes are widely utilized for the direct electrochemical detection of H_2O_2 due to their high sensitivity and electrocatalytic activity [144]. Recent technological advancements in thin-film FETs and capacitive sensors have enabled label-free detection of H_2O_2 by monitoring subtle impedance shifts or the modulation of gate potential upon its binding or reaction at the sensor interface.

3 | Self-Sustained Biosensing Neural Interfaces

In the rapidly evolving landscape of neural technologies, the push toward self-sustained neural interfaces marks a paradigm shift from passive, externally managed systems to autonomous, intelligent platforms that can sense, process, and respond to the body's dynamic biochemical and electrophysiological environment [213]. A self-sustained system in this context refers to a device that operates independently over extended periods, without the need for external intervention, maintenance, or tethered power supply. This autonomy is achieved through the integration of key elements: self-powered sensors, energy harvesters, local signal processing, and actuation modules, all embedded within a soft, biocompatible architecture (Figure 2).

Central to this vision is the concept of closed-loop systems, which actively monitor physiological signals, such as neurotransmitter concentrations or neural activity, and use this information to adjust their output in real-time [21–24, 26]. Unlike open-loop systems that deliver fixed stimulation regardless of biological feedback, closed-loop interfaces enable responsive neuromodulation, drug release, or electrical stimulation based on real-time

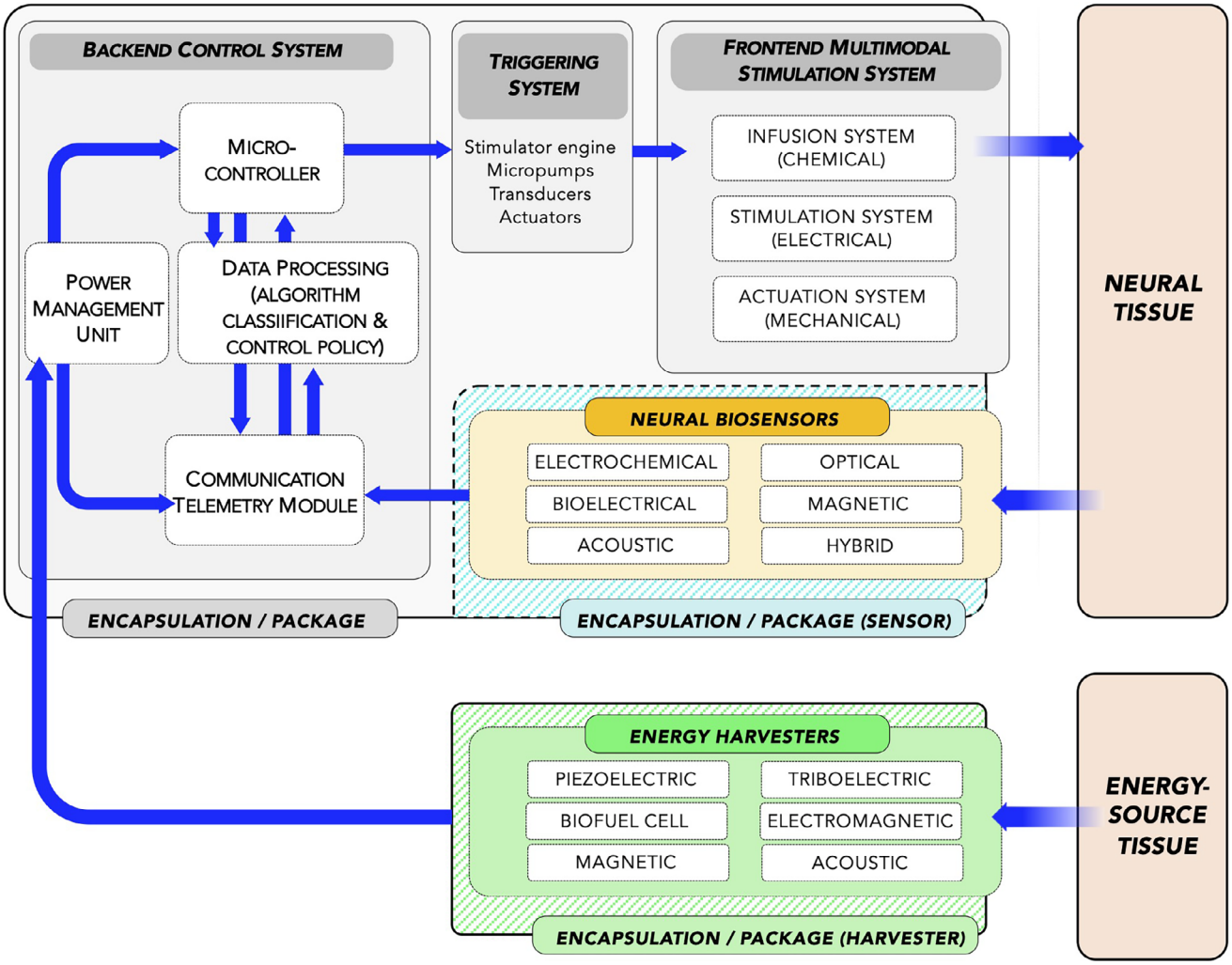

FIGURE 2 | Schematic of a multimodal self-sustained neural interface integrating neural biosensors (e.g., for dopamine), energy harvesters positioned on an energy-source tissue (e.g., biofuel cell or piezoelectric nanogenerator on the heart surface or muscles), back-end electronics for signal conditioning, control and wireless communication, and front-end electronics including a (multimodal) stimulation module. The role of the neural biosensor is to acquire neurochemical data.

needs, greatly enhancing therapeutic precision and minimizing adverse effects [214, 215]. A natural extension of this idea is the adaptive system, which not only responds to moment-to-moment fluctuations but also learns and optimizes its behavior over time, for instance, through machine learning algorithms or embedded feedback controllers that adapt stimulation protocols based on long-term trends in biomarker levels or neuronal responses [216, 217].

In parallel, the development of multimodal and multiplexed systems enables these interfaces to capture and integrate multiple data streams, such as electrophysiological signals, neurochemical profiles, temperature, and mechanical strain, within a single platform [218–221]. This multimodal sensing capacity provides a more holistic understanding of tissue states and allows for more informed and nuanced therapeutic strategies. Multiplexed sensing, often achieved through advanced materials or thin-film architectures, enables the simultaneous detection of multiple biomarkers (e.g., dopamine, glutamate, pH) using minimally invasive platforms. These capabilities are particularly important in the brain, where complex neurochemical interactions underlie behavioral and pathological states. Multi-analyte sensing is key to establishing functional relationships between neurotransmitter activity, metabolic state, and disease biomarkers.

Multiplexed electrochemical arrays integrate patterned microelectrodes with distinct recognition elements. Spatial resolution is achieved through photolithographic patterning, while electrical isolation between electrodes ensures minimal crosstalk. Arrays are typically fabricated on flexible polymers (e.g., polyimide, PDMS) and coated with functional materials using inkjet printing, vapor-phase deposition, or micro-contact printing.

Hybrid sensor systems combining optical (e.g., fluorescence, SERS), electrochemical, and piezoelectric modalities are emerging for enhanced selectivity and dynamic range. For example, integration of electrochemical sensors with plasmonic nanostructures enables dual-mode detection, fluorescence for quantification, and electrochemistry for temporal resolution.

Machine learning (ML)-enabled signal processing is increasingly employed to deconvolute overlapping signals in multiplexed

systems. ML algorithms can distinguish signal patterns associated with specific analytes, compensate for drift, and identify correlations among detected species.

A critical enabler of self-sustained operation is the inclusion of self-powered biosensors, which can operate using locally harvested energy [222–224]. These sensors often exploit energy harvesting techniques such as biofuel cells (e.g., glucose-oxidase-based), piezoelectric or triboelectric generators that convert mechanical motion into electrical energy [225], or wireless power transfer mechanisms using ultrasound or radiofrequency [16]. Self-powered sensors minimize the need for batteries, reduce device size, and extend operational lifetimes, key features for chronic implants.

Together, these components form the foundation of next-generation neural interfaces: compact, fully integrated systems capable of real-time, multimodal sensing and adaptive response, powered by ambient or bio-harvested energy. Table 2 reports some representative examples of self-sustained systems encompassing sensing, actuation, harvesting and processing, with indication of target tissue, degree of autonomy and long-term performances. The integration of these technologies will be crucial to realizing minimally invasive, intelligent implants that can function autonomously for long periods, bringing neural interfaces closer to clinical translation and personalized neurotherapies.

3.1 | Role of Biochemical Feedback in Self-Sustained Systems

Within closed-loop systems, sensing elements continuously monitor physiological parameters and dynamically adjust stimulation or actuation accordingly. This real-time feedback control allows for more precise, efficient, and personalized neuromodulation, compared to open-loop approaches. While traditional closed-loop systems have largely relied on electrical biomarkers such as local field potentials (LFPs), multi-unit activity (MUA), or electromyographic (EMG) signals, biochemical feedback is now gaining traction as a complementary or even superior source of information. The shift toward closed-loop, autonomous, and adaptive neural interfaces is tightly coupled with the ability to acquire high-fidelity, real-time biochemical information. Unlike electrophysiological signals, which provide fast but indirect insights into neural function, biochemical markers such as dopamine, glutamate, lactate, or cytokines reflect metabolic and neurochemical states with higher specificity. As a result, the integration of biosensors for small molecules and biomarkers is driving the next generation of smart neurotechnologies capable of personalized and context-aware therapeutic interventions.

Neurotransmitters such as dopamine, serotonin, acetylcholine, and glutamate are tightly linked to neurological function and behavior. Abnormalities in their concentrations have been implicated in various disorders including Parkinson's disease, depression, schizophrenia, and addiction. By embedding biosensors capable of detecting these analytes with high temporal and spatial resolution, closed-loop systems can tailor stimulation protocols in real-time based on the underlying neurochemical landscape. For instance, a closed-loop deep brain stimulation (DBS) system that adjusts its output in response to local dopamine levels could achieve more effective and side-effect-free treatment for Parkinsonian motor symptoms [233–235].

Beyond neurotransmitters, the monitoring of biomarkers such as inflammatory cytokines (e.g., IL-6, TNF-α), oxidative stress indicators (e.g., nitric oxide, ROS), metabolic intermediates (e.g., glucose, lactate), and hormones (e.g., cortisol) can provide crucial feedback in both neural and systemic applications. These biochemical cues can inform device operation, trigger safety shutdowns, initiate therapeutic release, or provide early warning of adverse tissue responses.

The integration of real-time biochemical sensing with embedded control algorithms and stimulation hardware necessitates compact, low-power, and biocompatible sensor platforms. Thin-film biosensors, owing to their conformability, mechanical compliance, and ease of integration with other microelectronic components, are particularly well-suited for this task. Additionally, advances in on-chip data processing and low-latency telemetry further enhance the feasibility of biochemical closed-loop systems in both experimental and clinical settings.

4 | Thin-Film Biosensing

The drive toward miniaturized, high-performance biosensors has placed a spotlight on thin-film technologies. These systems, typically fabricated with dimensions on the micron or sub-micron scale, provide a versatile platform for integrating biosensing functionality into flexible substrates [236]. Thin-film biosensors enable high surface-to-volume ratios, facilitating enhanced analyte accessibility and faster response times. Furthermore, their mechanical properties, particularly ultrathinness (<5 μm) and low bending stiffness, allow them to conform to dynamic biological surfaces such as the brain, spinal cord, or peripheral nerves without eliciting tissue damage or immune response [52, 237, 238]. From a materials perspective (see Subsection 4.3), functional thin-film coatings play a critical role in enabling specific and sensitive detection of biochemical targets. Conductive polymers (e.g., poly(3,4-ethylenedioxythiophene):polystyrenesulfonate, or PEDOT:PSS) [239], metal oxide nanostructures (e.g., ZnO, TiO_2) [240], carbon-based materials (e.g., graphene, carbon nanotubes) [241], and plasmonic nanostructures (e.g., gold nanorods, nanopillars) [62] are commonly employed to provide electrochemical activity or signal amplification. These materials are further functionalized with biorecognition elements such as aptamers, enzymes, antibodies, or molecularly imprinted polymers (MIPs) to ensure selective binding to target analytes.

In addition to classical electrochemical sensors, plasmonic and photoacoustic biosensors based on thin films have shown significant promise for optical or ultrasound-based biochemical detection. Localized surface plasmon resonance (LSPR) sensors fabricated on thin metal nanostructures can detect changes in refractive index due to molecular binding events, enabling label-free and multiplexed detection. Similarly, ultrasound-based biosensors utilize piezoelectric thin films to transduce biochemical interactions into acoustic signals, enabling deep-tissue readouts even in opaque environments.

TABLE 2 | Representative, experimentally validated self-sustained implantable systems that integrate biosensing, on-board or harvested energy sources, embedded signal processing and control electronics or closed-loop actuation/therapeutic output. For each example, the implantation duration, the target tissue, the integrated sensing modality, energy modality, degree of autonomy and demonstrated long-term performance limitations are reported.

System (Reference)	Target tissue/ application	Integrated sensing modality	Energy source (on-board/ harvested)	On-board processing/ control	Actuation/ therapeutic output	Implantation duration demonstrated	Degree of autonomy	Key limitations reported
Responsive Neurostimulation (RNS) System [226]	Human cortex — responsive epilepsy therapy	Continuous intracranial electrocorticographic sensing	Rechargeable internal battery (clinically managed)	On-board detection algorithms / programmable stim paradigms	Closed-loop electrical stimulation to abort seizures	Multi-year human implants (clinical use, long-term follow-up)	Semi-autonomous (device senses and stimulates automatically; requires clinical battery maintenance)	Clinical, validated performance but not energy-harvesting — relies on implanted battery and clinical recharge/replacement; regulatory/packaging constraints.
Wirelessly powered fully internal optogenetic implants [227]	Brain/spinal cord/peripheral nerves (rodent models)	Optical stimulation control + electrophysiological readout (μLED + recording electrodes)	RF/inductive wireless power (external transmitter) — battery-free	On-chip timing and control for stimulation patterns	Optical stimulation (μLEDs) for neuromodulation (closed-loop variants demonstrated)	Days to weeks in behaving rodents	High autonomy during experiment (wireless power delivered externally)	Requires external power transmitter; thermal and alignment constraints for chronic use; implant packaging and long-term biostability not fully validated long-term.
Wireless, battery-free subdermal optoelectronic tissue oximetry (fully implantable platform) [228]	Subdermal / brain tissue oximetry and local hemodynamics (mouse models)	Optical photodetectors + LEDs (continuous tissue oxygenation sensing)	Resonant magnetic / RF wireless power (battery-free)	Integrated microscale electronics for signal conditioning and wireless data encoding	Wireless telemetry; in some variants, on-demand stimulation possible	Acute to short-term chronic in animals (days–weeks)	Autonomous while within RF field; no implanted battery	Demonstrates continuous sensing with battery-free operation but still depends on external power field; scaling to long human chronic use remains to be shown.
Fully implantable, wireless, battery-free electrochemical catecholamine sensing and optogenetic stimulation [229]	Brain — real-time catecholamine dynamics (rodent models)	Electrochemical detection of catecholamines (microelectrodes)	Battery-free wireless power (RF/resonant)	Onboard low-power conditioning and control ASIC	Closed-loop optogenetic stimulation driven by chemical sensing (demonstrated control loops)	Acute to short chronic in rodents (days)	High functional autonomy when powered wirelessly	Powerful demo of integrated chemical sensing and actuation, but requires external power field; chronic biostability and long-term enzyme/fouling issues remain open.
Blood-glucose-powered metabolic fuel cell coupled to insulin-release capsule [230]	Subcutaneous metabolic control (mouse diabetes model)	Intrinsic glucose sensing via fuel-cell power output (metabolic sensing)	Glucose biofuel cell (implant converts excess glucose into electrical power)	Simple control logic coupling fuel-cell output to stimulation of insulin-releasing module (engineered cells / actuators)	Electrically triggered insulin release from engineered cell capsule (closed-loop restoration of normoglycemia in mice)	Acute proof-of-concept in mice (days)	Largely autonomous (self-sufficient closed loop demonstrated in vivo)	Prototype stage; enzyme/biocatalyst longevity, biocompatibility, and scalability to humans unproven; limited implantation duration reported.
Piezoelectrically powered drug-release (push-button and motion-activated) implant [231]	Subcutaneous therapeutic release (mouse diabetes model demonstrated)	Onboard chemical sensing / thresholding in variants; here mechanical actuation triggers release from engineered cells	Mechanical (finger press or motion) for piezoelectric harvesting (on-demand energy)	Simple control/electrical coupling to engineered cell chamber	Rapid actuation: electrical activation of cell capsule for insulin release (closed-loop or manual trigger)	Demonstrated restoration of normoglycemia in mice (acute to short-term)	Autonomous at activation (no battery), requires mechanical activation or motion	Demonstrates clever energy-economy for rare actuation events; not continuously self-sustaining for high-duty therapies; long-term biocompatibility and mechanical fatigue need study.
Cardiac motion–energy harvesters coupled to sensing modules (piezo/TENG + sensing) [232]	Cardiovascular interface / pacemaker concepts	Pressure/motion sensors (mechanical to electrical transduction)	Piezoelectric / triboelectric nanogenerators harvesting heartbeat motion	Extremely low-power conditioning and telemetry circuits (demonstrated)	Diagnostic telemetry; in concept can supply pacing or low-energy actuation	Short-term animal demonstrations; proof-of-concept pacing proposed	Potential for autonomous intermittent operation (dependent on motion amplitude)	Power density often low and intermittent; requires storage and power-management to support actuation; chronic reliability needs validation.

4.1 | Thin-Film Microfabrication Techniques

The intricate fabrication of advanced thin-film biosensors, especially those destined for chronic in vivo neural applications, critically hinges upon sophisticated micro- and nanofabrication techniques [242]. These methods enable the precise, high-resolution patterning of a diverse array of functional materials onto flexible or even stretchable substrates, ensuring mechanical compatibility with soft biological tissues and curved anatomical surfaces. The selection and combination of these techniques are paramount for achieving the desired sensitivity, specificity, stability, and integration capabilities of the final biosensing platform.

Among the cornerstone methodologies are photolithography (PhL) and electron-beam lithography (EBL). These are quintessential "top-down" lithographic methods that facilitate the patterning of thin films with remarkable precision. PhL, leveraging ultraviolet (UV) light to transfer a pattern from a photomask onto a photoresist-coated substrate, is broadly and economically employed for defining device features typically down to and including the micrometer scale (features ≥1 μm). This technique is highly scalable and forms the backbone of conventional semiconductor manufacturing. For features demanding even greater resolution, reaching into the nanometer regime, EBL becomes indispensable. EBL utilizes a focused beam of electrons to directly draw patterns onto an electron-sensitive resist, offering unparalleled resolution (down to tens of nanometers) for critical components such as sub-micron nanoelectrodes, high-density interconnects, or specialized plasmonic nanostructures. Both PhL and EBL are inherently compatible with standard complementary metal-oxide-semiconductor (CMOS) processing, which is a significant advantage as it facilitates the monolithic integration of biosensing elements directly alongside on-chip electronic circuitry for signal conditioning, amplification, and wireless data transmission, thereby creating highly compact and efficient sensor systems.

For the deposition of various material layers, physical vapor deposition (PVD) techniques are extensively utilized, such as sputtering and thermal evaporation. These deposit robust metallic layers, such as gold for electrodes or recognition element immobilization, platinum for catalytic surfaces or reference electrodes, and titanium or chromium as adhesion layers. They are also critical for depositing dielectric films like silicon dioxide (SiO_2) or aluminum oxide (Al_2O_3), which serve as insulating layers, passivation layers, or gate dielectrics in transistor-based sensors. PVD offers exceptional control over film thickness, composition, and stoichiometry, which are all essential parameters for ensuring the reproducibility and uniformity of large-scale sensor arrays.

Chemical vapor deposition (CVD) plays a vital role, particularly for growing high-quality semiconducting or carbon-based materials like single-layer or few-layer graphene and carbon nanotubes (CNTs). In CVD, volatile precursors react or decompose on a heated substrate surface to form a solid film, providing uniform coverage and controlled crystallinity [243]. Given the increasing use of flexible and temperature-sensitive polymeric substrates (e.g., polyimide, parylene) for neural biosensors, low-temperature CVD (LTCVD) or plasma-enhanced CVD (PECVD) variants are particularly important [244–246]. PECVD, for instance, uses plasma to activate precursors at much lower temperatures, preventing thermal degradation of the substrate while still enabling high-quality film growth.

Beyond vacuum-based deposition, printing techniques gained significant traction for their additive manufacturing capabilities, scalability, and cost-effectiveness [247–250]. Inkjet printing precisely deposits picoliter droplets of conductive inks (e.g., silver nanoparticle inks), biomaterial solutions (e.g., enzyme suspensions, antibody solutions), or nanoparticle suspensions onto specific locations. Screen printing is a versatile technique for depositing thicker films of conductive pastes or sensing materials through a patterned mesh [251, 252]. Aerosol jet printing offers finer resolution than traditional inkjet, using an atomized aerosol stream to deposit functional materials [253, 254]. These printing methods are highly compatible with roll-to-roll (R2R) processing, making them highly attractive for high-throughput, low-cost, and large-area biosensor fabrication on flexible films, enabling efficient mass production.

For the creation of highly conformal and stretchable biosensors, critical for intimate contact with dynamic biological tissues, soft lithography and transfer printing techniques are indispensable. Soft lithography, often involving microcontact printing, utilizes an elastomeric stamp (typically polydimethylsiloxane, PDMS) molded from a silicon master [255]. This stamp can be inked with molecules or nanoparticles and then used to "print" patterns onto a substrate, allowing for gentle, high-resolution patterning on delicate or non-planar surfaces. Elastomeric transfer printing involves the precise pick-and-place of pre-fabricated thin-film structures from a rigid growth substrate onto a compliant, elastomeric substrate such as PDMS or Ecoflex. This approach enables the fabrication of complex micro/nanostructured films that retain their electrical and mechanical integrity even when subjected to significant stretching or bending, thereby facilitating intimate and stable contact with soft tissues and intricately curved anatomical surfaces like the brain's gyri and sulci.

Finally, laser ablation and etching techniques offer precise material removal capabilities. Focused laser ablation uses highly concentrated laser energy to selectively remove material, enabling the precise definition of microscale sensor geometries, microfluidic channels, or electrical isolation trenches, particularly valuable in hybrid or multilayer devices where selective material removal is required without damaging underlying layers [256, 257]. Similarly, plasma etching utilizes chemically reactive plasmas to remove materials with high anisotropy and selectivity. These etching techniques are also crucial for the release of freestanding thin-film structures from their fabrication substrates or for patterning complex microfluidic channels for integrated analyte sampling, delivery, and waste removal, enhancing the overall functionality of integrated biosensing platforms [258, 259].

Ultimately, these advanced fabrication techniques are rarely used in isolation. Instead, they are often combined in hybrid processes to construct multilayer, multifunctional biosensors with increasingly complex and hierarchical architectures. Each distinct layer, whether it's the electrode material, a dielectric insulator, a functional recognition interface, or a protective passivation layer, plays a highly specific and integrated role

in the overall sensing mechanism, signal transduction, data transmission, and mechanical integration with the biological environment. This multi-technique approach is essential for pushing the boundaries of neural biosensor performance and clinical utility.

4.2 | Key Figures of Merit

The performance of thin-film biosensors is governed by several key figures of merit that define their utility in biomedical applications:

Sensitivity refers to the smallest change in analyte concentration that the sensor can detect. For electrochemical biosensors, sensitivity is typically expressed in terms of current (nA) per concentration unit (μM or nM), while for optical biosensors, it may relate to wavelength shift or absorbance change. High sensitivity is critical in neural interfaces where neurotransmitters like dopamine and glutamate fluctuate at sub-micromolar levels.

Selectivity describes the sensor's ability to distinguish the target analyte from interfering species. This is especially important in complex biological environments rich in potentially confounding molecules (e.g., ascorbic acid, uric acid, glucose). Strategies to enhance selectivity include the use of molecular recognition elements (enzymes, aptamers, antibodies), selective membranes (e.g., Nafion), or redox mediators.

Stability encompasses both operational stability (performance over time during active use) and shelf-life stability (storage durability). In vivo applications demand long-term functional stability, often over weeks or months, with minimal drift, fouling, or degradation. This depends on both material robustness and antifouling surface chemistry.

Response time is another critical parameter, defined by the time required to reach a steady-state signal after analyte exposure. Fast response (in the order of milliseconds to seconds) is essential for capturing transient neurotransmitter dynamics.

Limit of detection (LoD) and dynamic range are also relevant. The LoD defines the minimum detectable concentration with an acceptable signal-to-noise ratio, while the dynamic range defines the span of concentrations over which the sensor response remains linear or predictable.

Together, these metrics, summarized in Table 3, guide sensor design choices and help determine suitability for real-time, chronic, or multiplexed monitoring applications in neurotechnologies.

4.3 | Material Platforms: Metals, Polymers, and Hybrids

The choice of materials is undeniably one of the most critical determinants in the design and performance of microfabricated thin-film biosensors, particularly those intended for integration into flexible bioelectronic systems for in vivo applications (Figure 3). These materials directly dictate the resulting electrical, chemical, and mechanical properties of the device, profoundly influencing its functionality, efficiency, and long-term interaction with the biological environment. The materials must be inherently non-toxic, non-inflammatory, conformable to soft tissues, and demonstrate long-term safety upon continuous exposure to body tissues and fluids [17, 274, 275]. Crucially, they must also enable the efficient operation of the wireless system within the complex and heterogeneous dielectric environment of the human body, which comprises tissues of varying conductivity and permittivity [16].

Noble metals stand as foundational components in thin-film biosensor fabrication and wireless system interconnects due to their exceptional electrical conductivity, robust electrochemical stability, and inherent biocompatibility. Au, for instance, is widely employed for constructing electrodes, electrical interconnects [276], and as a versatile surface for immobilizing biorecognition elements (e.g., antibodies, aptamers) owing to its chemical inertness and well-established surface functionalization chemistries. Pt is another favored choice for working and counter electrodes due to its excellent electrocatalytic properties for various redox reactions (e.g., H_2 O_2 detection) and its biostability. For specialized applications like pH sensing and neural stimulation, IrO_x is highly regarded for its remarkable charge injection capacity (critical for efficient neural stimulation with minimal tissue damage) and its inherent biostability in physiological environments. Beyond noble metals, various transition metal oxides, such as Zinc Oxide (ZnO), Titanium Dioxide (TiO_2), and Tungsten Oxide (WO_3), are increasingly utilized. These oxides can serve as active sensing layers in enzymatic biosensors (e.g., providing high surface area for enzyme immobilization) or as semiconducting components in field-effect transistor (FET) configurations, often enhancing catalytic activity, charge transfer kinetics, or displaying tunable semiconducting behavior directly sensitive to analyte binding. In wireless power transfer and wireless data communication systems, the materials used in antennas, coils, and interconnects require high electrical conductivity to minimize ohmic losses and ensure efficient power transfer [16]. High dielectric materials with low loss, such as certain ceramics, are ideal for components requiring high capacitance with minimal energy dissipation, whereas materials with low dielectric constant and low loss, including specific polymers and carbon-based materials, are better suited for achieving mechanical flexibility and minimizing signal degradation in antennas and transmission lines.

Polymers offer a remarkable versatility in thin-film biosensor and flexible bioelectronic system design, broadly categorized into conductive and non-conductive types [277]. Conductive polymers, such as PEDOT and polyaniline (PANI), are highly attractive as they combine electronic conductivity with inherent mechanical flexibility, biocompatibility, and excellent bio-interfacing properties. PEDOT, in particular, often doped with polystyrenesulfonate (PSS), offers high conductivity, tunable redox states, and a porous structure ideal for enzyme entrapment and enhanced electrode surface area in electrochemical sensors [239, 278, 279]. These polymers can serve as active transducers or as scaffolds for bioreceptor immobilization. In contrast, non-conductive polymers are indispensable for their roles as robust substrates, encapsulants, and dielectric layers. Materials like parylene C, SU-8, and polyimide are extensively used due to their exceptional dielectric strength

TABLE 3 | Figures of merit of biosensors for detection of neurochemically-relevant species.

Figure of merit				
Name	**Unit**	**Symbol/Expression**	**Description**	**Refs.**
Limit of Detection (LoD)	Concentration (e.g., nM, pM, fM)	$LoD = \frac{3 \cdot \sigma_b}{m}$	The lowest concentration of an analyte that can be reliably detected and distinguished from a blank signal. σ_b is the standard deviation of the blank, and m is the slope of the calibration curve. Crucial for detecting low-abundance biomarkers.	[260–262]
Limit of Quantification (LoQ)	Concentration (e.g., nM, pM)	$LoQ = \frac{10 \cdot \sigma_b}{m}$	The lowest concentration of an analyte that can be quantified with acceptable precision and accuracy. Higher than LoD.	[263, 264]
Sensitivity	Current/Voltage per Unit Concentration (e.g., nA/nM, mV/nM)	$\frac{\Delta\,(signal)}{\Delta\,(concentration)}$ or slope of calibration curve	The change in sensor output (current, voltage, frequency, etc.) per unit change in analyte concentration. A higher sensitivity indicates a stronger response to a given amount of analyte.	[260, 265, 266]
Specificity / Selectivity	(Unitless, often % rejection or selectivity coefficient)	$K_{A,B} = \frac{m_A}{m_B}$ or % inhibition	The ability of the biosensor to selectively detect the target analyte in the presence of other potentially interfering substances (e.g., other neurotransmitters, drugs, metabolites). Quantified by selectivity coefficients ($K_{A,B}$ where A is target, B is interferent), or by demonstrating minimal signal from interferents.	[267, 268]
Linear Dynamic Range (LDR)	Concentration (e.g., nM to µM)	C_{min} to C_{max}	The range of analyte concentrations over which the biosensor's response is directly proportional to the analyte concentration. This defines the usable range for quantitative measurements.	[269, 270]
Response time (T90 or tmax)	Time (e.g., ms, s)	Time to reach 90% or max signal	The time taken for the sensor to reach a stable output (typically 90% of its final response) after the introduction of the analyte. Critical for real-time in vivo monitoring of rapid physiological events.	[266]
Recovery time / Reversibility	Time (e.g., s, min)	Time for signal to return to baseline	The time taken for the sensor signal to return to baseline after the analyte is removed or consumed. Important for continuous monitoring and preventing signal accumulation.	[266]
Stability (short-term & long-Term)	% Retention of Initial Signal over Time	$\frac{Signal\ at\ time\ t}{Signal\ at\ time\ 0}$ (%)	The ability of the biosensor to maintain its performance (e.g., sensitivity, LoD) over a period of time, both during a single experiment (short-term) and over weeks/months of continuous operation or storage (long-term). Influenced by enzyme degradation, biofouling, material degradation.	
Reproducibility / Repeatability	% Relative Standard Deviation (RSD%)	$RSD = (\frac{Standard\ deviation}{Mean}) \cdot 100$	The ability of a sensor to provide the same response for the same analyte concentration under identical conditions (repeatability) or across different sensors/batches (reproducibility). Often expressed as RSD% for multiple measurements.	[266]
Biocompatibility	(Qualitative, often ranked)	Inflammation scores, cell viability	The ability of the sensor material to interact with biological systems without causing adverse effects (e.g., inflammation, toxicity, foreign body response) and to avoid being degraded or fouled by the biological environment. Essential for implantable devices.	—

(Continues)

TABLE 3 | (Continued)

Figure of merit				
Name	**Unit**	**Symbol/Expression**	**Description**	**Refs.**
Biofouling Resistance	% Signal Loss / Surface Coverage over Time	Rate of signal degradation or surface protein adsorption	The ability of the sensor surface to resist non-specific adsorption of proteins, cells, or other biological components that can degrade performance over time. Crucial for chronic in vivo applications.	[271]
Miniaturization / Spatial resolution	Length (e.g., μm)	Electrode/Sensor Dimension	The physical size of the sensing element. Smaller sensors allow for localized measurements within specific neural structures and minimize tissue damage during implantation.	—
Power consumption	Power (e.g., μW, mW)	Power required for operation	The amount of electrical power required for the sensor to operate. Low power consumption is vital for portable, wearable, and implantable devices to extend battery life and reduce heat generation.	[272, 273]

(insulating properties), excellent chemical resistance, mechanical flexibility, and biocompatibility. Parylene C, deposited via chemical vapor deposition, forms highly conformal and pinhole-free coatings, making it an ideal choice for encapsulation layers that protect the active sensor elements from the harsh in vivo environment [274, 280–282]. SU-8 is widely used in photolithography to define microscale structures and channels [283, 284]. Polyimide offers excellent thermal stability and mechanical strength for flexible circuit boards [285–289]. Furthermore, hydrogels and ionomers (polymers containing ionic groups, such as Nafion) are specifically employed in biosensors to mediate ion transport (e.g., for ISEs), create permselective barriers to exclude interfering species (e.g., preventing ascorbic acid from reaching dopamine sensors), or encapsulate sensitive biological components while allowing analyte diffusion [290–292].

Recent advances in neural biosensing have increasingly focused on the rational design and synthesis of hybrid and composite materials, which synergistically combine the desirable properties of different material classes to overcome limitations inherent in single-component systems. For instance, the integration of carbon-based materials (e.g., graphene, CNTs) with metal nanoparticles (e.g., AuNPs, PtNPs) creates nanocomposites with vastly enhanced surface area, superior electrical conductivity, and significantly improved catalytic activity for electrochemical reactions. Such composites enable higher loading of recognition elements and amplified signals. Another powerful approach involves nanocomposites embedding enzymes or aptamers within polymer matrices (e.g., conductive polymers, hydrogels). This strategy effectively preserves the delicate bioactivity of the recognition element while simultaneously improving the overall mechanical robustness and stability of the sensing interface. Emerging platforms include MXenes (a class of 2D transition metal carbides, nitrides, or carbonitrides) and other 2D materials (beyond graphene) that offer a remarkable array of tunable electronic, chemical, and mechanical properties, making them highly promising for next-generation biosensors and flexible electronics [241, 293]. These materials can be engineered for high conductivity, unique sensing mechanisms, or enhanced biocompatibility.

4.4 | Surface Functionalization Strategies

To effectively detect specific biomolecules within the complex milieu of physiological fluids, thin-film biosensors necessitate precise functionalization with highly selective molecular recognition elements [294, 295] (Figure 3). This functionalization process directly confers the requisite target specificity, sensitivity, and operational stability of the biosensor. Improper functionalization strategies can lead to significant issues such as signal drift, pronounced biofouling, and a detrimental loss of sensitivity over time, particularly critical for applications involving chronic implantation or prolonged exposure to challenging biological matrices like sweat, interstitial fluid, or cerebrospinal fluid (CSF). Functionalization strategies can be broadly categorized into several sophisticated approaches.

Covalent immobilization relies on the formation of robust covalent bonds between the biosensor's surface and the molecular recognition element (MRE) [296, 297]. The sensor sur-

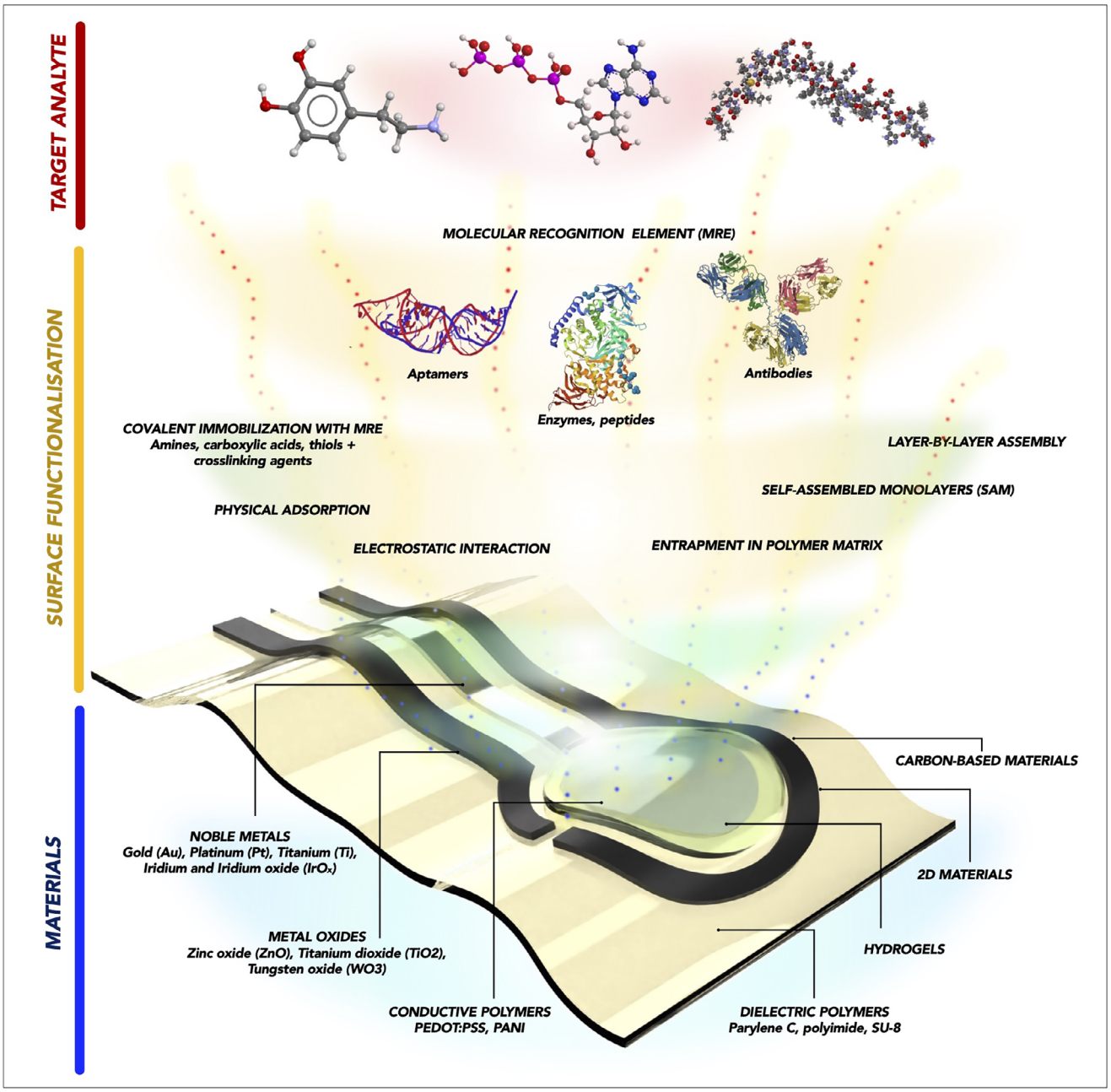

FIGURE 3 | Artwork showing the most common choices for materials and surface functionalization strategies for a microfabricated neural biosensor aimed at detecting neurological analytes.

face is typically engineered to present specific functional groups such as amines (-NH_2), carboxylic acids (-COOH), or thiols (-SH). These groups then react with complementary groups on the MREs (e.g., enzymes, antibodies, aptamers, peptides) through various chemical coupling reactions. Crosslinking agents are frequently employed to facilitate and stabilize these bonds. Common examples include glutaraldehyde, which forms Schiff bases with amine groups; EDC/NHS (1-ethyl-3-(3-dimethylaminopropyl)carbodiimide / N-hydroxysuccinimide), a widely used carbodiimide chemistry for amide bond formation between carboxyl and amine groups; and various silanes (e.g., aminopropyltriethoxysilane, APTES) which can form stable siloxane bonds with oxide surfaces and provide accessible amine groups for subsequent MRE attachment. While covalent binding offers superior stability, mechanical robustness, and resistance to desorption compared to non-covalent methods, it often necessitates prior surface pretreatment steps. These can include plasma activation (e.g., oxygen plasma to create hydroxyl groups), chemical etching, or silanization processes to introduce the desired reactive functional groups onto the otherwise inert thin-film material. A key challenge is to ensure that the covalent attachment does not compromise the native conformation or biological activity of the MRE.

Noncovalent approaches are generally simpler and more straightforward to implement, often favored for proof-of-concept studies or applications requiring reversible or temporary sensing layers [298]. They include (i) physical adsorption, (ii) electro-

static interaction, (iii) entrapment/embedment in a polymer matrix.

Physical adsorption involves non-specific interactions such as van der Waals forces, hydrophobic interactions, and weak electrostatic forces between the MRE and the sensor surface [299]. It's easy to implement but often leads to random orientation of MREs and is highly prone to desorption or denaturation under mechanical stress, thermal fluctuations, or changes in ionic strength.

Electrostatic interaction relies on the attractive forces between oppositely charged groups on the sensor surface and the MRE [300]. Surface charge can be tailored by pH or by modifying the surface with polyelectrolytes. While offering some degree of orientation control, it is susceptible to changes in ionic strength and pH of the physiological fluid, potentially leading to MRE leaching.

Entrapment in a polymer matrix consists of physically confining the MRE within the porous structure of a polymer film (e.g., hydrogels like polyHEMA, or conductive polymers like PEDOT) [301]. This method can protect the MRE from denaturation and provide a diffusion-controlled environment. However, it can limit the accessibility of the analyte to the MRE and is still prone to MRE leakage from the matrix over time, especially with larger pore sizes or mechanical agitation. While simpler, these non-covalent methods are inherently more prone to issues such as desorption (loss of the MRE from the surface), denaturation (loss of MRE activity due to conformational changes), and fouling due to non-specific interactions.

Self-assembled monolayers (SAMs) represent a highly elegant and versatile functionalization strategy, enabling the creation of well-defined and precisely tunable surface architectures [302, 303]. These are typically formed by the spontaneous adsorption and organization of amphiphilic molecules (molecules with both hydrophobic and hydrophilic parts) onto a solid surface from solution. For instance, thiol-based SAMs readily form on gold surfaces, where the sulfur atom strongly binds to gold, leaving a functional head group exposed to the solution [304, 305]. Similarly, silane-based SAMs are commonly employed on oxide surfaces (e.g., SiO_2, TiO_2) via the formation of stable siloxane bonds [306, 307]. The terminal functional groups of these SAMs (e.g., -COOH, -NH_2, PEG chains) can then be precisely engineered for subsequent covalent attachment of MREs or for imparting specific surface properties. A significant advantage of SAMs is their ability to include antifouling moieties, such as short PEG chains or zwitterionic groups, within the monolayer itself [308]. These antifouling layers create a highly hydrated and sterically repulsive barrier that effectively prevents non-specific protein adsorption and cellular adhesion, thereby significantly prolonging the in vivo stability and operational lifetime of the biosensor.

Layer-by-Layer (LbL) assembly is a highly versatile and controlled thin-film deposition technique that involves the sequential alternate deposition of oppositely charged polyelectrolytes (or other interacting species like nanoparticles, proteins) from aqueous solutions [309, 310]. Each adsorption step is driven by electrostatic interactions (or other non-covalent forces), resulting in a precise build-up of nanometer-thick layers. By carefully selecting the polyelectrolytes and the incorporation of functional layers (e.g., enzyme layers, nanoparticle layers), LbL assembly can be used to fabricate highly sophisticated multi-analyte sensors by creating distinct functional layers for different MREs. It is also particularly useful for designing stimuli-responsive sensors (e.g., pH-responsive, temperature-responsive) where changes in the environment can alter the film's properties or release an encapsulated analyte. The multi-layered nature also provides mechanical stability and can protect embedded MREs.

Beyond molecular-level modifications, the physical nanotopography and architecture of the sensor surface itself play a critical role in enhancing biosensor performance. Nanostructured surfaces, such as arrays of nanopillars, nanowires, porous films, or precisely engineered microelectrode arrays, dramatically increase the active surface area available for MRE immobilization. This increased surface area directly translates into higher sensor sensitivity by allowing more recognition events to occur per unit macroscopic area [311–313]. Furthermore, it enables high-density multiplexing, allowing for the integration of multiple sensing elements for different analytes within a very confined space. The engineered surface nanotopography also critically influences various surface phenomena, including protein adsorption dynamics, cellular interaction (e.g., guiding cell adhesion or repulsion), and significantly impacts the overall biofouling resistance of the device. For instance, specific nanoscale roughness or patterned hydrophilic/hydrophobic domains can deter the formation of a dense protein corona, thus preserving sensor function over time.

Functionalization is not merely an afterthought in biosensor design; it is a pivotal determinant of the sensor's operational reliability and analytical performance. The optimization of surface modification protocols, often involving sophisticated combinatorial approaches of these techniques, is absolutely critical. This is especially true in the demanding context of chronic in vivo implantation, where the biosensor is continuously exposed to complex and aggressive biological fluids like interstitial fluid, or cerebrospinal fluid.

5 | Electrochemical Biosensors

Electrochemical (EC) biosensors have rapidly advanced to become one of the most compelling modalities for monitoring dynamic biochemical changes in vivo, particularly within the intricately complex landscapes of the central and peripheral nervous systems [270, 277]. These sophisticated devices excel at converting specific chemical information, most commonly the precise concentration of analytes such as neurotransmitters, metabolic byproducts, or inflammatory mediators, into quantifiable electrical signals. Their inherent miniaturizability, seamless compatibility with flexible [314] and even stretchable [315] substrates, and remarkable responsiveness to real-time biochemical fluctuations make EC biosensors well-suited for integration into advanced neural interface applications. This section delves into the primary electrochemical modalities, elucidating their fundamental mechanisms of action, and detailing how they are tailored to function effectively within demanding neural environments (see Table 4 for a list of sensors shown in previous works).

TABLE 4 | Examples of electrochemical biosensors for neurotransmitters, biomarkers, and small molecules.

Category/Description	Target analyte	Platform/Materials	Sensitivity/Limit of detection	Application stage	Refs.
Amperometric					
Screen-printed carbon MEA, thick-film carbon ink electrodes (SU-8 insulated) for analyte oxidation	Nitric oxide	Screen-printed carbon ink on quartz; SU-8 insulation	n/a (sensitivity demonstrated at +900 mV)	In vitro (tissue slices)	[373]
Glutamate enzyme microelectrode array	L-Glutamate	Ceramic (Al_2O_3) substrate with Pt microelectrodes; glutamate oxidase/Nafion coatings	7.6×10^{-3} nA/μM (slope); LOD ~0.92 μM	In vivo (rats)	[374]
Choline enzyme microprobe array	Choline	Silicon microprobe with thin-film Pt electrodes; choline oxidase/phosphorylase membranes	157 $\mu A\cdot mM^{-1}cm^{-2}$; LOD <1 μM	In vivo	[375]
Voltammetric					
Carbon-fiber GluOx + FSCV, carbon-fiber microbiosensor coated with glutamate oxidase, detected by fast-scan cyclic voltammetry	Glutamate (via H_2O_2 reporter); Dopamine	Carbon fiber microelectrode; GluOx hydrogel coating	(Sensitivity ~33 pA/μM for glutamate); LOD ~μM	In vivo (rat striatum)	[376]
Carbon-nanotube yarn CFMEs, CNT yarn fiber microelectrodes for FSCV	Serotonin	Carbon nanotube yarn electrode; FSCV waveform	(Enhanced sensitivity vs. CFME; fouling-resistant)	In vitro	[377]
3D fuzzy graphene MEA, vertically grown graphene nanoflakes on microelectrode array for FSCV	Dopamine	3D graphene nanostructured carbon microelectrode array	LOD ≈364 pM; sensitivity ≈2.12 $nA\cdot nM^{-1}$	In vitro (buffer perfused)	[378]
FSCV microelectrode array for dopamine	Dopamine	Pyrolyzed photoresist (carbon) electrodes on Si/SiO_2 with Si_3N_4 insulation (microfabricated)	n/a	In vivo (rat)	[379]
Dual-electrode voltammetric dopamine sensor	Dopamine	Pyrolyzed photoresist carbon dual microelectrodes (8 μm spacing) on SiO_2 surface	n/a	In vitro	[380]

(Continues)

TABLE 4 | (Continued)

Category/Description	Target analyte	Platform/Materials	Sensitivity/Limit of detection	Application stage	Refs.
Enzyme-based					
Si microprobe with GOx/ChOx, silicon microprobe with recessed Pt microelectrodes coated with enzyme membranes (GOx for glucose, ChOx for choline, etc.)	Choline, L Glutamate	Silicon probe; Pt microelectrodes; enzyme (ChOx, GluOx) in polymer film	Sensitivity: ~95–132 $\mu A \cdot mM^{-1} \cdot cm^{-2}$; LOD <0.5 μM	In vitro and in vivo	[381]
Tyrosinase/C-MOF CFME, carbon-fiber microelectrode with chitosan/ceria/tyrosinase layer (low-potential DA reduction)	Dopamine	Carbon fiber (~100 μm Ø); chitosan/ceria/Tyr on tip	LOD = 1 nM; sensitivity 14.2 $nA \cdot \mu M^{-1}$	In vivo (rat brain)	[382]
Carbon-fiber with AChE/ChOx, CF electrode immobilized with acetylcholinesterase and choline oxidase, layered with HRP/Os mediator and permselective coatings	Acetylcholine, Choline	Carbon fiber; AChE and ChOx co-immobilized in gel/film	LOD = 1 μM (for both ACh and Ch)	In vivo (rat hippocampus)	[383]
Platinized CFME + LOx, Pt-deposited carbon-fiber microelectrode with lactate oxidase cross-linked in polyurethane/Permselective layers	L-Lactate	Pt-coated carbon fiber; lactate oxidase (+ mPD, PU coatings)	(High sensitivity; LOD not reported)	In vitro (hippocampal slices)	[384]
Aptamer-based					
Ferrocene-tagged aptamer on Au SPE – ferrocene-labeled DNA aptamer immobilized on a gold screen-printed electrode	Dopamine	Au screen-printed electrode; thiolated ferrocene aptamer	LOD ≈60 pM (CV) – 20 pM (EIS)	In vitro (buffer)	[385]
Gold electrode with 5-HT aptamer – thiolated DNA aptamer for serotonin on Au electrode, read out by EIS	Serotonin	Gold working electrode; thiolated serotonin aptamer	LOD = 5.6 nM	In vitro (flow system)	[386]
OECTs					
PEDOT:PSS OECT array, microfabricated OECT array with PEDOT:PSS channel and Pt pseudo-reference gates (chitosan-modified)	Dopamine	PEDOT:PSS channel; Pt gate electrodes, chitosan-modified	LOD ≈1 nM	In vitro (artificial CSF)	[387]
PEDOT:PSS OECT multiplexed array, flexible OECT array for mapping catecholamines (PEDOT:PSS channel, Ag/AgCl gate)	Dopamine (and catecholamines)	PEDOT:PSS channels on flexible substrate; on-chip Ag/AgCl reference	LOD ~1 nM	In vivo (rat brain)	[342]
PEDOT:PSS OECT aptamer, single PEDOT:PSS transistor with epinephrine-specific aptamer on gate electrode	Epinephrine (adrenaline)	PEDOT:PSS channel OECT; Au gate with covalently attached aptamer	LOD = 90 pM	In vitro	[388]
Laser-scribed graphene OECT, flexible dual-gate OECT (PEDOT:PSS on LSG) with one gate modified by chitosan and the other by GlutOx enzyme	Dopamine, Glutamate	Laser-scribed graphene transistor; chitosan and GluOx on gate surfaces	LOD ≈5 nM (DA) and ≈1 μM (Glu)	In vitro	[389]

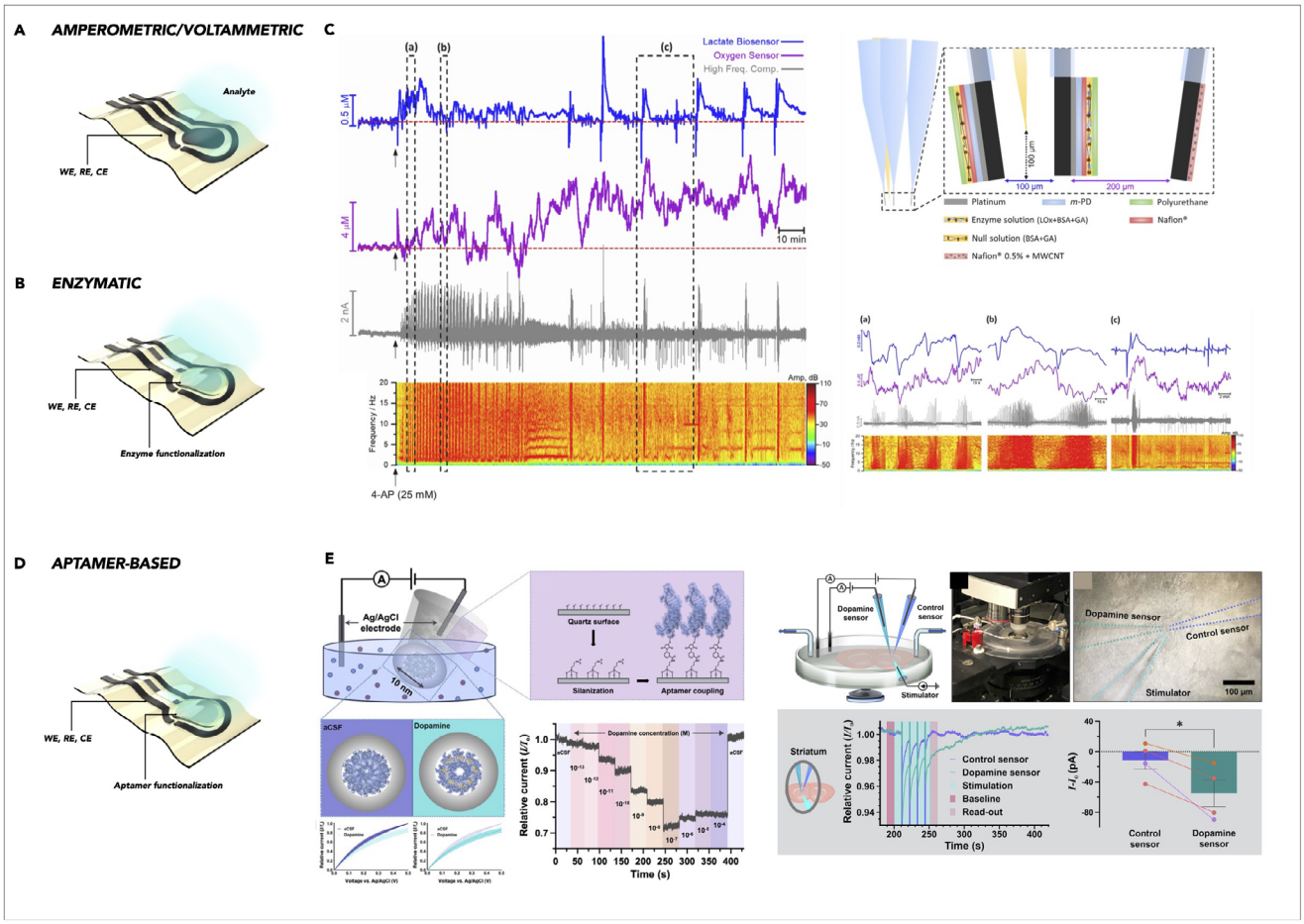

FIGURE 4 | Electrochemical neural biosensors: (A) Amperometric/voltammetric, (B) enzymatic, (D) aptamer-based. (C) Example of enzyme-functionalised amperometric biosensor integrated with micropipettes. Representative recordings are displayed of the concurrent measurement of lactate (blue), oxygen (purple) and local field potential (LFP) in the cortex of anaesthetized rats (AP: −4.0; ML: −2.5; DV: −1.5) during *status epilepticus* after 4-AP injection. High frequency component (grey) (1–20 Hz FFT band pass) of the amperometric recording and power spectrum analysis of the high component. Dotted red lines represent the baseline level. Reproduced from [338]. Creative Commons CC-BY. (E) Example of aptamer-modified nnopipette for dopamine detection. Characterization in artificial cerebrospinal fluid (aCSF): the schematic shows dopamine-specific aptamers covalently modified on the inner surface of nanopipettes with ~10 nm orifices, with sequential surface chemistry to tether thiolated dopamine aptamers to the quartz surface. Conformational changes of the dopamine aptamer upon target recognition alter the surface charge distribution within the nanoscale pore, altering the conductivity. The current–voltage (I–V) sweeps in aCSF demonstrate a decrease in current response upon dopamine detection (100 µM, 14.2 ± 4.9%) relative to the respective baseline measurement (I_o) in aCSF at 0.5 V. Reproduced from [339]. Creative Commons CC-BY.

5.1 | Amperometric and Voltammetric Detection

Amperometric and voltammetric biosensors represent the cornerstone technologies in electrochemical sensing, both fundamentally relying on the principle of redox reactions occurring at an electrode surface (Figure 4A). These electron transfer events are then transduced into measurable electrical currents, the magnitude and characteristics of which are directly indicative of the presence and concentration of the target analytes.

Amperometric sensors operate by applying a fixed potential to the working electrode, which is strategically chosen to facilitate either the oxidation or reduction of electroactive species present in the surrounding medium [124, 126, 242]. The resulting steady-state current, known as the faradaic current, is then measured. The magnitude of this current is directly proportional to the concentration of the electroactive analyte, assuming mass transport to the electrode surface is the rate-limiting step [316]. Amperometry is particularly prevalent in enzymatic biosensors where the enzyme catalyzes a reaction that yields an electroactive product, such as H_2O_2. For instance, in an amperometric dopamine sensor, a constant positive potential (e.g., +0.6 V vs. Ag/AgCl) is applied to the electrode, which oxidizes DA to dopamine-o-quinone, generating an electron flow that registers as a current signal directly proportional to the dopamine concentration [317, 318]. This technique offers excellent temporal resolution, limited primarily by the diffusion of the analyte to the electrode; this temporal resolution typically ranges from milliseconds to tens of milliseconds. This speed allows them to capture the transient spikes of neurotransmitter concentration that occur during exocytosis (the release of neurotransmitters from vesicles) at individual synapses or cells [319].

Voltammetric sensors, in contrast to amperometry's fixed potential, systematically vary the electrode potential over time while simultaneously measuring the resultant current [320]. This

dynamic approach yields significantly more detailed electrochemical information about the redox processes occurring at the electrode-solution interface, typically presented as a current-voltage (I-V) curve or voltammogram. This richer dataset confers superior selectivity, enabling the differentiation of multiple electroactive species even if they possess similar oxidation or reduction potentials. Prominent voltammetric techniques include cyclic voltammetry (CV), which sweeps the potential in both forward and reverse directions to probe reversible and irreversible redox reactions; square-wave voltammetry (SWV), which superimposes a square-wave potential on a staircase ramp, offering enhanced sensitivity by discriminating against non-faradaic currents; and differential pulse voltammetry (DPV), which applies small potential pulses superimposed on a linear potential ramp, providing improved signal-to-noise ratios and better peak resolution for qualitative and quantitative analysis. For in vivo neural interfaces, FSCV stands out as a widely adopted technique [74]. This employs very rapid potential sweeps across a defined range, allowing for millisecond-resolution tracking of transient neurotransmitter dynamics, which is crucial for capturing rapid release and reuptake events in synaptic clefts [74]. Microelectrodes, often fabricated from carbon fiber (5–10 μm diameter) or platinum wire, are commonly configured into thin-film arrays, ensuring minimally invasive implantation and facilitating precise spatial mapping of neurochemical activity across specific brain regions.

5.2 | Enzymatic Electrochemical Sensors

Enzymatic electrochemical biosensors ingeniously integrate specific biological recognition elements, most frequently oxidoreductase enzymes, that exhibit selectivity in reacting with target molecules [321] (Figure 4B). These enzyme-catalyzed reactions lead to the production of either electrons or electroactive by-products that are subsequently detected via an electrochemical transducer. The fundamental architecture of such a sensor typically comprises three interconnected components: (1) a precisely immobilized recognition enzyme layer that confers analyte specificity, (2) an electrochemical transducer (the electrode) that converts the biochemical event into an electrical signal, and (3) a signal processor that interprets and quantifies the electrical output.

Commonly employed enzymes for neural applications include: GOx, LOx, ChOx, acetylcholinesterase (AChE), GluOx. GOx and LOx are essential in glucose and lactate sensing, respectively [126, 129], catalyzing in particular the oxidation of glucose to gluconolactone, and the oxidation of lactate to pyruvate, both generating H_2O_2. The electrochemically active H_2O_2 is then quantified via oxidation at a fixed positive potential at the underlying electrode surface (e.g., using platinum or Prussian blue-modified electrodes). ChOx and AChE are utilized in a two-step cascade for ACh sensing and the detection of related metabolites like choline. GluOx is critical in glutamate biosensors, catalyzing the oxidation of glutamate to α-ketoglutarate and H_2O_2. These sensors are vital for monitoring excitotoxic levels of glutamate in models of neural injury (e.g., stroke, TBI) or disease, given glutamate's role as the primary excitatory neurotransmitter.

The effective immobilization techniques for these enzymes are paramount to preserving their catalytic activity and ensuring sensor stability. As discussed in Section 4.4, strategies include robust covalent bonding to functionalized electrode surfaces (e.g., via EDC/NHS coupling to surface amines or carboxyls), physical entrapment in biocompatible hydrogels (e.g., poly(2-hydroxyethyl methacrylate) or PEG diacrylate hydrogels) that provide a protective, permeable microenvironment, or crosslinking using bifunctional agents like glutaraldehyde that create a stable polymeric network. To further enhance performance, nanomaterials such as graphene, carbon nanotubes, or various metal nanoparticles (e.g., gold, platinum nanoparticles) are frequently incorporated into the enzyme immobilization matrix [322] (Figure 4C). These nanomaterials dramatically increase the active surface area for enzyme loading, facilitate more efficient electron transfer between the enzyme and the electrode, and can improve overall enzyme stability.

For neural interface applications, enzymatic electrochemical biosensors are often integrated onto microelectrode arrays or flexible polymeric substrates. This allows for their chronic implantation into specific deep brain regions, such as the striatum (for dopamine, glucose, lactate) or hippocampus (for glutamate, acetylcholine), enabling long-term, continuous monitoring of metabolic states or neurotransmitter fluctuations. Inherent challenges persist, including enzyme denaturation over time (due to temperature, pH changes, or proteases), biofouling (non-specific protein adsorption and cellular encapsulation that limits analyte diffusion), and oxygen dependence (as many oxidases require oxygen as a co-substrate), which collectively motivate ongoing research into alternative non-enzymatic strategies.

5.3 | Aptamer-Functionalized Electrodes

Aptamer-based electrochemical sensors represent an innovative non-enzymatic approach, employing synthetic single-stranded nucleic acids (DNA or RNA) or, less commonly, peptides, as molecular recognition elements [323, 324] (Figure 4D). These engineered aptamers are selected in vitro (e.g., via SELEX – Systematic Evolution of Ligands by Exponential Enrichment) to bind to target molecules with remarkable specificity and high affinity, akin to antibodies [325, 326]. A significant advantage of aptamers over enzymes is their inherent chemical stability (resisting denaturation by temperature, pH, or proteases), lower immunogenicity, and the ability to be selected de novo against a vastly broader range of targets, encompassing small molecules, peptides, proteins, and even whole cells, for which antibodies might be difficult to generate [327]. Unlike enzymes that degrade, aptamers are remarkably robust and can often be regenerated chemically (e.g., by changing pH or ionic strength to release the target) or electrochemically (e.g., by applying a potential pulse to induce conformational change and release), allowing for repeated measurements over extended periods without the need for sensor replacement [328, 329]. Their integration into implantable neural probes provides a highly promising non-enzymatic alternative, with lower susceptibility to biological degradation and potentially longer operational lifetimes in vivo.

The fundamental principle of apta-sensing relies on the target molecule's binding to the aptamer, which induces a specific

conformational change in the aptamer structure. This conformational change is then transduced into a measurable electrical signal by affecting the electrochemical properties of the electrode-interface. Several sophisticated detection schemes are employed.

(1) *Label-free detection via EIS*. In this configuration, the aptamer is directly immobilized onto the electrode surface. Upon target binding, the conformational change or the mass of the bound target alters the charge transfer resistance or capacitance at the electrode-solution interface, which is sensitively monitored by EIS. This method eliminates the need for bulky labels [91, 330, 331].

(2) *Redox-labeled aptamers (aptamer beacons)*. Here, a redox reporter molecule (e.g., methylene blue, ferrocene) is covalently attached to the aptamer [332–334]. In the unbound state, the aptamer is designed to keep the redox reporter close to the electrode, facilitating electron transfer and generating a clear signal. Upon target binding, the aptamer undergoes a conformational switch (e.g., forming a hairpin or loop), moving the redox reporter away from the electrode surface or impeding its electron transfer, thus modulating the observed redox peak current (Figure 4E).

Aptamer-functionalized sensors have demonstrated considerable success in detecting various neurochemical species relevant to neural interfaces, including neurotransmitters like dopamine and serotonin, key inflammatory cytokines such as IL-6 and TNF-α, and critical neurodegenerative disease biomarkers like Aβ peptides. When these aptamer layers are integrated with nanostructured electrode surfaces, such as gold nanodendrites, reduced graphene oxide (rGO) nanosheets, or carbon nanotubes, the greatly increased active surface area and enhanced electron transfer properties allow the sensitivity of these platforms to reach impressive sub-nanomolar to picomolar levels [335–337].

5.4 | Organic Electrochemical Transistors (OECTs)

Organic Electrochemical Transistors (OECTs) represent a profoundly powerful and rapidly advancing class of biosensing devices distinguished by their capacity for amplified electrical signals and their intrinsic compatibility with soft, flexible, and biocompatible substrates [51, 53, 340–342] (Figure 5A). Unlike conventional field-effect transistors (FETs) that rely primarily on electrostatic gating, OECTs operate through a unique mechanism that modulates the current flowing through an organic semiconductor channel (PEDOT:PSS) via ionic interactions with the surrounding electrolyte [343–346].

The working principle of an OECT involves three fundamental electrodes: a source, a drain, and a gate electrode. The organic semiconductor channel (e.g., PEDOT:PSS film) connects the source and drain. When a voltage is applied to the gate electrode, which is in direct contact with an ionic electrolyte (and typically with the organic channel), ions from the electrolyte are electrochemically driven into the bulk of the organic semiconductor channel [347, 348]. This volumetric ion ingress acts as a form of "volumetric doping", effectively modulating the concentration of charge carriers within the entire thickness of the organic channel. This mechanism results in a substantial and highly efficient modulation of the channel's electrical conductivity. This volumetric doping mechanism is the key differentiator from traditional inorganic FETs, leading to exceptionally high transconductance (the ratio of change in drain current to change in gate voltage) and, consequently, significant signal amplification, making OECTs sensitive transducers for subtle changes in the local ionic environment [349] (Figure 5B).

For biosensing applications, the critical step involves functionalizing the gate electrode with specific biomolecules, such as enzymes, antibodies, or aptamers, that are designed to selectively interact with the analyte of interest [350, 351]. The binding event between the functionalized gate and the target analyte (or an enzymatic reaction occurring at the gate) either directly alters the local ionic environment near the gate (e.g., by consuming or releasing ions, or altering local pH) or generates charged species. These localized biochemical changes, in turn, subtly modulate the gate potential effectively "gating" the transistor and thereby inducing a substantial change in the drain current flowing through the organic semiconductor channel. This provides an amplified readout of the biochemical event [352].

OECTs have demonstrated applicability in various neural interface scenarios. OECTs can effectively transduce the redox activity of dopamine at a functionalized gate electrode into significant and amplified modulation of the drain current, offering both high sensitivity and intrinsic signal amplification, crucial for detecting low-level fluctuations [353, 354] (Figure 5C).

Additionally, when the gate electrode is functionalized with LO_x, these enzyme-functionalized OECTs exhibit high selectivity for lactate and can operate continuously in physiologically relevant fluids like cerebrospinal fluid analogs, providing real-time metabolic insights [355]. With antibodies or aptamers specifically targeting inflammatory markers immobilized on their gates, OECTs are capable of detecting very low levels of cytokines (e.g., IL-6, TNF-α), which is critical for assessing neuroinflammatory responses post-implantation or in neurodegenerative conditions [356, 357].

The inherent advantages of OECTs for neural interfaces are compelling [53, 340, 341, 358]: they operate at low operating voltages (compatible with biological systems), exhibit biocompatibility (especially with PEDOT:PSS), possess excellent mechanical flexibility (allowing seamless integration with soft tissues), and are highly compatible with scalable additive manufacturing techniques such as inkjet printing and large-area processing. Their successful integration into conformable polymeric substrates like Parylene C, PDMS (polydimethylsiloxane), or even natural biopolymers like silk fibroin has paved the way for the fabrication of high-density, multi-analyte biosensing arrays [359–361].

However, their long-term stability in physiological environments and their susceptibility to signal drift stemming from ionic accumulation or non-specific adsorption within the organic channel pose ongoing engineering hurdles. To mitigate these limitations and enhance chronic in vivo performance, intensive research is focused on developing robust encapsulation strategies and implementing advanced gate passivation layers to protect the active

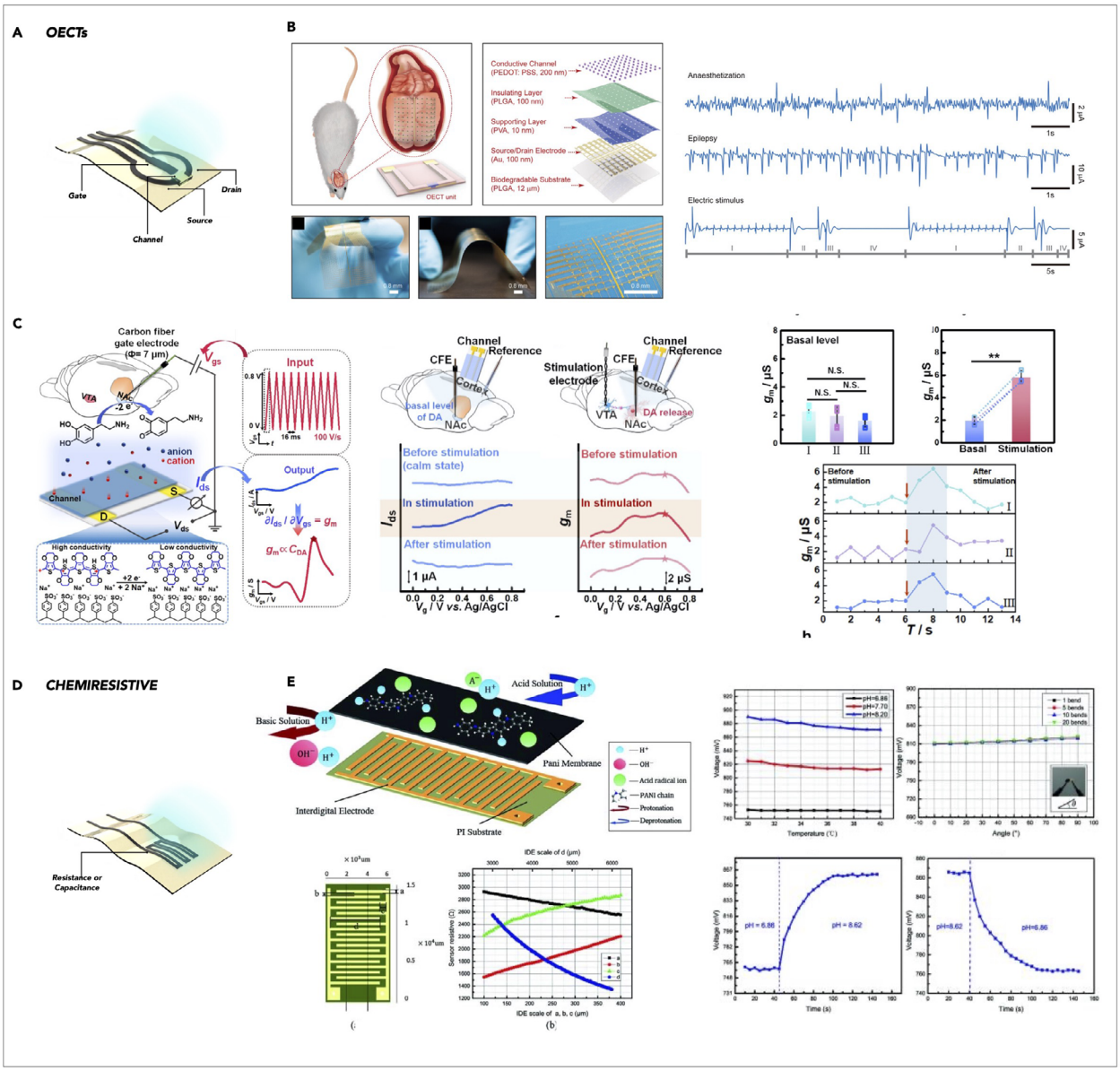

FIGURE 5 | Electrochemical neural biosensors (cont.): (A) OECTs, (D) chemiresistive. (B) Ultrathin, soft, high-throughput transient OECT array as a core platform for a high-fidelity brain-machine interface. The OECTs are placed on the cerebral cortex in the animal model for μ-ECoG signals recording (thickness of ≈15 μm, and weight of 99.3 mg). Characterization of μ-ECoG signals for three representative stimuli. Time-domain signals of rat a) in state of anaesthetization; b) during seizures; c) with electric stimulus at 1 Hz and 3 V. Reproduced from [341]. Creative Commons CC-BY. (C) Fast scanning potential-gated OECT for in vivo DA assay, constructed with a carbon fiber electrode and a PEDOT:PSS-modified channel. Typical transfer and g_m–V_{gs} curves of the OECT for DA assay are shown with g_m as an analytical parameter. Results of in vivo DA monitoring are shown. Reproduced with permission from [354]. Copyright 2022 John Wiley and Sons. (E) pH sensor consisting of a PANI membrane on interdigital electrodes (IDEs) supported by a PI substrate. The sensor relies on the transformation of PANI protonated in acid solution and deprotonated in basic solution. The initial resistance of the IDEs depends on the geometric parameters. The increasing sizes of the longitudinal (red line) and transverse (green line) spacing enhance the initial resistance, whereas both the grid width (black line) and the length (blue line) weaken the initial resistance. Flexibility and temperature experiments of the pH sensors. The dynamic response of the pH sensor for a step pH change shows a rising time from pH 6.86 to 8.62 and an inverse fall time from pH 8.62 to 6.86. Reproduce from [372]. Creative Commons CC-BY.

organic semiconductor channel from biological degradation and ionic interference [362–364].

5.5 | Chemiresistive Sensors

Chemiresistive sensors may be considered a subset of electrochemical sensors as they transduce a chemical event into a measurable change in the electrical resistance of a sensing material [365] (Figure 5D). These sensors typically consist of a conductive or semiconductive material whose electrical properties are highly sensitive to surface adsorption or chemical reactions [366]. The sensing element is usually a thin film, nanoparticle network, or nanowire of a metal oxide (e.g., ZnO, SnO_2 , WO_3) [367], carbon-based material (e.g., graphene, carbon nanotubes [368]), or conductive polymer (e.g., polyaniline). When a target analyte

(e.g., a gaseous molecule, a charged ion, or a binding protein) interacts with the sensor surface, it induces a change in the charge carrier concentration, mobility, or band structure of the sensing material [369]. For instance, the adsorption of reducing gases can donate electrons to an n-type metal oxide semiconductor, increasing its conductivity (decreasing resistance), while oxidizing gases would decrease its conductivity [370, 371]. In liquid-phase neurochemical sensing, the interaction of charged analytes or enzymatic reaction products with the surface of a chemiresistive material can cause a localized change in surface potential, altering the resistance or capacitance (Figure 5E). These sensors are not the preferred choice for implantable applications: the primary challenges are often low selectivity (as many molecules can alter resistance non-specifically) and susceptibility to environmental factors like humidity and temperature, requiring careful design and compensation strategies for in vivo use.

6 | Optical Biosensors

Optical biosensors, harnessing the intricate interactions of light with biological matter, have emerged as indispensable tools for probing biochemical changes within living systems, particularly within the central and peripheral nervous systems [390–393]. These devices translate specific optical phenomena, such as fluorescence emission, light absorption, or refractive index shifts, into quantifiable signals indicative of the presence and concentration of target analytes (see Table 5). Their non-invasive or minimally invasive nature, coupled with high sensitivity, spatial resolution, and the potential for real-time monitoring, renders them exceptionally well-suited for advanced neural interface applications.

6.1 | Colorimetric Sensors

The simplest class of optical biosensors includes colorimetric sensors, which rely on a measurable and often visible change in color or light absorbance/transmittance in response to the presence and concentration of a target analyte [394]. The transduction mechanism hinges on a specific chemical or biochemical reaction that produces a colored product, consumes a colored reagent, or induces a shift in the absorption spectrum of an indicator molecule. In neurochemical sensing, colorimetric assays are commonly deployed on miniaturized analytical platforms, such as paper-based devices, microfluidic chips, or lateral flow assays, enabling point-of-care diagnostics with minimal instrumentation and sample volume [395–398]. These formats are particularly well-suited for low-resource settings and can achieve multiplexing through spatial separation of reagents or barcode-based visual encoding.

A widely used example is the enzyme-mediated colorimetric assay for detecting glucose or lactate, where enzymes such as glucose oxidase or lactate oxidase catalyze the oxidation of their respective substrates, producing H_2O_2 as a byproduct. This peroxide subsequently reacts with chromogenic substrates like 3,3′,5,5′-tetramethylbenzidine (TMB) or o-dianisidine in the presence of horseradish peroxidase (HRP), yielding a colored compound whose absorbance intensity is proportional to analyte concentration [399]. Emerging designs incorporate nanomaterials such as gold nanoparticles (AuNPs) [400], carbon dots [401], or metal-organic frameworks (MOFs) [402] that exhibit peroxidase-mimicking activity or that act as colorimetric enhancers through aggregation-induced optical changes, thereby improving the sensitivity and dynamic range of detection.

Colorimetric biosensors have also been developed for neurotransmitters like dopamine and serotonin, utilizing reactions with quinone derivatives, polydopamine films, or functionalized nanoparticle substrates that produce visible signals upon analyte binding. Integration with smartphone-based imaging systems has further advanced their utility, enabling real-time quantification with image-processing apps. Despite their inherent simplicity and portability, limitations persist, including lower sensitivity compared to fluorescence or electrochemical techniques, interference from colored biological fluids, and challenges in in vivo deployment due to reagent instability and background signal. Nevertheless, their low cost, rapid readout, and ease of miniaturization make colorimetric sensors ideal for preliminary screening, clinical validation, and complementary use in multimodal neurochemical sensing platforms.

6.2 | Fluorescence-Based Sensors

Fluorescence-based biosensors leverage the intrinsic or engineered ability of certain molecules, known as fluorophores, to absorb light at a specific excitation wavelength and subsequently re-emit light at a longer, characteristic emission wavelength [48, 403] (Figure 6A). The transduction principle hinges on how the interaction between the fluorophore and the analyte of interest alters this fluorescence signature, manifesting as changes in fluorescence intensity, lifetime, or a spectral shift in either the excitation or emission spectrum. This optical readout provides a highly sensitive and often spatially resolved means of detecting biochemical events.

For neurotransmitter detection, a significant leap has been made with the development of genetically encoded fluorescent indicators (GEFIs) [404]. These sophisticated biosensors are chimeric proteins, typically incorporating a fluorescent protein (like GFP or its derivatives) fused to a ligand-binding domain or a transmembrane receptor. When the specific neurotransmitter (e.g., dopamine, serotonin, acetylcholine, glutamate) binds to its engineered recognition domain, it induces a conformational change in the GEFI, which in turn alters the fluorescence properties of the attached fluorophore (Figure 6B). Examples include the GRAB (GPCR-Activation-Based) sensor family, which utilizes G protein-coupled receptors to detect a wide array of neurotransmitters with high specificity and millisecond kinetics [405, 406]. These GEFIs are expressed directly within neurons or glial cells using viral vectors, allowing for real-time, in vivo visualization of neurotransmitter release and dynamics in specific neural circuits, often in conjunction with optogenetics for precise control of neuronal activity [407]. Their application extends to understanding synaptic plasticity, reward pathways, and the pathophysiology of neurological disorders.

Similarly, for ion detection, fluorescent ion indicators are widely employed. These are small-molecule fluorophores designed to

TABLE 5 | Examples of optical biosensors for neurotransmitters, biomarkers and small molecules.

Category/Description	Target analyte	Platform/Materials	Sensitivity/Limit of detection	Application stage	Refs.
Fluorescence-based					
A small fiber-optic probe with quantum dots (QDs) on the tip; Dopamine quenches QD fluorescence. Integrated microspectrometer and wireless module.	Dopamine	Optical fiber tip coated with CdSe/ZnS quantum dots	LoD ~ 100 nM High selectivity to ascorbic acid (90:1) and uric acid (36:1)	In vivo (brain)	[479]
Proof-of-concept "brain-on-chip" integrating CRANAD-2 fluorescence to detect Aβ fibrils. Demonstrated linear fluorescence response to Aβ and reduced sample volumes	Amyloid-β	Microfluidic channel with fluorescent probe (CRANAD-2)	n/a	In vitro (on chip)	[480]
Array of fiber-optic probes each with a different fluorescent sensing film. Allows simultaneous real-time monitoring of pH, dissolved oxygen, glucose, and temperature in brain tissue	pH, O_2, glucose, temp.	Array of optical fibers with sol–gel fluorescent coatings	n/a	In vivo (brain ex vivo)	[393]
Fiber tip coated with a hydrogel containing pH-sensitive fluorescent microspheres. Implanted in mouse brain; fluorescence ratio readout tracks pH with ~0.0014 unit resolution, detecting pH drops during ischemia and seizures	pH (brain)	Silica multimode fiber + hydrogel + pH-sensitive fluorescent beads	~0.0014 unit resolution	In vivo (mouse)	[481]
SPR- and LSPR-based					
Dopamine is captured by a thin-film of chitosan doped with graphene quantum dots on the Au surface	Dopamine	Gold SPR chip with chitosan/graphene-QDs multilayer	LoD sub-fM	In vitro (sensor)	[482]
Aptamer-functionalized gold nanostructures on chip (LSPR) bind dopamine, causing refractive-index shifts. Enables ultra-sensitive dopamine sensing in whole blood (real-time plasmonic readout)	Dopamine	Microfluidic chip with plasmonic nanostructures functionalized with DA aptamer	n/a	In vitro (blood)	[457]
Plasmonic fiber grating (Au-coated, graphene-enhanced) functionalized with a Dopamine aptamer. Aptamer folding on Dopamine binding shifts the grating resonance (LSPR).	Dopamine	Etched fiber Bragg grating + Au/graphene film + Dopamine aptamer	LoD 10^{-13} M	In vitro (serum)	[483]

(Continues)

TABLE 5 | (Continued)

Category/Description	Target analyte	Platform/Materials	Sensitivity/Limit of detection	Application stage	Refs.
Raman and SERS-based					
Ag+4-MPBA film for dopamine	Dopamine	Ag nanostructured film (one-step sputtered) functionalized with 4-mercaptophenylboronic acid	Linear 1 pM–100 nM (LoD ≈1 pM)	In vitro (serum)	[484]
Liquid SERS assay (PSALM) with Fe^{3+}-bridged Au nanoparticles	Neurotransmitters (e.g. dopamine)	Gold nanoparticles + Fe^{3+} ions in solution (SERS hotspots)	LoD below physiological urine levels	In vitro (urine)	[485]
3D-printed hydrogel-integrated SERS device (PEGDA/SA)	Dopamine	3D-printed device with PEGDA/SA hydrogel and plasmonic SERS substrate	LoD = 1 nM	In vitro (blood)	[486]
Nanoparticle cluster SERS with cucurbit[7] host–guest assembly	Dopamine, serotonin, epinephrine	Au nanoparticle colloids + cucurbit[7] for uniform gaps	LoD ~10^{-9} M (1 nM)	In vitro (urine)	[487]
Colorimetric					
Dopamine oxidizes $FeCl_3$ to Fe^{2+}, which reacts with 1,10-phenanthroline to form a red complex. The color change on paper strips is read by camera.	Dopamine	Wax-printed paper microchannels, Fe^{3+}/phenanthroline reagents	LoD ~0.37 μM	In vitro (serum)	[395]
Photonic crystal					
Graphene–Si microring resonator.	Dopamine	CMOS-compatible silicon microring with patterned CVD graphene overlay	Detects <10 μM (Δresonance)	In vitro	[488]
Interferometric					
Microfiber MZI with SiO_2 spheres	Serotonin	Tapered silica optical fiber interferometer decorated with mesoporous SiO_2 nanospheres	LoD 84 fM (linear 0.1 pM–1 μM)	In vitro	[489]

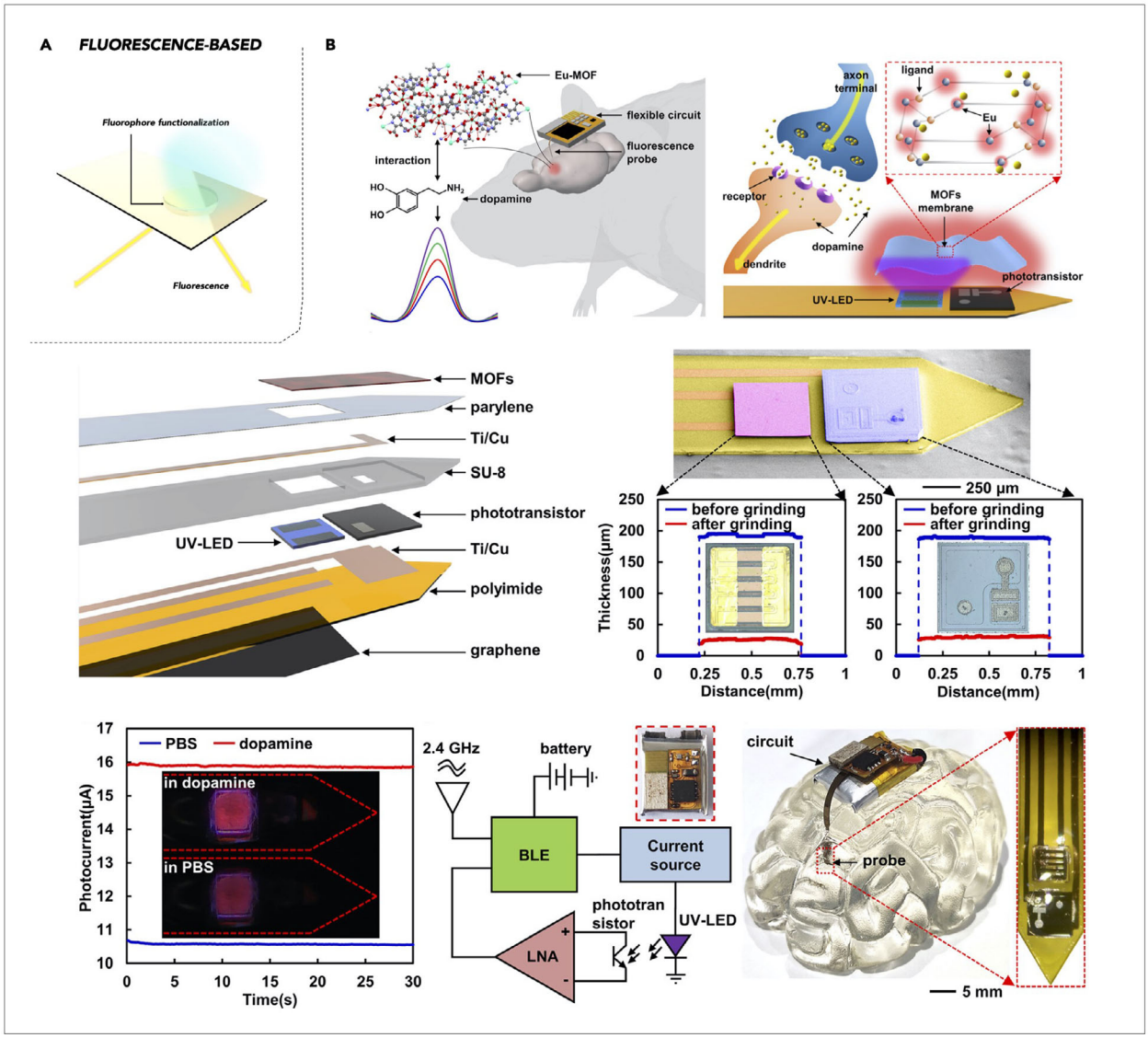

FIGURE 6 | Optical biosensors: (A) fluorescence-based. (B) Implantable fluorescence probe for deep brain dopamine sensing. A fluorescent MOF film that specifically binds dopamine was modified onto the probe, which simultaneously excited the fluorescence and detected the fluorescence intensity. The multilayer structure of the probe contains a UV-LED as a light source and a phototransistor for fluorescence detection. Photocurrent response of the fluorescence probe is reported in PBS and high-concentration dopamine solution, respectively. A brain phantom was implanted with a flexible fluorescence probe and a flexible wireless circuit. Reprinted with permission from [429]. Copyright 2024, American Chemical Society.

exhibit a change in their fluorescence properties upon binding to specific ions. For instance, Fura-2 and Fluo-4 are popular indicators for intracellular calcium (Ca^{2+}), where Ca^{2+} binding alters their quantum yield or excitation/emission spectra, allowing for ratiometric or intensity-based measurements of intracellular calcium transients, which are fundamental to neuronal excitability and signaling [408–411]. Similarly, SBFI is used for sodium (Na^{+}) detection [412, 413] and PBFI for potassium (K^{+}) [414–416], providing insights into ion homeostasis and dysregulation during conditions like ischemic stress or spreading depression. These indicators enable real-time monitoring of ion flux, crucial for understanding neuronal activity, synaptic transmission, and pathological events like excitotoxicity.

The advantages of fluorescence-based sensors are compelling: they offer high sensitivity, enabling the detection of low analyte concentrations; provide excellent spatial resolution when coupled with advanced microscopy techniques (e.g., confocal, two-photon microscopy), allowing for visualization of molecular events at the sub-cellular level; and facilitate real-time imaging of dynamic processes. However, inherent limitations exist, including photobleaching (irreversible degradation of the fluorophore upon prolonged light exposure), phototoxicity (cellular damage induced by light and reactive oxygen species), and the fundamental need for an external light source and detector, which can be bulky for in vivo applications [417]. Furthermore, light scattering and absorption by biological tissues significantly limit the depth of penetration, restricting direct in vivo imaging to superficial brain regions. To circumvent depth limitations, integration with optical fibers (e.g., fiber photometry) allows for light delivery and collection from deeper brain structures, albeit with a loss of spatial resolution compared to direct microscopy [418–422]. Recent advances suggest as well potential pathways for extending optical sensing beyond superficial tissue layers. The

use of near-infrared fluorophores operating in the NIR-I (700–900 nm) and NIR-II (1000–1700 nm) windows reduces scattering and hemoglobin absorption, enabling improved signal penetration and signal-to-background ratios at depth [423]. Complementary approaches such as time-gated and fluorescence lifetime-based detection can further suppress tissue autofluorescence and enhance contrast in highly scattering environments [424, 425]. In parallel, computational scattering-correction techniques, including model-based light transport inversion and data-driven reconstruction, have been explored to partially recover spatial and temporal information from distorted fluorescence signals. While these strategies show promise in acute or experimental settings, their application to chronic implants introduces additional challenges. Fluorophore photostability, long-term toxicity, and potential immune responses remain concerns for extended implantation, particularly in neural tissue [426]. Time-resolved detection schemes increase system complexity, power consumption, and integration demands, while computational correction methods are sensitive to motion artifacts, tissue heterogeneity, and gradual biological remodeling over time [427, 428]. As such, these emerging approaches should be viewed as enabling technologies rather than fully mature solutions, and their successful translation to chronic deep-brain fluorescence sensing will likely require coordinated advances in fluorophore chemistry, low-power optoelectronics, and long-term in vivo validation.

6.3 | SPR and Plasmonic Sensors

Plasmonic biosensors have emerged as exceptionally powerful tools for the detection of biomolecules, distinguished by their label-free, highly sensitive, and real-time detection capabilities [430–432]. These biosensors ingeniously leverage the intricate interaction of light with free electrons within engineered metallic nanostructures. This interaction, upon biomolecular binding, translates into detectable changes in the local refractive index, providing a direct and quantifiable readout of the binding event. The successful implementation of plasmonic biosensors in thin-film formats has been pivotal, enabling their seamless integration into flexible and implantable devices that are ideally suited for chronic neural interface applications.

6.3.1 | SPR Principles

SPR is a captivating optical phenomenon that occurs when p-polarized (transverse magnetic, TM) light, incident at a specific angle, strikes a thin metallic film (typically gold or silver) at a metal-dielectric interface (Figure 7A). At this precise angle, the incident light's evanescent field resonantly couples with and excites surface plasmons, coherent, collective oscillations of the free electrons (plasmons) at the metal surface [433]. This resonance condition is sensitive to the refractive index of the dielectric medium immediately adjacent to the metal surface. Consequently, when biomolecules bind to the functionalized surface of the metal film, they induce a minute change in the local refractive index within the evanescent field region (typically extending ~200-300 nm from the surface). This shift in refractive index perturbs the resonance condition, altering the precise angle or wavelength at which the resonance occurs, which is then optically detected. Modern SPR sensors employ various interrogation schemes, including angular interrogation (scanning the incident angle at a fixed wavelength and detecting the minimum reflected intensity) [434], wavelength modulation (scanning the incident wavelength at a fixed angle and detecting the minimum reflected intensity) [435], or intensity detection (monitoring changes in reflected light intensity at a fixed angle and wavelength) [436].

Key parameters that influence the performance of an SPR sensor include: the thickness of the metal film (typically 40–60 nm for gold, optimized for maximum resonance dip); the surface roughness of the metal film (which can scatter plasmons and broaden the resonance); the polarization of the incident light (only p-polarized light can efficiently excite surface plasmons); and the prism coupling configuration, most commonly the Kretschmann-Raether geometry, which facilitates efficient excitation of surface plasmons by matching the momentum of the incident light with that of the surface plasmons. SPR has found widespread application in the label-free detection and kinetic analysis of a vast array of biomolecules, including proteins, nucleic acids, and small molecules. For the specific detection of neurotransmitters and disease biomarkers relevant to neural interfaces, the sensor surface is functionalized with highly specific biorecognition elements such as antibodies, aptamers, or molecularly imprinted polymers (MIPs) designed to selectively capture the target analyte [437–440].

6.3.2 | Localized Surface Plasmon Resonance (LSPR) and Nanostructures

In contrast to the propagating surface plasmons on planar interfaces characteristic of conventional SPR, Localized Surface Plasmon Resonance (LSPR) occurs when incident light interacts with metallic nanoparticles or specifically engineered nanostructures (e.g., nanorods, nanodisks, nanoholes) whose dimensions are smaller than the wavelength of light [441] (Figure 7A). In this scenario, the resonant oscillation of conduction electrons is confined to the nanoparticle scale, leading to non-propagating plasmonic modes localized at the nanoparticle surfaces.

LSPR sensors exhibit several distinct advantages [442–445]: they create strong field enhancement (often referred to as "hotspots") immediately adjacent to the nanoparticle surface, which significantly amplifies the local electromagnetic field; they display sharp and tunable resonance peaks typically in the UV-visible to near-infrared (NIR) range, whose position is highly sensitive to the nanoparticle's material, size, shape, and surrounding dielectric environment; and they possess high sensitivity to the local refractive index within a very confined region (typically within ~10–30 nm from the nanoparticle surface), making them ideal for detecting molecular binding events.

These plasmonic nanostructures can be precisely fabricated using either "top-down" (EBL, nanoimprint lithography) or "bottom-up" (colloidal synthesis, self-assembly) approaches. Regardless of the fabrication method, the specific geometries (e.g., aspect ratio of nanorods, diameter of nanodisks), material compositions (e.g., gold, silver, copper), and subsequent surface functional-

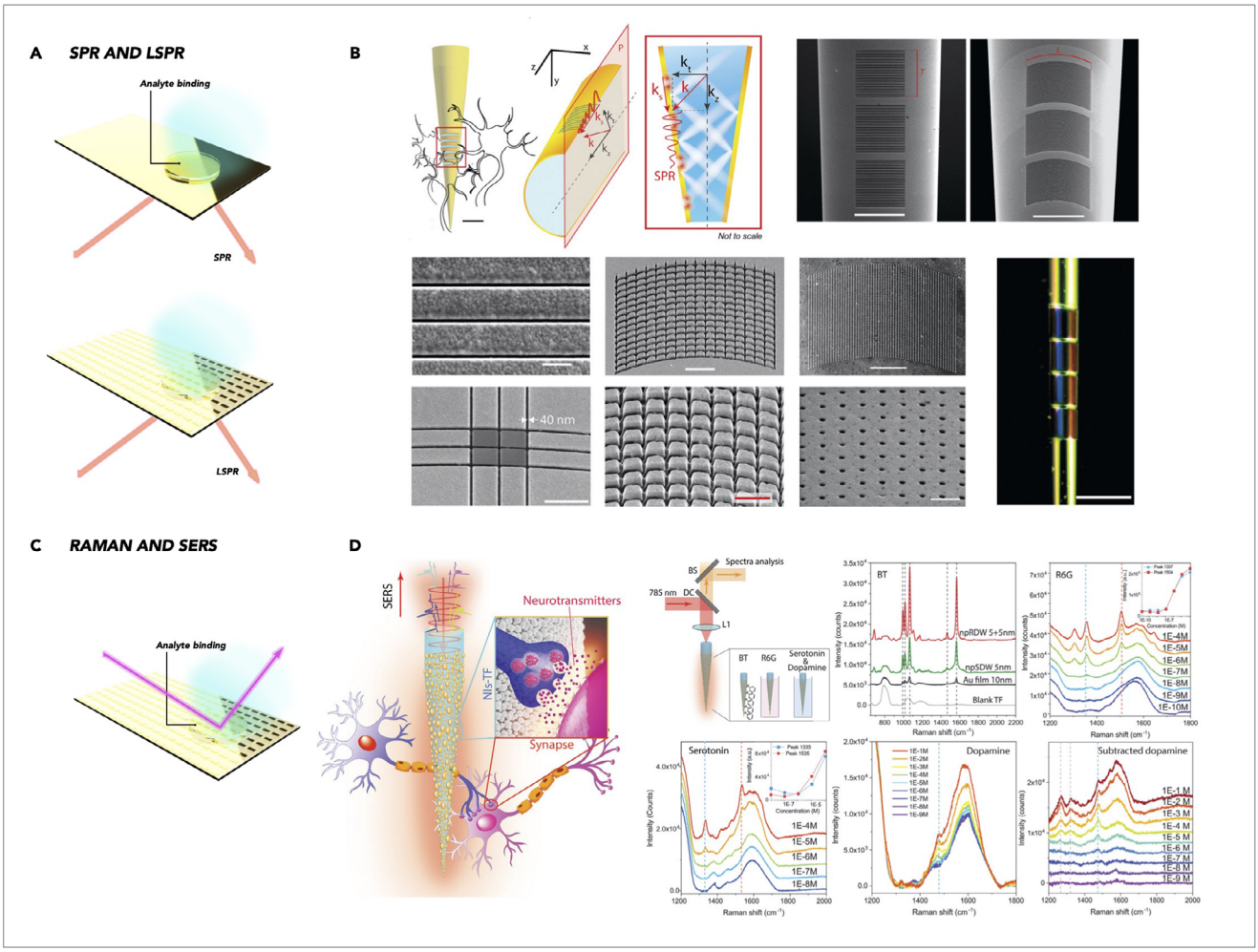

FIGURE 7 | Optical biosensors (cont.): (A) SPR and LSPR, (C) Raman and SERS. (B) Metal-coated tapered optical fiber hosting a plasmonic nanostructure with footprint comparable to the soma of a single neuron (the scale bar is 25 μm). When broadband light guided in the taper illuminates the nanograting, the superficial component k_s of the guided light couples with the grating periodicity. An SPR is then generated at the dielectric-metal interface. Close-ups of different nanostructures milled on the fiber are shown: (left) minimum feature size of 40 nm for a curved (top) and crossing curved lines on the taper surface; top left and bottom left scale bars are 1 μm. Middle: a 2D curved array of nanoplatelets (top) and a zoom on the nanoplatelets (bottom); top middle and bottom middle scale bars are 1 μm. Right: a curved array of nanoholes (top, inverted grayscale) and a close-up on 100 nm diameter nanoholes on the fiber's surface; top right scale bar is 2 μm, bottom right scale bar is 2 μm. Reprinted with permission from [62]. Copyright 2021. John Wiley and Sons. (D) Tapered optical fibers decorated with gold nanoislands by nonplanar repeated dewetting, for neurotransmitters' SERS signal detection. The probes were functionalized with BT molecule, R6G, and soaked in neurotransmitters (dopamine and serotonin) aqueous solutions. SERS response of BT molecule functionalized repeadet-dewetting (red curve), single-dewetting (green curve), 10 nm gold film coated (black curve), and blank (gray curve) TFs, the dashed vertical lines indicate the molecular signature peaks at 992, 1015, 1065, 1465, and 1567 cm^{-1}. Detection of R6G, serotonin, and dopamine aqueous solutions is reported with concentrations varying from 10^{-10} to 10^{-4} M, from 10^{-8} to 10^{-4} M, and from 10^{-9} to 10^{-1} M, respectively. Reprinted with permission from [432]. Copyright 2022, John Wiley and Sons.

ization strategies critically determine the LSPR sensor's overall sensing performance. Key configurations include gold nanorods [446], whose LSPR peaks are highly dependent on their aspect ratio, allowing for tunable resonances; nanohole arrays in thin metal films [447], which exhibit extraordinary optical transmission phenomena highly sensitive to surface modifications; and nanosphere lithography-based arrays, which provide a scalable way to create ordered arrays of plasmonic nanoparticles [448]. LSPR biosensors are particularly well-suited for integration into flexible and implantable devices due to their miniaturized format, compatibility with low-temperature fabrication processes, and inherent potential for multiplexed readout on a single platform. Crucially, they offer real-time monitoring without the need for fluorescent or radioactive labels, simplifying assays and reducing potential phototoxicity.

6.3.3 | Label-Free Optical Detection of Neurotransmitters and Biomarkers

Plasmonic thin-film biosensors are exceptionally effective for detecting a wide array of neurochemical targets without the necessity of additional labeling agents [432, 449]. This label-free nature is a significant advantage, as it simplifies the assay protocol, reduces processing time, and, importantly, preserves the

native biological activity and conformation of the analyte, leading to more accurate measurements.

For the detection of neurotransmitters, plasmonic sensors have been functionalized with various biorecognition elements [301]. For dopamine, this includes highly specific dopamine-binding aptamers or even conductive polymer layers like polyaniline, which can undergo redox changes upon dopamine interaction that subtly alter the local refractive index [450]. Serotonin can be detected using anti-serotonin antibodies or molecularly imprinted polymers (MIPs) engineered to selectively bind serotonin [451]. For glutamate and acetylcholine, which are not directly electroactive for plasmonic detection, sensors typically integrate enzymatic coatings (e.g., glutamate oxidase for glutamate, or acetylcholinesterase/choline oxidase for acetylcholine). The enzymatic reactions produce by-products (like H_2O_2) or consume oxygen, leading to localized changes in refractive index or pH that can be detected as a shift in the plasmonic resonance. The label-free detection extends to various small molecules crucial for metabolic monitoring. Glucose and lactate sensing involves the integration of their respective enzyme layers (glucose oxidase, lactate oxidase) with plasmonic nanostructures.

Beyond neurotransmitters and small molecules, plasmonic biosensors are highly capable of detecting a range of biomarkers associated with neurological disorders. For cytokines such as IL-6 and TNF-α, SPR chips functionalized with specific antibodies enable highly sensitive detection down to sub-nanomolar concentrations, providing crucial insights into neuroinflammatory processes [452]. Similarly, for key neurodegenerative hallmarks like Aβ peptides and Tau proteins, peptide- or antibody-modified gold nanostructures are employed. The binding of these proteins to the functionalized surface induces a detectable refractive index change, offering a promising avenue for early Alzheimer's disease diagnosis and monitoring.

6.3.4 | Integration With Flexible and Implantable Substrates

The successful integration of plasmonic biosensors with flexible, stretchable, and ultimately implantable substrates is not merely an engineering convenience but an absolute necessity for developing devices that can conform intimately to and mechanically interact harmoniously with soft, curvilinear biological tissues, such as the brain parenchyma, peripheral nerves, or the spinal cord, minimizing mechanical mismatch and chronic inflammation.

The selection of appropriate substrate materials is paramount: the most ideal candidates are polydimethylsiloxane (PDMS) (excellent biocompatibility, inherent mechanical flexibility, optical transparency), Parylene-C (conformality, transparency, biocompatibility, ability to be deposited as very thin, pinhole-free layers), polyimide (PI) (thermal stability, mechanical flexibility). Various fabrication approaches are employed to achieve this integration. Transfer printing is a versatile technique where prefabricated plasmonic nanostructures (e.g., gold nanoparticles, nanohole arrays) are precisely transferred from a rigid growth substrate onto a soft, flexible polymeric substrate [453, 454]. In situ nanoparticle growth directly on flexible surfaces allows for direct fabrication without transfer steps [455]. Furthermore, nanopatterning via soft lithography techniques, such as nanoimprint lithography or microcontact printing, enables the direct patterning of plasmonic features onto flexible substrates at low temperatures. Mechanical considerations are critical for long-term in vivo performance. Designing devices with thin films minimizes bending strain and mechanical stress on the delicate surrounding tissues. The use of serpentine or kirigami-inspired patterns in the interconnects and active areas significantly enhances the overall stretchability and conformability of the device, accommodating tissue movements without fracturing. Moreover, effective encapsulation with permeable but protective layers (e.g., thin films of parylene, or even biocompatible biopolymers like silk fibroin) is essential to shield the active plasmonic elements from the harsh biofluid environment while allowing analyte diffusion [274, 282, 456].

Implantable plasmonic devices have already demonstrated compelling in vivo functionality. Examples include real-time dopamine detection in the striatum of freely moving rats, providing dynamic insights into neurochemical signaling [447, 457]; the continuous monitoring of IL-6 levels in cerebrospinal fluid, offering a window into neuroinflammatory processes [458]; and the successful implementation of multiplexed biomarker detection using flexible SPR arrays in small animal models [459], showcasing the potential for comprehensive neurochemical profiling. By combining these advanced sensing capabilities with emerging wireless readout technologies (e.g., miniaturized smartphone-based detectors, integrated photodiodes for direct signal conversion), plasmonic thin-film biosensors are poised to revolutionize neurological diagnostics and research, serving as intelligent, continuous implants for monitoring complex biochemical dynamics within the nervous system.

An advantageous combination is the coupling of optical fibers with plasmonic nanostructures, which have emerged as powerful tools for biosensing and photometry in the brain, offering highly sensitive, minimally invasive methods for probing neural activity and biochemical dynamics [460–462]. These hybrid systems exploit the unique light-guiding properties of optical fibers and the LSPR effects of metallic nanostructures, such as gold or silver nanoparticles, which dramatically enhance the detection of molecular interactions (Figure 7B). When integrated into brain tissue, the optical fibers serve as conduits for delivering light and collecting signals, while the plasmonic components amplify the optical responses of biomolecular binding events, enabling real-time monitoring of neurochemical fluctuations at picomolar concentrations [62, 432]. This is particularly valuable for detecting neurotransmitters, peptides, or other biomarkers associated with neurological function and disease. In photometry, the same configuration allows for precise measurement of fluorescence or optogenetic signals deep within brain regions, facilitating the correlation of neuronal activity with behavioral states or drug interventions [418, 422]. When combined with neuropharmacology, these platforms offer a transformative approach to studying drug effects on neural circuits with unprecedented spatial and temporal resolution [463]. For instance, the dynamic monitoring of dopamine release in response to pharmacological agents can be achieved with high fidelity, informing both basic neuroscience and therapeutic development. Moreover, the integration of func-

tionalized plasmonic surfaces with targeted ligands permits selective detection of specific analytes, expanding the capability to simultaneously study multiple neurochemical pathways. The versatility of this technology also supports closed-loop systems, where biosensing data can guide on-demand drug delivery via microfluidic channels or light-activated release mechanisms.

6.4 | Raman and Surface-Enhanced Raman Spectroscopy (SERS) Biosensors

Raman spectroscopy is a powerful analytical technique based on the inelastic scattering of monochromatic light (typically from a laser) by molecules [464–466]. When photons interact with a molecule, most are elastically scattered (Rayleigh scattering), but a small fraction undergoes inelastic scattering, losing or gaining energy. This energy shift corresponds to the vibrational, rotational, and other low-frequency modes of the molecule, producing a unique "fingerprint" spectrum characteristic of its chemical structure. This molecular fingerprint provides highly specific chemical information, enabling the identification and quantification of analytes without the need for labels. However, the inherent weakness of the normal Raman scattering signal (typically 10^{-6} to 10^{-8} of the incident light intensity) severely limits its applicability for detecting low-concentration analytes in complex biological matrices [467]. This limitation has been dramatically overcome by the advent of Surface-Enhanced Raman Spectroscopy (SERS) [468] (Figure 7C). SERS leverages the unique optical properties of plasmonic nanostructures (typically noble metals like gold or silver) to enormously amplify the Raman signal, often by factors ranging from 10^6 to an astounding 10^{14} or even higher. This extraordinary enhancement allows for the detection of molecules at ultra-low concentrations, down to single-molecule levels in some cases.

The SERS mechanism is primarily attributed to two synergistic effects [469]. The first and dominant mechanism is the electromagnetic (EM) enhancement, arising from the excitation of localized surface plasmons (LSPs) on the metallic nanostructures when illuminated by the incident laser. These LSPs create highly confined and intensely amplified electromagnetic fields (the "hotspots") at the nanostructure surface. Molecules adsorbed within these hotspots experience a vastly enhanced incident field and a similarly enhanced scattered field, leading to a multiplicative increase in the Raman signal. A secondary mechanism is the chemical (CM) enhancement, which involves charge transfer interactions between the adsorbed molecule and the metal surface. This can alter the polarizability of the molecule, further contributing to the Raman signal enhancement.

SERS biosensors for neural sensing are advantageous [470–472]: they are label-free, simplifying assay development and avoiding potential perturbations to biological systems; they offer highly specific molecular fingerprinting, allowing for unambiguous identification of analytes even in complex mixtures; they enable multiplexing by detecting multiple analytes simultaneously based on their distinct Raman spectra; and they exhibit minimal interference from water, which is a strong absorber in other optical techniques but a weak Raman scatterer, making them ideal for aqueous biological samples.

On the other hand, implementing in vivo SERS for neural applications presents unique challenges, primarily related to light scattering and absorption by biological tissues, which limit penetration depth, and potential photothermal effects at high laser powers. Strategies to overcome these include using near-infrared (NIR) excitation lasers, which penetrate tissue more deeply [473]; developing miniaturized fiber optic SERS probes for targeted delivery and collection of light from deep brain regions [432] (Figure 7D); and fabricating biocompatible SERS substrates that minimize foreign body response and maintain long-term stability in vivo.

The reproducibility of SERS substrate fabrication remains a significant engineering challenge, as the enhancement factor is highly dependent on the precise morphology and arrangement of the plasmonic nanostructures. Achieving consistent and uniform "hotspots" across large areas is difficult. Furthermore, quantitative analysis with SERS can be challenging due to variations in enhancement factors and molecular orientation on the surface. Finally, while NIR lasers reduce photothermal effects, careful control of laser power is still necessary to prevent photothermal damage to delicate neural tissues during prolonged in vivo measurements.

6.5 | Photonic Crystal and Interferometric Biosensors

Photonic crystal (PhC) biosensors and interferometric biosensors represent advanced optical sensing modalities that exploit light's interaction with nanostructured materials or precisely controlled optical paths. These label-free techniques offer high sensitivity to changes in the refractive index of the surrounding medium, making them powerful for detecting biomolecular binding events.

PhC are periodic dielectric nanostructures that control the flow of light in a similar way that semiconductors control the flow of electrons. They possess a "photonic bandgap," a range of frequencies that cannot propagate through the crystal. Defects or cavities introduced into this periodic structure can localize light at specific wavelengths within the bandgap, creating highly sensitive resonant modes [474, 475]. For biosensing, the surface of a PhC structure (e.g., a 1D grating, a 2D slab with a periodic array of holes) is functionalized with a biorecognition element [476]. When a target analyte binds to the surface, it causes a change in the local refractive index within the evanescent field of the localized light mode. This minute refractive index change leads to a measurable shift in the resonance wavelength or the intensity of the light transmitted or reflected by the photonic crystal. The sharp resonance peaks associated with PhCs allow for extremely precise detection of these wavelength shifts, translating into very high sensitivity for biomolecular binding, often in the picomolar to femtomolar range.

Interferometric biosensors operate on the principle of optical interference, where a phase difference is introduced between two coherent light beams (or two parts of the same beam) due to an interaction with the analyte, leading to a measurable change in interference pattern or intensity [477]. Common configurations include Mach–Zehnder interferometers, Young's interferometers,

and surface grating couplers [478]. In a typical Mach-Zehnder interferometer, light is split into two paths: a sensing arm and a reference arm. The surface of the sensing arm is functionalized with a biorecognition layer. When the target analyte binds to the sensing arm, it causes a localized change in the effective refractive index of the waveguide or optical path. This change introduces a phase shift in the light propagating through the sensing arm relative to the reference arm, resulting in a detectable change in the interference pattern observed at the detector. Interferometric sensors offer high sensitivity, as phase changes can be measured with very high precision. Like PhCs, they are label-free, compact, and compatible with integrated photonics, allowing for multiplexing and miniaturization suitable for implantable devices. Both PhC and interferometric biosensors are being explored for detecting neurotransmitters, proteins, and DNA biomarkers in neural fluids, offering promising avenues for high-performance, integrated optical neurochemical sensing.

7 | Ultrasound-Assisted and Acoustic Biosensors

The application of ultrasound in biomedical engineering has evolved beyond imaging and therapeutic interventions, establishing itself as a compelling strategy for powering and enhancing implantable biosensing platforms [490–493]. Within the landscape of neural interfaces, ultrasound-assisted and acoustic biosensors offer a promising avenue for non-invasive, deep-tissue operation, wireless communication, and signal amplification. These biosensors rely on the mechanical and acoustic properties of ultrasound waves to enable detection of biochemical and physiological signals relevant to brain health and function (Table 6).

7.1 | Mechanisms of Ultrasound-Driven Sensing

Ultrasound-based biosensing exploits the interactions between acoustic waves and soft biological tissues or micro/nanostructures embedded within implantable sensors. At the core of many ultrasound-responsive biosensors lies the principle of piezoelectricity, where materials such as zinc oxide (ZnO), barium titanate ($BaTiO_3$), or lead zirconate titanate (PZT) generate electrical potentials in response to mechanical deformation [494–497]. When integrated into thin-film biosensors, these piezoelectric elements can convert incident ultrasound waves into electric signals, providing a power source or transduction mechanism for sensing events.

In particular, ultrasound can modulate the behavior of biosensors in several ways. For passive systems, it induces mechanical vibrations or displacement of sensing membranes, which can be transduced into an electrical signal by piezoelectric or triboelectric effects. For active biosensors, focused ultrasound can trigger localized heating, induce cavitation effects, or modulate the permeability of hydrogel matrices, thereby enhancing molecular diffusion and signal kinetics. This approach has been effectively employed to improve the temporal resolution and sensitivity of neurotransmitter detection, particularly for dopamine and glutamate in deep-brain structures.

Furthermore, the development of microbubble-based or gas vesicle-based sensing elements provides additional layers of functionality [498, 499]. These gas-filled structures can oscillate in response to ultrasound waves, producing mechanical signals or changing their optical properties. When combined with functionalized films, such as enzyme- or aptamer-coated layers, they enable biochemical sensing with acoustic readouts or actuation [500].

7.2 | Ultrasound for Wireless Actuation and Signal Enhancement

One of the most attractive features of ultrasound in neural implantable biosensors is its capability for wireless energy transfer and data modulation. Acoustic energy can penetrate deep tissues with low attenuation and without the electromagnetic interference associated with RF or inductive powering [16]. This makes ultrasound a suitable modality for chronically implanted neural sensors, especially in regions shielded by bone or cerebrospinal fluid.

Wireless powering using ultrasound is typically realized through the use of miniaturized piezoelectric transducers integrated into the biosensor platform [501]. These transducers harvest incident ultrasonic waves and convert them into electrical energy that can sustain the operation of low-power electronics such as signal amplifiers, microcontrollers, or even electrochemical sensing modules [502]. Compared to conventional batteries, these ultrasonic power sources allow for reduced device size, increased longevity, and elimination of percutaneous wires or connectors.

Additionally, acoustic modulation can be used to encode sensing signals for data transmission. This is accomplished by modulating the amplitude, phase, or frequency of ultrasound backscatter from the implanted device in response to biochemical analyte levels. Techniques such as pulse-echo time-of-flight or acoustic backscatter modulation have been demonstrated in proof-of-concept devices for glucose and lactate sensing [502].

Beyond power and telemetry, ultrasound can directly enhance the sensitivity of biosensors by improving analyte transport. For example, low-intensity pulsed ultrasound (LIPUS) has been shown to increase tissue permeability and enhance interstitial fluid movement [503–505]. This can facilitate the diffusion of target analytes such as interleukins or neurotransmitters toward the sensor surface, reducing the response time and improving the lower detection limit.

7.3 | Applications in Biochemical Monitoring

Ultrasound-assisted biosensors are particularly well-suited for monitoring biochemical events, where traditional optical or electromagnetic methods face limitations. These sensors, powered and interrogated acoustically, can operate without wired connections or large external hardware, allowing for experiments in freely moving animals.

Furthermore, these biosensors have been applied in models of neurodegenerative diseases such as Alzheimer's and Parkinson's

TABLE 6 | Examples of acoustic and FET-based biosensors for neurotransmitters, biomarkers and small molecules.

Category/Description	Target analyte	Platforms/Materials	Sensitivity/Limit of detection	Application stage	Refs.
Acoustic					
Surface Acoustic Wave (SAW) Love-wave immunosensor for BoNT-A	Botulinum toxin A (BoNT-A)	Quartz SAW device (120 MHz) with gold electrodes, antibody monolayer receptor layer	n/a	In vitro	[534]
SAW dopamine sensor (CoPc nanopillars)	Dopamine	Quartz SAW device (110 MHz) coated with cobalt phthalocyanine nanopillars (sensing film)	~1.6° phase shift per nM (LOD ~0.1 nM)	In vitro	[532]
SAW-assisted SERS for dopamine	Dopamine	$LiNbO_3$ SAW device + Ag nanoparticle aerosol (forming SERS clusters)	~10 fM with SAW (~1 pM without SAW)	In vitro	[535]
FET					
Graphene aptamer transistor	Dopamine	CVD-grown graphene channel with dopamine-specific DNA aptamer, integrated on Si substrate	LOD ~1 aM; range up to 100 μM	In vitro	[536]
Polysilicon nanowire FET	Dopamine	Low-temperature poly-Si nanowires (sidewall spacer technique) on silicon substrate	fM-level sensitivity	In vitro	[537]
Single-CNT aptasensor (smFET)	Serotonin	Single-walled carbon nanotube with covalently attached aptamer (smFET configuration)	Single-molecule detection (1 molecule)	In vitro	[538]
Dual-gate SOI FET with extended gate (EGFET)	Dopamine	Silicon-on-insulator dual-gate FET + dopamine-sensitive extended gate	Sensitivity 373.98 mV/decade (10 fM–1 μM)	In vitro	[508]

disease, where monitoring chronic changes in cytokine levels or oxidative stress markers like H_2O_2 is crucial [506] (Figure 8A). Recent studies have also explored the integration of ultrasound biosensors with neuromodulatory systems. [12, 71] By coupling sensing modules with ultrasonic neural stimulators, closed-loop systems can be developed wherein the detection of a specific biochemical threshold (e.g., a spike in IL-6 or nitric oxide) triggers an adaptive therapeutic response. Such systems are envisioned as the foundation of intelligent neural implants capable of personalized, autonomous intervention.

8 | Field-Effect Transistor (FET)-Based Biosensors

Field-Effect Transistor (FET)-based biosensors represent a highly sensitive and versatile class of electrochemical transducers, leveraging the sensitivity of a semiconductor channel's electrical conductivity to changes in its immediate dielectric environment [507]. These devices are particularly attractive for microfabricated biosensors aimed at detecting neurotransmitters, biomarkers, and small molecules due to their inherent signal amplification capabilities, miniature footprint, and compatibility with standard microfabrication processes [508–510] (Table 6). The core principle involves a gate electrode (or the analyte itself acting as a gate) modulating the charge carrier density within a semiconductor channel, leading to a measurable change in current flowing between the source and drain electrodes (Figure 8B). FETs and OECTs are both used as biosensors, but they differ fundamentally in their operating mechanisms and materials [511]. OECTs (a specific variant of organic field-effect transistors, OFETs) operate through bulk ion penetration into an organic semiconductor, making them highly sensitive to ionic and biochemical signals in aqueous environments. In contrast, FET sensors modulate current through an electric field applied at a gate, with signal detection occurring primarily at the interface, which makes them faster but generally less sensitive to ionic concentration changes. Additionally, OECTs offer better biocompatibility and lower operating voltages, while FETs typically provide higher-speed responses and better integration with traditional electronics.

Despite their optimal sensitivity under controlled in vitro conditions, the performance of FET-based biosensors in clinically relevant biofluids remains a critical challenge for translation. In complex matrices such as serum, interstitial fluid, or cerebrospinal fluid, high ionic strength leads to strong Debye screening that attenuates charge-based signal transduction, while electroactive interferents (e.g., ascorbic acid, uric acid, glucose) and nonspecific protein adsorption introduce signal drift and false positives [512, 513]. These effects are further compounded over time by biofouling and changes in the local biochemical environment, which can obscure analyte-specific responses. To mitigate these limitations, specificity can be improved through

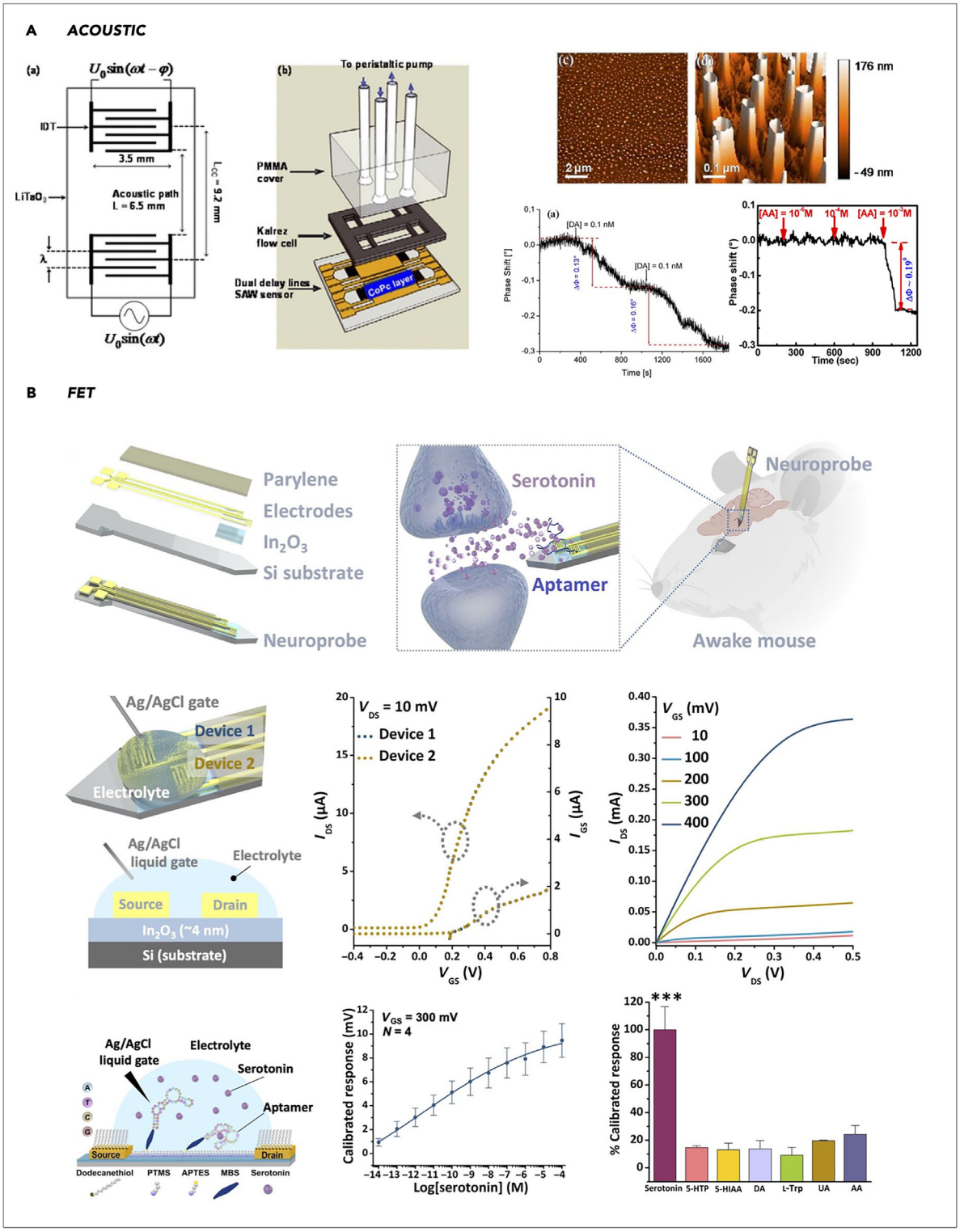

FIGURE 8 | Acoustic (A) and (B) FET-based sensors. (A) $LiTaO_3$ surface acoustic wave sensor for detection of dopamine. The AFM images show a 2D scan of 50 nm thick cobalt phthalocyanine (CoPc) film grown over the gold sensing platform of the SAW sensor, and the 3D view of the high-magnification image of CoPc films. Response of the CoPc-based SAW sensor is shown for different ascorbic acid concentrations. Reprinted from [532]. Copyright 2014, American Chemical Society. (B) FET-based Si neuroprobe for detection of serotonin. Representative transfer characteristics (I_{DS}-V_{GS}; left) and leakage current (I_{GS}-V_{GS}; right) for two transistors (curves are overlaid) on a single probe in phosphate-buffered saline. Representative transfer characteristics (I_{DS}-V_{DS}) is also shown at different gate voltages showing typical transistor behavior with saturation. A surface functionalization for In_2O_3 transistor channels is based on PTMS, trimethoxy(propyl)silane, APTES, (3-aminopropyl)triethoxysilane, MBS, 3-maleimidobenzoic acid *N*-hydroxysuccinimide ester. Serotonin aptamer-FET response curve in artificial cerebrospinal fluid (aCSF) is shown, together with its responsiveness to biologically relevant concentrations of interferents versus serotonin in aCSF (100 nM): 100 μM l-5-hydroxytryptophan (l-5-HTP), 5-hydroxyindoleacetic acid (5-HIAA), DA, l-tryptophan (l-Trp), 50 μM uric acid (UA), or 200 μM ascorbic acid (AA). Reproduced from [533]. Creative Commons CC-BY.

surface functionalization strategies that minimize the effective sensing distance and suppress nonspecific interactions, including the use of short recognition elements (e.g., aptamers, nanobodies, or antibody fragments), antifouling polymer and zwitterionic coatings, and PEGylated or biomimetic passivation layers [308, 514]. Additional approaches such as differential reference architectures, charge-modulation schemes, and operation in low-ionic-strength microenvironments have enabled partial recovery of sensitivity in real biofluids. However, these demonstrations typically involve short-term measurements, underscoring the need for further validation of long-term stability, specificity, and reproducibility before FET biosensors can be reliably deployed in chronic clinical settings.

8.1 | Silicon Nanowire FETs for Neurochemical Sensing

Silicon Nanowire (SiNW) FETs have emerged as a prominent platform for high-performance neurochemical sensing, capitalizing on the unique electrical and physical properties of silicon nanowires [515–517]. These devices utilize a semiconductor channel fabricated from silicon, typically grown or patterned into a one-dimensional (1D) nanowire geometry. The defining characteristic of SiNW FETs for sensing is their high surface-to-volume ratio. This geometric advantage maximizes the interaction between the sensing surface and the analyte in the surrounding solution, enhancing sensitivity significantly. The transduction mechanism in a SiNW FET involves a change in the local electric field near the nanowire surface, induced by the binding of charged analytes or by biochemical reactions that alter the local charge density or dielectric constant. This change directly modulates the electrostatic potential along the nanowire channel, leading to a substantial and quantifiable change in the drain current (current flowing from source to drain).

The operational principle for neurochemical sensing typically involves modifying the surface of the SiNW with a specific recognition layer [517]. For instance, neurotransmitter detection can be achieved by functionalizing the silicon dioxide (SiO_2) native oxide layer on the nanowire surface with specific receptors or enzymes [518]. For example, for dopamine detection, the SiNW surface can be modified with a dopamine receptor, or with an enzyme like tyrosinase which catalyzes dopamine oxidation, generating products that alter the local potential [519]. The binding of charged dopamine molecules or the products of its enzymatic reaction would directly gate the nanowire, causing a detectable change in its conductance. Similarly, for ion detection, such as H+ (pH sensing), K+, or Na+, the SiNW surface can be functionalized with ion-selective membranes or ionophores. The binding of these ions to the functional layer leads to a change in the surface potential that directly modulates the conductance of the underlying silicon nanowire channel [520, 521]. The high sensitivity of SiNW FETs allows for the detection of physiological and even sub-physiological concentrations of these critical ions, essential for monitoring neuronal excitability and pathological conditions like ischemia.

SiNW FETs offer several compelling advantages for neural sensing. Their inherent signal amplification means that small changes in surface charge or potential result in large, easily measurable changes in drain current, leading to ultra-high sensitivity, often achieving picomolar (pM) to femtomolar (fM) limits of detection for certain analytes. The miniature size of nanowires (typically tens to hundreds of nanometers in diameter) allows for high-density integration into arrays, enabling multiplexed detection of various analytes simultaneously within a localized area, crucial for understanding complex neurochemical interactions. Furthermore, their compatibility with standard silicon fabrication processes facilitates batch production and integration with sophisticated on-chip signal processing circuitry, paving the way for compact, autonomous sensing systems.

8.2 | Graphene and 2D Material-Based FETs

The advent of two-dimensional (2D) materials, particularly graphene, has revolutionized the field of FET-based biosensors, offering unprecedented levels of sensitivity and flexibility for neurochemical sensing [522]. Graphene, a single layer of carbon atoms arranged in a hexagonal lattice, possesses extraordinary electrical properties, including exceptionally high electron mobility and ambipolar (electron and hole) conduction. Crucially for sensing, every atom in graphene is a surface atom, making its electrical properties sensitive to changes in the surrounding environment. Beyond graphene, other 2D materials like molybdenum disulfide (MoS_2) [523], tungsten disulfide (WS_2) [524], and black phosphorus (BP) [525] are also being explored, each offering unique bandgap characteristics and surface chemistries.

The transduction mechanism in a graphene FET (GFET) biosensor is similar to SiNW FETs, where the binding of an analyte or a local biochemical event alters the surface charge density or the local dielectric constant in the vicinity of the graphene channel. This change directly shifts the Dirac point (the gate voltage at which graphene's conductivity is minimal) or modulates the conductivity of the graphene channel itself, leading to a measurable change in the source-drain current [526]. For instance, the adsorption of charged neurotransmitters or proteins onto the graphene surface directly acts as an electrostatic gate, inducing charge carriers in the graphene and changing its conductance. For dopamine or serotonin, aptamers can be immobilized onto graphene. Upon binding of the target neurotransmitter, the conformational change of the aptamer or the charge of the bound molecule itself directly alters the electrical properties of the underlying graphene. Similarly, for metabolic small molecules like glucose or lactate, enzymes (e.g., glucose oxidase, lactate oxidase) are immobilized onto the graphene surface. The enzymatic reaction produces electroactive species (like H_2O_2) or changes local pH, both of which can be detected as a shift in the GFET's transconductance. For biomarker detection, such as proteins (e.g., cytokines like IL-6, etc.), antibodies or peptide receptors can be linked to the graphene [527].

The ultra-high sensitivity of 2D material-based FETs stems from the atomic thinness of the channel, meaning even minute surface charge variations significantly impact overall conductance, leading to exceptionally low limits of detection (often at the fM to aM range). Their inherent mechanical flexibility and optical transparency make them ideal for integration onto flexible and transparent substrates, enabling conformable neural interfaces that minimize tissue damage and allow for multimodal

integration (e.g., with optical imaging). Furthermore, graphene's unique electronic properties, including its ambipolarity, offer new avenues for engineering highly efficient sensors. Despite their favorable electrical properties and atomically thin sensing interfaces, 2D material FETs face significant challenges, including the precise and reproducible functionalization of 2D material surfaces, scalable fabrication of high-quality, pristine 2D materials for large-scale sensor array, and long-term surface stability in biological environments [528, 529]. Wafer-scale synthesis and transfer processes often introduce defects, grain boundaries, and interfacial contamination that lead to variability in device performance and hinder reproducible large-area integration. These issues are compounded in chronic implant settings, where biofouling and protein adsorption can rapidly degrade sensitivity and baseline stability. Approaches to address these limitations include: material-specific antifouling strategies, e.g., ultrathin polymeric or zwitterionic coatings that preserve electrostatic coupling [514]; dynamic or stimuli-responsive surface layers that adapt to changing biological conditions [530]; and nanostructured or textured interfaces that reduce nonspecific adsorption while maintaining analyte accessibility [531]. These approaches represent promising directions, however, their compatibility with wafer-scale processing and their durability over long implantation times remain largely unvalidated.

9 | Magnetic Biosensors

Magnetic and magnetoresistive biosensors represent a rapidly advancing class of analytical tools, distinguished by their ability to detect biomolecular interactions through changes in magnetic fields or electrical resistance under magnetic influence. These sensors offer unique advantages for applications in neuroscience, particularly for in vivo monitoring of neurotransmitters, biomarkers, and small molecules, due to their potential for high sensitivity, low background noise from biological samples, and compatibility with miniaturization and implantable designs [539]. Unlike optical or electrochemical methods that can be susceptible to sample turbidity or electrochemical interferences, magnetic sensing often provides a cleaner signal in complex biological matrices [540].

9.1 | Principles of Magnetic Sensing

The fundamental principle behind magnetic biosensors lies in the precise detection of magnetic nanoparticles (MNPs), which are functionalized as labels to bind specifically to target analytes [541]. These MNPs, typically superparamagnetic iron oxide nanoparticles [542], possess unique magnetic properties: they exhibit strong magnetic responses when an external magnetic field is applied but show no residual magnetism when the field is removed, preventing aggregation and non-specific magnetic interactions. This superparamagnetic behavior is crucial for their application as highly sensitive tags in biosensing. The detection scheme involves a biorecognition event that brings these MNPs into close proximity with a magnetic sensor. The presence and concentration of these MNPs, and thus the target analyte, are then quantified by measuring their effect on a magnetic field or a magnetic sensor's electrical properties [543]. This is achieved through various magnetic sensing techniques, which differ in their underlying physics and readout mechanisms. One common approach involves measuring the stray magnetic field generated by the MNPs after they have bound to the target on the sensor surface. When an external magnetic field is applied, the MNPs become magnetized, producing a local stray field. The magnitude of this stray field is directly proportional to the number of bound MNPs and, consequently, the concentration of the target analyte. Sensors like Hall effect sensors [544], Giant Magnetoresistance (GMR) sensors [545, 546], or Tunnel Magnetoresistance (TMR) sensors [547] are sensitive to these localized magnetic field changes. Hall effect sensors, for instance, detect the voltage generated perpendicular to both a current flow and an applied magnetic field in a semiconductor. While effective, GMR and TMR sensors generally offer significantly higher sensitivities for biosensing applications.

GMR sensors are based on the quantum mechanical phenomenon observed in multilayer structures composed of alternating ferromagnetic (FM) and non-magnetic (NM) conductive layers (e.g., Fe/Cr, CoFe/Cu). The electrical resistance of such a multilayer stack changes dramatically depending on the relative orientation of the magnetization vectors in adjacent ferromagnetic layers. When the magnetizations are aligned parallel, resistance is low; when they are antiparallel, resistance is high. This "giant" change in resistance is exploited for sensing. In an implantable GMR biosensor, the surface of the GMR stack is functionalized with a capture probe (e.g., antibodies, aptamers). When the target analyte is present in the biological fluid (e.g., cerebrospinal fluid, interstitial fluid), it binds to the capture probe. Subsequently, magnetic nanoparticles (MNPs), conjugated to a detection probe (e.g., another antibody), bind to the captured analyte, bringing the MNPs into close proximity to the GMR sensing element. These MNPs generate a localized stray magnetic field, which perturbs the magnetization alignment within the GMR stack's "free layer." This perturbation causes a measurable change in the GMR device's electrical resistance, directly correlating with the number of bound MNPs and thus the concentration of the target analyte. GMR sensors offer high sensitivity (often in the picomolar to femtomolar range for biomolecules), excellent signal-to-noise ratio, and are relatively stable in physiological environments. They can be fabricated into miniaturized arrays, allowing for multiplexed detection of multiple targets from a small sample volume. For neural applications, GMR sensors have been explored for detecting neurotransmitters labeled with MNPs, or for inflammatory biomarkers and proteins associated with neurodegenerative diseases.

TMR sensors represent an even more sensitive class of magnetoresistive devices. A TMR sensor is typically a magnetic tunnel junction (MTJ), consisting of two ferromagnetic layers separated by an ultrathin insulating barrier (e.g., CoFeB/MgO/CoFeB) [548]. Electrons quantum mechanically "tunnel" through this insulating barrier. The tunneling probability, and thus the electrical resistance of the MTJ, is sensitive to the relative alignment of the magnetization vectors of the two ferromagnetic layers. Similar to GMR, parallel alignment results in low resistance, while antiparallel alignment leads to high resistance. TMR sensors generally exhibit a larger magnetoresistance ratio (the percentage change in resistance) compared to GMR, translating into even higher sensitivity [549]. This enhanced sensitivity makes TMR sensors particularly attractive for detecting extremely

low concentrations of neural biomarkers. For implantable TMR biosensors, the insulating barrier or one of the ferromagnetic layers can be functionalized. As MNPs bind to the recognition layer on the TMR sensor surface, their stray magnetic fields directly influence the magnetization of the sensing ferromagnetic layer, leading to a measurable change in the tunneling current or resistance. TMR sensors offer extremely low power consumption, high bandwidth, and can be fabricated into very small footprints, making them highly suitable for power-constrained, miniaturized implantable neural probes. Researchers are exploring TMR biosensors for the detection of subtle changes in neurotransmitter levels, cytokines indicative of neuroinflammation, and protein biomarkers associated with traumatic brain injury or neurodegenerative disorders [549, 550].

Another principle involves detecting changes in the magnetic susceptibility or magnetic relaxation of the MNPs. Nuclear Magnetic Resonance (NMR) relaxometry, for example, can exploit the superparamagnetic properties of MNPs [551, 552]. When MNPs are present, they induce local magnetic field inhomogeneities that accelerate the relaxation of nearby water protons (T_2 relaxation). The change in the measured T_2 relaxation rate of water molecules in the sample is directly proportional to the concentration of MNPs, which are indirectly linked to the target analyte. This approach is particularly advantageous as it is less susceptible to background biological noise.

Furthermore, some magnetic biosensors operate by detecting the magnetic moments of cells or other biological entities directly labeled with MNPs, or by using MNPs to exert mechanical forces on biomolecules, which can then be detected optically or electrically. The key advantage across all these principles is the low magnetic background noise inherently present in biological samples, as most biological tissues are diamagnetic or weakly paramagnetic. This provides a high signal-to-noise ratio compared to optical or electrochemical methods, which can suffer from autofluorescence or electrochemical interferences.

9.2 | Emerging NMR Microprobes for Neural Biomarkers

Nuclear Magnetic Resonance (NMR) spectroscopy is a powerful analytical technique widely used for structural elucidation and quantitative analysis of metabolites in complex biological samples. Its strengths include high reproducibility, quantitative accuracy, and the ability to non-destructively analyze native tissue specimens. While traditional high-field NMR spectrometers are bulky and confined to laboratory settings, the emergence of miniaturized NMR microprobes is opening new avenues for in vivo or near-in vivo detection of neural biomarkers and small molecules, leveraging the principles of magnetic resonance in a microfabricated format [553].

The core concept of NMR microprobes involves shrinking the key components of an NMR system, primarily the RF coil used for both exciting and detecting nuclear spins, to the microscale. These microcoils, often planar or solenoid in design, are fabricated using microelectromechanical systems (MEMS) technology. By dramatically reducing the coil size, the mass sensitivity (sensitivity per unit mass of analyte) of the NMR system is significantly enhanced because the magnetic coupling between the RF coil and the tiny sample volume it interrogates is maximized. This allows for the detection of metabolites and biomarkers from very small sample volumes (e.g., nanoliters to microliters), which is crucial for in vivo neural applications where sample availability is limited [554].

The transduction mechanism relies on the fundamental principles of NMR. Atomic nuclei with a net nuclear spin (such as 1H, 31P, 13C) behave like tiny magnets. When placed in a strong external static magnetic field (B_0), these nuclear spins align either with or against the field, creating a slight population difference. Applying a resonant RF pulse tips these aligned spins, causing them to precess and emit their own characteristic RF signal, which is detected by the microcoil. The frequency of this signal (chemical shift) is unique to the chemical environment of the nucleus, allowing for direct identification of specific molecules (e.g., lactate, glucose, glutamate, choline metabolites). The intensity of the signal is proportional to the concentration of the molecules. For neural biomarker detection, NMR microprobes can be designed to perform highly localized metabolomics, providing a "metabolic fingerprint" of specific brain regions [554, 555]. For instance, lactate accumulation is a key biomarker for ischemic injury or anaerobic metabolism, while glutamate and GABA levels reflect excitatory and inhibitory neurotransmission. Choline-containing compounds (e.g., phosphocholine, glycerophosphocholine) are indicators of membrane turnover, often associated with neuroinflammation or tumor growth. The NMR microprobe can provide quantitative, spatially resolved information on these metabolites, crucial for understanding pathological states.

A particularly promising approach involves Diagnostic Magnetic Resonance (DMR), which combines micro-NMR (μNMR) chips with magnetic nanoparticles (MNPs) as proximity sensors to amplify molecular interactions [556, 557]. In this scheme, specific antibodies or aptamers are conjugated to MNPs. When a target biomarker (e.g., peptides, inflammatory cytokines) is present, it bridges these MNP-bioreceptor conjugates, causing the MNPs to aggregate. These aggregates significantly increase the local magnetic field inhomogeneity, leading to a much stronger perturbation of the T_2 relaxation time of surrounding water protons compared to dispersed MNPs. The μNMR microcoil then detects this enhanced T_2 relaxation, providing a highly sensitive readout amplified by the collective magnetic field of the MNP aggregates. This method allows for highly sensitive (down to picomolar to femtomolar range) and selective multiplexed detection of various biomarkers in unprocessed biological samples (e.g., CSF, blood plasma), even in turbid media, without relying on optical signals or bulky fluidics.

Current limitations of NMR microprobes for neural applications include their relatively lower sensitivity compared to optical or electrochemical methods for in vivo detection of very low-concentration analytes (nM- μM range for direct NMR, lower for MNP-amplified DMR), and the need for stronger magnetic fields (even if from miniaturized permanent magnets) and sophisticated RF electronics. The development of more sensitive microcoils, integration with microfluidics for sample handling, and miniaturization of the entire NMR system for truly implantable designs are active areas of research, paving the way

for NMR to provide real-time, comprehensive metabolic profiling within the nervous system.

10 | Self-Powered Biosensors and Energy Harvesting

The vision of truly autonomous, long-term, and implantable biosensors for continuous monitoring of neurotransmitters, biomarkers, and small molecules within the human body is critically dependent on addressing the fundamental challenge of power supply. Traditional battery-powered devices are limited by battery size, lifespan, and the need for invasive replacement surgeries [16]. Self-powered biosensors directly address this limitation by integrating energy harvesting capabilities, drawing power from the biological environment itself. This paradigm shift enables the creation of devices that are perpetually operational, reducing maintenance, increasing patient comfort, and minimizing the risk of complications associated with power source depletion. Various energy harvesting modalities exist [225]: a detailed review of all of them is out of the scope of this work. Two main examples will be considered, i.e., piezoelectric and triboelectric nanogenerators. The integration of energy harvesters with microfabricated biosensors paves the way for truly self-sustained wireless neural interfaces.

10.1 | Piezoelectric and Triboelectric Nanogenerators for Autonomous Sensing

The human body is a rich source of various forms of mechanical energy, primarily generated by physiological movements such as heartbeat, breathing, blood flow, muscle contraction, and everyday activities. Piezoelectric Nanogenerators (PENGs) and Triboelectric Nanogenerators (TENGs) are emerging technologies that efficiently convert this ambient mechanical energy into usable electrical power, making them ideal candidates for powering autonomous biosensors. These nanogenerators operate on distinct physical principles, yet both offer high energy conversion efficiency at small scales, making them suitable for implantable applications.

PENGs exploit the piezoelectric effect, where certain materials generate an electric potential when subjected to mechanical stress or strain. Conversely, they deform when an electric field is applied. For energy harvesting, piezoelectric materials (e.g., PZT, ZnO, polyvinylidene fluoride (PVDF), $BaTiO_3$, aluminium nitride (AlN)) are designed to undergo repeated mechanical deformation from physiological movements [225, 558–561]. When a piezoelectric material is compressed or stretched, its internal crystal structure distorts, leading to a separation of positive and negative charges and the generation of an electric potential across the material. When this stress is released, the charges recombine, producing an alternating current.

In the context of biosensors, PENGs can be designed as thin films or nanowire arrays integrated directly onto or near regions of the body experiencing rhythmic movements. For example, PENGs positioned near the diaphragm or heart can harvest energy from breathing or heartbeat, respectively [562]. PENGs incorporated into flexible neural probes can convert the micro-movements of brain tissue or surrounding cerebrospinal fluid flow into electrical power [563]. The generated voltage and current can then be rectified and stored in a micro-supercapacitor or thin-film battery to continuously power the biosensing elements. The specific material choice, geometry (e.g., nanowires, thin films, composite structures), and encapsulation are critical for maximizing energy output and ensuring biocompatibility.

TENGs, on the other hand, convert mechanical energy into electrical energy based on the coupling of triboelectrification (charge transfer between two materials upon contact and separation) and electrostatic induction [564, 565]. When two materials with different electron affinities repeatedly come into contact and separate, charges are transferred, creating static electricity. If electrodes are placed on the surfaces of these materials, the periodic change in the separation distance between the charged surfaces induces an alternating current flow in the external circuit as charges move to screen the separated surface charges.

TENGs are typically constructed from two distinct triboelectric layers (often polymeric, e.g., PDMS, polyimide, nylon) that are brought into contact and separated, or slid against each other [566–569]. The specific design can be based on contact-separation mode, sliding mode, single-electrode mode, or freestanding triboelectric-layer mode. For in vivo applications, TENGs can harvest energy from skin stretching, muscle contraction, blood vessel pulsation, or even the movement of internal organs. For instance, a flexible TENG patch implanted near a pulsing artery can continuously generate power. The materials used must be robust, biocompatible, and possess a high triboelectric disparity to maximize charge transfer. TENGs generally produce higher output voltages but lower currents compared to PENGs, requiring different power management circuitry [225, 564, 570, 571].

10.2 | Integration of Energy Harvesters With Electrochemical and FET Sensors

The successful realization of self-powered biosensors lies in the effective and efficient integration of these energy harvesting units with the actual biosensing elements, such as electrochemical and FET sensors.

For electrochemical biosensors, which typically require a low but continuous current bias or potential for their operation (e.g., amperometric sensors) or for short pulses (e.g., voltammetric sensors), the harvested energy needs to be rectified and stored. A common integration strategy involves connecting the PENG or TENG to a rectifier circuit (e.g., a full-wave bridge rectifier) for AC/DC conversion. This DC power is then fed into a power management unit (PMU), which typically includes a voltage regulator and an energy storage component like a micro-supercapacitor or a thin-film rechargeable battery. The micro-supercapacitor, due to its high power density and rapid charge/discharge cycles, is well-suited for buffering the intermittent energy harvested from body movements and providing stable power to the electrochemical sensor. For example, a flexible PENG harvesting energy from respiration can trickle-charge a micro-supercapacitor, which then provides the stable potential for an amperometric glucose or lactate sensor, enabling continuous metabolic monitoring without external power [572]. The challenges in this integration

include matching the output impedance of the nanogenerator to the input impedance of the power management unit, minimizing conversion losses, and ensuring the stability of the harvested voltage/current for the sensitive electrochemical measurements.

Similarly, for FET-based biosensors, which typically operate at low voltages (a few volts) and low currents but require stable gate biasing and source-drain voltage, the integration strategy follows a similar rectification and storage principle. The PENG or TENG generates the raw AC power, which is rectified and regulated by the PMU. The regulated DC voltage is then applied to the source and drain terminals, and a precise gate voltage can be generated internally or from the PMU. The ultralow power consumption of modern FETs, especially those fabricated with 2D materials, makes them highly compatible with energy harvesting solutions. For instance, a flexible TENG integrated into a subcutaneous neural probe could harvest kinetic energy from body movements to power a graphene FET array for continuous detection of neurotransmitters or inflammatory cytokines [573]. A key aspect here is managing the power duty cycle: the nanogenerators generate power intermittently, while the biosensors may require continuous or pulsed operation. The energy storage element acts as a buffer, ensuring the biosensor always receives the necessary power, even during periods of low mechanical activity. Furthermore, advanced integration can involve self-gating mechanisms, where the triboelectric charges directly modulate the gate of an FET, potentially eliminating the need for complex external gate control circuits, leading to truly simplified and highly efficient self-powered sensing [574]. The choice of packaging and encapsulation is crucial for both energy harvester and sensor to withstand the physiological environment and maintain long-term functionality.

Table 7 provides a comparative power-budget framework that relates physiologically achievable harvested power to the typical consumption of sensing, signal conditioning, data processing, wireless communication, and actuation modules in closed-loop implants. This analysis clarifies which system functions can be supported continuously, which may require duty cycling or event-driven operation, and where hybrid energy strategies (e.g., harvesting combined with microstorage or intermittent wireless replenishment) are likely necessary.

11 | Other Biosensor Modalities

Beyond the established electrochemical, optical, magnetic, and self-powered platforms, a diverse array of other biosensor modalities are actively being explored and developed for neurochemical sensing.

11.1 | Micro- and Nanoelectromechanical Systems (MEMS/NEMS) for Neural Sensing

MEMS and their nanoscale counterparts, Nanoelectromechanical Systems (NEMS), represent a class of integrated devices that combine electrical and mechanical components at the micro- and nanoscale [581]. These systems transduce a physical or chemical input into a mechanical response (e.g., deflection, resonance frequency shift) that is then converted into an electrical signal. For neural sensing, MEMS/NEMS offer unique advantages, particularly for label-free, mass-sensitive detection, and for creating integrated platforms capable of both sensing and actuation.

The core principle of MEMS/NEMS biosensors for neural applications often revolves around resonant sensors [582]. These devices typically consist of a micro- or nanocantilever, resonator, or diaphragm, coated with a specific biorecognition layer [583]. When the target analyte binds to the recognition layer, it increases the mass of the resonator. This mass addition causes a detectable shift in the resonator's fundamental resonance frequency, which can be precisely measured using piezoelectric, piezoresistive, or capacitive transduction methods. The extremely small mass of NEMS resonators (e.g., carbon nanotube resonators) allows for detection of incredibly small mass changes, enabling ultrahigh sensitivity, potentially down to single-molecule detection [584]. For example, a nanocantilever functionalized with an antibody specific to a neurodegenerative biomarker like Aβ would show a frequency shift upon Aβ binding, allowing for label-free quantification [585].

Beyond mass sensing, MEMS/NEMS devices can also be designed to measure other physical changes induced by biochemical interactions. For instance, surface stress-based sensors utilize the differential surface stress induced on a functionalized cantilever upon molecular binding, causing the cantilever to bend. This bending can be detected optically or piezoresistively [586]. Moreover, MEMS can form the basis of miniaturized fluidic systems for sample handling, drug delivery, or integrated cell culture platforms for in vitro neural studies. For in vivo neural interfaces, MEMS/NEMS technology enables the fabrication of highly integrated probes that can simultaneously perform electrophysiological recording (via microelectrodes), chemical sensing (via integrated biosensors), and even local drug delivery (via microfluidic channels), all on a single, compact, and flexible device [587].

11.2 | Hybrid Biosensors for Multimodal Detection

The complexity of the neural environment, characterized by dynamic interactions between electrical activity, diverse neurochemical signals, and ongoing cellular processes, often necessitates a more holistic approach to sensing. Hybrid biosensors for multimodal detection represent a powerful paradigm shift, integrating two or more distinct biosensing modalities onto a single platform. This synergistic combination provides a more comprehensive and accurate picture of complex biological events, allowing for simultaneous measurement of different types of signals (e.g., electrical and chemical, or chemical and physical), cross-validation of results, and enhanced robustness against individual sensor limitations.

A common and highly impactful form of hybrid biosensor in neural interfaces is the electrochemical-electrophysiological probe. These devices combine microelectrode arrays (MEAs) for recording neuronal electrical activity (local field potentials, single-unit spikes) with integrated electrochemical biosensors (e.g., amperometric or voltammetric sensors) for simultaneous detection of neurotransmitters (e.g., dopamine, serotonin, gluta-

TABLE 7 | Realistic continuous average power budgets (typical ranges), key variability factors and feasibility for continuous operation, for common energy harvesters described in literature [14, 16, 24, 225, 567, 575–580].

Energy harvester/Subsystem	Realistic continuous average power (typical range)	Key variability factors	Feasibility for continuous operation
Harvesters			
Inductive (near-field, dedicated external TX)	0.5–50 mW (practical: 1–20 mW)	Coupling, alignment, distance, coil size; continuous if external TX present	Yes (with external transmitter)
Dedicated RF power transfer (focused)	10 μW – 5 mW	Tx power limits, alignment, regulatory limits	Maybe (lower mW with careful link)
Ambient RF harvesting	nW–10 μW	RF environment, distance to emitters	No (insufficient for active wireless/actuation)
Thermoelectric (TEG; body gradient)	0.1 μW–100 μW (typical implant: 1–20 μW)	Local temp gradient, surface area, thermal interface	Maybe for ultra-low power nodes
Mechanical / piezo (motion, heartbeat)	0.1 μW–1 mW (typical: 1–500 μW, highly intermittent)	Motion amplitude/frequency and coupling	Maybe (for intermittent or duty-cycled loads)
Triboelectric (TENGs)	∼μW-mW (motion dependent)	Contact mechanics, encapsulation losses	Maybe (for intermittent or duty-cycled loads)
Biofuel cell (glucose, enzymatic)	0.5 μW–500 μW (typical continuous: 1–10^2 μW)	Local glucose concentration, enzyme lifetime, fouling	Maybe for low-power systems; hard for mW loads
Subdermal photovoltaic (with external light)	1 μW–10 mW (with strong illumination: mW range)	Skin attenuation, illumination, external light source	Yes if reliable external illumination; otherwise No
Subsystems (typical ranges)			
Sensing (low-bandwidth biochemical, low-noise front end)	1 μW–500 μW (typical low: 10–100 μW)	Bandwidth, multiplexing, sensor type	Often compatible with enzymatic / TEG / motion
Signal conditioning / ADC	1 μW–1 mW (depending on sampling rate and resolution)	ADC resolution, sampling duty cycle	Depends on duty cycling
Processing / ML inference (tinyML)	1 μW–10 mW (typical sleep μW; active inference 10–10^3 μW)	Model complexity, duty cycle	Often requires harvesting + storage or duty cycling
Wireless telemetry (BLE, low-rate)	Active TX: 5–50 mW; duty-cycled average: <100 μW – few mW	TX duty cycle, transmit power, link budget	Continuous streaming requires inductive/dedicated RF; suitable for intermittent
Closed-loop electrical actuation (neural stim)	Pulse instantaneous power: mW–10^2 mW; average depends on duty cycle (μW up to mW)	Stim amplitude, pulse width, frequency, electrode impedance	Usually requires inductive or stored energy + recharge
Drug-delivery actuator (microvalve, pump)	Mostly μW average, but occasional pulses can be mW–10^2 mW	Type of actuator, dosing schedule	Feasible with harvesting + storage if actuation rare

mate) [588]. For example, a flexible polyimide probe might embed both platinum microelectrodes for neuronal firing and carbon fiber microelectrodes functionalized with oxidase enzymes for real-time glucose and lactate monitoring [589, 590]. This multimodal approach allows researchers and clinicians to directly correlate neural electrical activity with concurrent neurochemical changes, providing deeper insights into brain function in health and disease (e.g., how specific firing patterns relate to neurotransmitter release, or how metabolic changes influence neuronal excitability during ischemia or seizure).

Another emerging type of hybrid sensor combines optical sensing with electrochemical detection. For instance, an SPR or LSPR plasmonic chip (for label-free protein biomarker detection) could

be integrated with electrochemical electrodes (for neurotransmitter analysis) on the same platform [591]. Such a device could simultaneously monitor real-time protein binding kinetics and also quantify specific electroactive small molecules from a single sample. Some advanced concepts also explore integrating MEMS/NEMS devices (for mass sensing or physical manipulation) with optical waveguides or electrochemical cells, creating intricate lab-on-a-chip systems for highly parallelized and comprehensive analysis of neural samples. For example, a MEMS-based microfluidic system could sort and deliver individual cells to an optical waveguide-based sensor for real-time analysis of intracellular biomarkers, while simultaneously, electrochemical sensors quantify extracellular neurotransmitters [592, 593].

The key advantages of hybrid biosensors are manifold. First, the simultaneous acquisition of diverse data types provides a more complete understanding of neurobiological processes. The cross-validation between modalities can also improve the confidence in detected signals and reduce false processes. By combining sensors with different selectivity mechanisms, the overall specificity of the system can be improved, helping to deconvolute signals in complex biological environments. Additionally, the ability to integrate multiple functions onto a single, compact microfabricated platform minimizes device footprint and surgical invasiveness for implantable applications. Hybrid designs can be customized to specific research questions or clinical needs, ranging from combining neural recording with optogenetic stimulation, or chemical sensing with localized drug delivery. Table 8 summarizes advantages and limitations of all the sensing modalities described in this review, including hybrid ones.

12 | Conclusions and Future Perspectives

The burgeoning demand for adaptive bioelectronic systems, highly personalized diagnostics, and responsive neuromodulation platforms has firmly established thin-film biosensors as a pivotal technology. These innovative devices enable the creation of multifunctional, minimally invasive, and multimodal neural interfaces, offering unprecedented windows into the dynamic complexities of the nervous system. Our exploration has detailed the fundamental principles, advanced materials, and sophisticated transduction mechanisms that underpin the development of electrochemical, plasmonic, and even emerging ultrasound-based thin-film biosensors, all tailored for the precise detection of neurotransmitters, minute small molecules, and critical disease-relevant biomarkers. Seamlessly integrated into flexible, implantable, and wearable systems, these sensing modalities unlock extraordinary opportunities for real-time monitoring and sophisticated closed-loop feedback in a broad spectrum of neurological and systemic disorders.

The profound impact of thin-film materials and sophisticated surface functionalization strategies cannot be overstated; they are absolutely critical for enhancing sensitivity, ensuring biocompatibility, and enabling radical device miniaturization. This dynamic field is experiencing an exhilarating pace of progress, propelled by groundbreaking innovations across nanomaterials, ultrasoft substrates, and ingenious biointerface designs. Together, these advancements are fundamentally transforming the performance metrics and clinical potential of chemical biosensors, steadily bridging the gap from conceptual studies to robust in vivo applications and, ultimately, to clinically viable systems.

Advancing functional materials. There is an urgent need to forge advanced functional materials that simultaneously exhibit tissue-like mechanical properties, unwavering long-term biostability, and biochemical specificity. These functional layers must be engineered to reliably detect incredibly low-abundance analytes within the constantly shifting and complex biological milieu, all while avoiding detrimental immune responses and debilitating sensor biofouling. The intrinsic complexity of neural tissues, soft, wet, and dynamically moving, demands ultrasoft and conformal materials for implantable interfaces to prevent mechanical mismatch, chronic inflammation, and gliosis. Materials like parylene C, polyimide, PDMS, and hydrogels form the bedrock of next-generation flexible and stretchable probes, designed to undergo large deformations without compromising integrity. Furthermore, incorporating antifouling strategies, such as hydrophilic coatings (e.g., PEG, zwitterionic polymers) or dynamic surface chemistries, is crucial for resisting non-specific protein adsorption and cellular encapsulation that degrade sensor performance over time. Continued breakthroughs in organic electronics, novel 2D materials, and bioinspired interface designs will be indispensable in actualizing these next-generation biosensors, often involving thin films or serpentine patterns to minimize mechanical strain and improve conformability with neural tissues.

Improving integration with wireless and closed-loop systems. For thin-film biosensors to truly ascend as integral components of intelligent therapeutic platforms, they must seamlessly merge with efficient wireless powering and robust data telemetry. Wireless technologies like RF, Bluetooth Low Energy (BLE), and ultrasonic links enable untethered operation, reducing patient discomfort and infection risks. Wireless power transfer modalities such as inductive coupling and ultrasonic power delivery are critical for battery-free operation, ensuring power reaches even deep-brain implants [16]. Beyond just transmitting data, future systems are envisioned to support bidirectional communication, where the rich data streamed from the biosensors directly informs real-time decision-making within adaptive, closed-loop architectures. This enables automated therapeutic interventions, such as precisely timed electrical stimulation or localized drug release, in response to detected neurochemical changes or abnormal neural activity. These self-sustained wireless neural interfaces, powered by energy harvesting from physiological movements or body heat, aim for continuous, long-term, and minimally invasive operation, promising transformative impact on neurological disease management and research.

Enhancing sensor robustness and longevity. The pursuit of chronic implantation demands materials and device architectures that can steadfastly endure sustained mechanical deformation, constant fluid exposure, and persistent biological degradation over extended periods, often spanning years. This requires moving beyond merely biocompatible materials to those with inherent durability and corrosion resistance. Research efforts must intensify on designing fatigue-resistant sensor architectures, pioneering more effective and hermetic encapsulation strategies using materials like parylene C or ALD-grown alumina, and even exploring self-healing materials capable of autonomously

TABLE 8 | Key advantages and limitations of different sensing modalities described in this review. This table provides a qualitative comparison based on previous literature reviews [242, 390, 507, 543, 594].

Sensing modality	Typical transduction mechanism	Detection principle	Key advantages	Key limitations	Temporal resolution	Depth / invasiveness	Chronic implantation considerations
Electrochemical	Amperometric microelectrodes	Faradaic current from oxidation/reduction of neurotransmitters	• Very high sensitivity • Direct chemical detection • Compact • Mature technology	• Poor intrinsic selectivity • Interferents • Fouling and drift	sub-ms–ms	Invasive; local	• Requires antifouling coatings and recalibration • Encapsulation reduces mass transport
	Fast-scan cyclic voltammetry (FSCV)	Voltage sweeps generate analyte-specific redox signatures	• Excellent temporal resolution • Analyte discrimination	• High background currents • Complex signal processing	sub-ms	Invasive	• Long-term stability limited by electrode degradation
	Enzyme-modified electrodes	Enzymatic conversion generates electroactive species	• Improved selectivity	• Enzyme degradation • Oxygen dependence	ms–s	Invasive	• Limited enzyme lifetime in chronic implants
FET–based	Silicon nanowire FETs	Surface charge modulates channel conductance	• Label-free; high sensitivity; CMOS-compatible	• Debye screening • Biofouling • Variability	ms–s	Invasive	• Stability and reproducibility remain challenges
	Graphene / 2D FETs	Carrier density modulation by molecular binding	• Ultrathin sensing interface; high mobility	• Fabrication variability • Fouling	ms–s	Invasive	• Wafer-scale uniformity and chronic surface stability unresolved
	Organic electrochemical transistors (OECTs)	Ionic–electronic coupling modulates channel doping	• High signal gain; operates in physiological ionic strength	• Slower response • Material degradation	ms–s	Invasive	• Organic material stability over long term
Optical	Fluorescent dyes	Intensity or spectral shift upon binding	• High specificity • Multiplexing	• Shallow penetration • Photobleaching	ms–s	Minimally invasive to invasive (optics)	• Photostability and chronic optical access
	Genetically encoded indicators	Fluorescence change via conformational shift	• Cell-type specificity • High selectivity	• Requires genetic manipulation • imited depth	ms–s	Moderately invasive	• Long-term expression stability
	Plasmonic (SPR/LSPR)	Resonance shift due to refractive index change	• Label-free • High surface sensitivity	• Shallow sensing depth • Complex optics	ms–s	Invasive	• Integration and fouling challenges
Acoustic	Ultrasound backscatter modulation	Neurotransmitter-induced changes in acoustic properties	• Deep penetration; non-ionizing	• Indirect chemical specificity	ms–s	Low invasiveness	• Limited molecular selectivity
Magnetic	GMR / TMR sensors	Magnetic nanoparticle binding alters resistance	• Deep tissue penetration • Low background noise	• Requires magnetic labels	ms–s	Low to moderate	• Nanoparticle clearance and biocompatibility
	NMR / relaxometry-based	Neurotransmitter-modulated relaxation times	• High chemical specificity	• Bulky hardware; low temporal resolution	s–min	Non-invasive (external)	• Not suitable for implantable chronic sensing
Hybrid	Electrochemical–optical	Complementary chemical + optical readout	• Improved specificity and validation	• High system complexity	Modality-dependent	Increased invasiveness	• Power, packaging, and failure-mode coupling
	FET–electrochemical	Dual electrical transduction	• Redundancy • Improved robustness	• Integration challenges	ms–s	Invasive	• Increased fabrication and calibration burden

repairing minor damage, all aimed at preserving optimal sensor function in vivo. However, hermeticity contrasts the intrinsic function of a biosensor, which has to interact with the external surroundings. For applications where permanent implants are undesirable, bioresorbable (transient) systems offer a compelling alternative, designed to degrade harmlessly after a temporary functional period, eliminating the need for surgical removal. Regardless of the intended lifespan, integrating all sensor components, electronics, and encapsulation layers into a cohesive, mechanically robust structure is vital for sustained function and clinical acceptance.

Expanding sensing targets and multiplexing. While current endeavors have commendably concentrated on pivotal neurotransmitters and essential metabolic molecules, the next generation of biosensors should broaden its scope to include the multiplexed detection of a far wider spectrum of biomarkers. This encompasses inflammatory cytokines, subtle oxidative stress markers, and crucial hormonal signals. The ability to precisely monitor these diverse neurochemical signals in real-time could unlock deeper insights into disease progression, therapeutic response, and fundamental brain function. Combining such multi-analyte readout with sophisticated machine learning-based data analysis will dramatically elevate diagnostic precision and enable more finely tuned therapeutic adaptation, moving beyond single-analyte snapshots to comprehensive neurochemical profiling.

Leveraging multi-modality and multifunctionality. The ambition extends to leveraging multi-modality and multifunctionality within a single, integrated platform. The elegant integration of chemical biosensing with complementary modalities such as electrophysiology (for real-time neural activity recording), optical stimulation (for precise neuronal control), and mechanotransduction (for physical tissue properties) will unlock remarkably powerful tools for both studying and precisely modulating complex physiological processes. Hybrid systems that harmoniously combine sensing, electrical stimulation, and targeted therapeutic release within a singular, unified microfabricated platform are poised to define the very essence of next-generation bioelectronic medicine. These sophisticated devices will enhance brain-machine interfaces by adding chemical context to electrical signals, paving the way for adaptive neuromodulation, personalized medicine, and advanced disease monitoring.

Paving the way for clinical translation. Finally, a dedicated and concerted effort to pave the way for clinical translation is non-negotiable. For thin-film biosensors to genuinely impact human health, collaborative efforts must converge on improving manufacturability to enable scalable production, diligently ensuring rigorous regulatory compliance (a complex and lengthy process), and conclusively validating their long-term safety and efficacy in human subjects. Manufacturing scalability remains a concern, particularly for devices relying on complex nanomaterials or custom microfabrication. Furthermore, critical considerations for systems transmitting sensitive biological information wirelessly include robust data privacy and cybersecurity.

Beyond signal drift and acute biofouling, the long-term clinical viability of thin-film biosensors is fundamentally constrained by challenges associated with chronic implantation. Prolonged exposure to the physiological environment can lead to gradual degradation of thin-film materials and encapsulation layers through hydrolysis, corrosion, or mechanical fatigue, as well as the release of leachables that may compromise both sensor performance and tissue compatibility [285, 595, 596]. In parallel, the foreign body response evolves over months to years from acute inflammation toward chronic fibrotic encapsulation, altering the mechanical, chemical, and transport properties of the tissue–sensor interface. The formation of dense collagenous capsules and adherent cellular layers increases diffusion distances and electrical insulation, resulting in progressive attenuation of signal amplitude, reduced sensitivity, and delayed temporal response [597].

Encapsulation-induced changes in the local microenvironment, such as altered pH, oxygen availability, and analyte transport, further decouple the sensor from the target physiological signal, particularly for thin-film electrochemical and chemical sensing modalities [598]. Emerging strategies to address these limitations include the use of mechanically compliant and tissue-matched substrates to reduce micromotion-induced inflammation, anti-fibrotic and immunomodulatory surface chemistries to mitigate capsule formation, and adaptive calibration, redundancy, or self-diagnostic architectures to compensate for gradual performance degradation [599]. While these approaches have shown promise in short-term or preclinical studies, their long-term efficacy and reliability in chronic human implantation remain largely unproven, underscoring the need for extended in vivo validation and system-level design approaches that explicitly account for biological evolution over time.

All this necessitates close collaborations across diverse disciplines, including materials science, biomedical engineering, neurosciences, clinical medicine, and regulatory science, all working in concert to achieve real-world deployment and unlock their full clinical promise.

Acknowledgments

M.M. heartfeltly dedicates this work to Franco C. (oenologist). MM also acknowledges two institutions (Italian Institute of Technology, école Polytechnique Fédérale de Lausanne) for their contribution to fuel his personal curiosity in self-powered systems and biosensors.

Conflicts of Interest

The author declares no conflict of interest.

References

1. D. Boufidis, R. Garg, E. Angelopoulos, D. K. Cullen, and F. Vitale, "Bio-Inspired Electronics: Soft, Biohybrid, and "Living" Neural Interfaces," *Nature Communications* 16 (2025): 1861.

2. C. Sun, Z. Cheng, J. Abu-Halimah, and B. Tian, "Perspectives on tissue-like bioelectronics for neural modulation," *iScience* 26 (2023): 106715.

3. P. Gutruf, V. Krishnamurthi, A. Vázquez-Guardado, et al., "Fully Implantable Optoelectronic Systems for Battery-free, Multimodal Operation in Neuroscience Research," *Nature Electronics* 1 (2018): 652–660, https://doi.org/10.1038/s41928-018-0175-0.

4. P. Gutruf, R. T. Yin, K. B. Lee, et al., "Wireless, Battery-free, Fully Implantable Multimodal and Multisite Pacemakers for Applications in

Small Animal Models," *Nature Communications* 10 (2019): 5742, https://doi.org/10.1038/s41467-019-13637-w.

5. I. R. Minev, P. Musienko, A. Hirsch, Q. Barraud, and N. Wenger, "Electronic Dura Mater for Long-term Multimodal Neural Interfaces," *Science* 347 (2015): 159–163.

6. J. Li, Y. Liu, L. Yuan, et al., "A Tissue-Like Neurotransmitter Sensor for the Brain and Gut," *Nature* 606 (2022): 94–101, https://doi.org/10.1038/s41586-022-04615-2.

7. D. T. Simon, S. Kurup, K. C. Larsson, et al., "Organic Electronics for Precise Delivery of Neurotransmitters to Modulate Mammalian Sensory Function," *Nature Materials* 8 (2009): 742–746, https://doi.org/10.1038/nmat2494.

8. S. I. Park, G. Shin, A. Banks, et al., "Ultraminiaturized Photovoltaic and Radio Frequency Powered Optoelectronic Systems for Wireless Optogenetics," *Journal of Neural Engineering* 12 (2015): 056002–056002, https://doi.org/10.1088/1741-2560/12/5/056002.

9. J.-W. Jeong, J. G. McCall, G. Shin, et al., "Wireless Optofluidic Systems for Programmable In Vivo Pharmacology and Optogenetics," *Cell* 162 (2015): 662–674, https://doi.org/10.1016/j.cell.2015.06.058.

10. Y. Yang, M. Wu, A. Vázquez-Guardado, et al., "Wireless Multilateral Devices for Optogenetic Studies of Individual and Social Behaviors," *Nature Neuroscience* 24 (2021): 1035–1045, https://doi.org/10.1038/s41593-021-00849-x.

11. M. J. Weber, Y. Yoshihara, A. Sawaby, J. Charthad, T. C. Chang, and A. Arbabian, "A Miniaturized Single-Transducer Implantable Pressure Sensor with Time-Multiplexed Ultrasonic Data and Power Links," *IEEE Journal of Solid-State Circuits* 53 (2018): 1089–1101, https://doi.org/10.1109/JSSC.2017.2782086.

12. J. F. Hou, M. O. G. Nayeem, K. A. Caplan, et al., "An Implantable Piezoelectric Ultrasound Stimulator (ImPULS) for Deep Brain Activation," *Nature Communications* 15 (2024): 4601, https://doi.org/10.1038/s41467-024-48748-6.

13. J. Li, Y. Long, F. Yang, and X. Wang, "Degradable Piezoelectric Biomaterials for Wearable and Implantable Bioelectronics," *Current Opinion in Solid State and Materials Science* 24 (2020): 100806, https://doi.org/10.1016/j.cossms.2020.100806.

14. S. Yoo, J. Lee, H. Joo, S.-H. Sunwoo, S. Kim, and D.-H. Kim, "Wireless Power Transfer and Telemetry for Implantable Bioelectronics," *Advanced Healthcare Materials* 10 (2021): 2100614, https://doi.org/10.1002/adhm.202100614.

15. M. Mariello, J. D. Rosenthal, F. Cecchetti, et al., "Wireless, Battery-free, and Real-time Monitoring of Water Permeation Across Thin-film Encapsulation," *Nature Communications* 15 (2024): 7443, https://doi.org/10.1038/s41467-024-51247-3.

16. M. Mariello and C. M. Proctor, "Wireless Power and Data Transfer Technologies for Flexible Bionic and Bioelectronic Interfaces: Materials and Applications," *Adv Mater Technol* 2400797.

17. S. P. Lacour, G. Courtine, and J. Guck, "Materials and Technologies for Soft Implantable Neuroprostheses," *Nature Reviews Materials* 1 (2016): 1–14, https://doi.org/10.1038/natrevmats.2016.63.

18. A. G. Rouse and M. H. Schieber, "Advancing Brain-machine Interfaces: Moving Beyond Linear state Space Models," *Frontiers in Systems Neuroscience* 9 (2015): 108, https://doi.org/10.3389/fnsys.2015.00108.

19. A. L. Benabid, T. Costecalde, A. Eliseyev, et al., "An exoskeleton controlled by an epidural wireless brain–machine interface in a tetraplegic patient: A proof-of-concept demonstration," *The Lancet Neurology* 18 (2019): 1112–1122, https://doi.org/10.1016/S1474-4422(19)30321-7.

20. E. Musk, Neuralink, "An Integrated Brain-Machine Interface Platform with Thousands of Channels," *Journal of Medical Internet Research* 21 (2019): e16194, https://doi.org/10.2196/16194.

21. Y. S. Choi, H. Jeong, R. T. Yin, et al., "A Transient, Closed-loop Network of Wireless, Body-Integrated Devices for Autonomous Electrotherapy," *Science* 376 (2022): 1006–1012, https://doi.org/10.1126/science.abm1703.

22. K. Scholten and E. Meng, "A Review of Implantable Biosensors for Closed-loop Glucose Control and Other Drug Delivery Applications," *International Journal of Pharmaceutics* 544 (2018): 319–334, https://doi.org/10.1016/j.ijpharm.2018.02.022.

23. C. Kathe, F. Michoud, P. Schönle, et al., "Wireless Closed-loop Optogenetics Across the Entire Dorsoventral Spinal Cord in Mice," *Nature Biotechnology* 40 (2022): 198–208, https://doi.org/10.1038/s41587-021-01019-x.

24. F. Del Bono, N. D. Trani, D. Demarchi, A. Grattoni, and P. M. Ros, "Wireless Power Transfer Closed-Loop Control for Low-Power Active Implantable Medical Devices," *IEEE Sensors* (2022): 1–4, https://doi.org/10.1109/SENSORS52175.2022.9967268.

25. D. Lee, S. H. Jeong, S. Yun, et al., "Totally Implantable Enzymatic Biofuel Cell and Brain Stimulator Operating in Bird Through Wireless Communication," *Biosensors and Bioelectronics* 171 (2021): 112746, https://doi.org/10.1016/j.bios.2020.112746.

26. G. Li, Y. Tian, L. Jiang, et al., "A Bimodal Closed-loop Neuromodulation Implant Integrated With Ultraflexible Probes to Treat Epilepsy," *Biosensors and Bioelectronics* 271 (2025): 117071, https://doi.org/10.1016/j.bios.2024.117071.

27. S. Liu, Y. Zhao, W. Hao, X.-D. Zhang, and D. Ming, "Micro- and Nanotechnology for Neural Electrode-tissue Interfaces," *Biosensors and Bioelectronics* 170 (2020): 112645, https://doi.org/10.1016/j.bios.2020.112645.

28. R. I. Teleanu, A.-G. Niculescu, E. Roza, O. Vladâcenco, A. M. Grumezescu, and D. M. Teleanu, "Neurotransmitters—Key Factors in Neurological and Neurodegenerative Disorders of the Central Nervous System," *International Journal of Molecular Sciences* 23 (2022): 5954, https://doi.org/10.3390/ijms23115954.

29. Z. Wu, D. Lin, and Y. Li, "Pushing the Frontiers: Tools for Monitoring Neurotransmitters and Neuromodulators," *Nature Reviews Neuroscience* 23 (2022): 257–274, https://doi.org/10.1038/s41583-022-00577-6.

30. S. Friberg, C. Lindblad, F. A. Zeiler, et al., "Fluid Biomarkers of Chronic Traumatic Brain Injury," *Nature Reviews Neurology* 20 (2024): 671–684, https://doi.org/10.1038/s41582-024-01024-z.

31. M. Khalil, C. E. Teunissen, S. Lehmann, et al., "Neurofilaments as biomarkers in neurological disorders — towards clinical application," *Nature Reviews Neurology* 20 (2024): 269–287, https://doi.org/10.1038/s41582-024-00955-x.

32. V. K. Sharma, T. G. Singh, V. Mehta, and A. Mannan, "Biomarkers: Role and Scope in Neurological Disorders," *Neurochemical Research* 48 (2023): 2029–2058, https://doi.org/10.1007/s11064-023-03873-4.

33. P. Siwach, E. Levy, L. Livshits, Y. Feldman, and D. Kaganovich, "Water Is a Biomarker of Changes in the Cellular Environment in Live Animals," *Scientific Reports* 10 (2020): 9095, https://doi.org/10.1038/s41598-020-66022-9.

34. A. Alvarsson and S. A. Stanley, "Remote Control of Glucose-sensing Neurons to Analyze Glucose Metabolism," *American Journal of Physiology-Endocrinology and Metabolism* 315 (2018): E327–E339.

35. B. E. Levin, "Glucosensing Neurons Do More Than Just Sense Glucose," *International Journal of Obesity* 25 (2001): S68–S72, https://doi.org/10.1038/sj.ijo.0801916.

36. M. Cai, H. Wang, H. Song, et al., "Lactate Is Answerable for Brain Function and Treating Brain Diseases: Energy Substrates and Signal Molecule," *Frontiers in Nutrition* 9 (2022): 800901, https://doi.org/10.3389/fnut.2022.800901.

37. A. B. Knott and E. Bossy-Wetzel, "Nitric Oxide in Health and Disease of the Nervous System," *Antioxidants & Redox Signaling* 11 (2009): 541–553, https://doi.org/10.1089/ars.2008.2234.

38. P. Picón-Pagès, J. Garcia-Buendia, and F. J. Muñoz, "Functions and Dysfunctions of Nitric Oxide in Brain," *Biochimica et Biophysica Acta - Molecular Basis of Disease* 1865 (2019): 1949–1967.

39. N. Xu, X. Li, and Y. Zhong, "Inflammatory Cytokines: Potential Biomarkers of Immunologic Dysfunction in Autism Spectrum Disorders," *Mediators of Inflammation* 2015 (2015): 531518, https://doi.org/10.1155/2015/531518.

40. A. Thomas, J. Guo, D. Reyes-Dumeyer, et al., "Inflammatory Biomarkers Profiles and Cognition Among Older Adults," *Scientific Reports* 15 (2025): 2265, https://doi.org/10.1038/s41598-025-86309-z.

41. T. Woodcock and C. Morganti-Kossmann, "The Role of Markers of Inflammation in Traumatic Brain Injury," *Frontiers in Neurology* 4 (2013).

42. D. M. Holtzman, "CSF Biomarkers for Alzheimer's Disease: Current Utility and Potential Future Use," *Neurobiology of Aging* 32 (2011): S4–S9, https://doi.org/10.1016/j.neurobiolaging.2011.09.003.

43. K. Blennow, N. Mattsson, M. Schöll, O. Hansson, and H. Zetterberg, "Amyloid biomarkers in Alzheimer's disease," *Trends in Pharmacological Sciences* 36 (2015): 297–309, https://doi.org/10.1016/j.tips.2015.03.002.

44. S. Schraen-Maschke, N. Sergeant, C.-M. Dhaenens, et al., "Tau as a Biomarker of Neurodegenerative Diseases," *Biomarkers in Medicine* 2 (2008): 363–384, https://doi.org/10.2217/17520363.2.4.363.

45. S. Holper, R. Watson, and N. Yassi, "Tau as a Biomarker of Neurodegeneration," *International Journal of Molecular Sciences* 23 (2022): 7307, https://doi.org/10.3390/ijms23137307.

46. F. Gonzalez-Ortiz, M. Turton, P. R. Kac, et al., "Brain-derived Tau: A Novel Blood-based Biomarker for Alzheimer's Disease-type Neurodegeneration," *Brain* 146 (2023): 1152–1165, https://doi.org/10.1093/brain/awac407.

47. Z. Meng, Y. Zhang, L. Yang, et al., "Application of Advanced Biosensors in Nervous System Diseases," *Interdisciplinary Medicine* 2 (2024): e20240024, https://doi.org/10.1002/INMD.20240024.

48. A. V. Leopold, D. M. Shcherbakova, and V. V. Verkhusha, "Fluorescent Biosensors for Neurotransmission and Neuromodulation: Engineering and Applications," *Frontiers in Cellular Neuroscience* 13 (2019).

49. G. Goumas, E. N. Vlachothanasi, E. C. Fradelos, and D. S. B. Mouliou, "Artificial Intelligence Biosensors, False Results and Novel Future Perspectives," *Diagnostics* 15 (2025): 1037.

50. Lun-De Liao, Chin-Teng Lin, K. McDowell, et al., "Biosensor Technologies for Augmented Brain–Computer Interfaces in the Next Decades," *Proceedings of the IEEE* 100 (2012): 1553–1566, https://doi.org/10.1109/JPROC.2012.2184829.

51. C. Sun, X. Wang, M. A. Auwalu, S. Cheng, and W. Hu, "Organic Thin Film Transistors-Based Biosensors," *EcoMat* 3 (2021): e12094.

52. P. Oldroyd, S. E. Hadwe, D. G. Barone, and G. G. Malliaras, "Thin-film Implants for Bioelectronic Medicine," *MRS Bulletin* 49 (2024): 1045–1058, https://doi.org/10.1557/s43577-024-00786-7.

53. P. Oldroyd, S. Velasco-Bosom, S. L. Bidinger, T. Hasan, A. J. Boys, and G. G. Malliaras, "Fabrication of Thin-film Electrodes and Organic Electrochemical Transistors for Neural Implants," *Nature Protocols* 20 (2025): 2100–2124, https://doi.org/10.1038/s41596-024-01116-6.

54. L. Ding, Z. Zhong, C. Chen, et al., "Advances in Multiplexed Photoelectrochemical Sensors for Multiple Components," *Chemical Engineering Journal* 505 (2025): 159319, https://doi.org/10.1016/j.cej.2025.159319.

55. S. Ma, Z. Wan, C. Wang, et al., "Ultra-Sensitive and Stable Multiplexed Biosensors Array in Fully Printed and Integrated Platforms for Reliable Perspiration Analysis," *Advanced Materials* 36 (2024): 2311106, https://doi.org/10.1002/adma.202311106.

56. J. Viventi, D.-H. Kim, L. Vigeland, et al., "Flexible, Foldable, Actively Multiplexed, High-density Electrode Array for Mapping Brain Activity in Vivo," *Nature Neuroscience* 14 (2011): 1599–1605, https://doi.org/10.1038/nn.2973.

57. R. Green and M. R. Abidian, "Conducting Polymers for Neural Prosthetic and Neural Interface Applications," *Advanced Materials* 27 (2015): 7620–7637, https://doi.org/10.1002/adma.201501810.

58. N. K and C. S. Rout, "Conducting Polymers: A Comprehensive Review on Recent Advances in Synthesis, Properties and Applications," *RSC Advances* 11 (2021): 5659–5697, https://doi.org/10.1039/D0RA07800J.

59. R. Vidu, M. Rahman, M. Mahmoudi, M. Enachescu, T. D. Poteca, and I. Opris, "Nanostructures: A Platform for Brain Repair and Augmentation," *Frontiers in Systems Neuroscience* 8 (2014): 91, https://doi.org/10.3389/fnsys.2014.00091.

60. A. Domínguez-Bajo, J. M. Rosa, A. González-Mayorga, et al., "Nanostructured Gold Electrodes Promote Neural Maturation and Network Connectivity," *Biomaterials* 279 (2021): 121186, https://doi.org/10.1016/j.biomaterials.2021.121186.

61. B. L. Rodilla, A. Arché-Nunez, S. Ruiz-Gómez, et al., "Flexible metallic core–shell nanostructured electrodes for neural interfacing," *Scientific Reports* 14 (2024): 3729, https://doi.org/10.1038/s41598-024-53719-4.

62. F. Pisano, M. F. Kashif, A. Balena, et al., "Plasmonics on a Neural Implant: Engineering Light–Matter Interactions on the Nonplanar Surface of Tapered Optical Fibers," *Advanced Optical Materials* 10 (2022): 2101649, https://doi.org/10.1002/adom.202101649.

63. M. Boulingre, R. Portillo-Lara, and R. A. Green, "Biohybrid Neural Interfaces: Improving the Biological Integration of Neural Implants," *Chemical Communications* 59: 14745–14758, https://doi.org/10.1039/D3CC05006H.

64. E. K. Buschbeck, A. Duc Le, C. Kelley, M. A. Hoque, and N. T. Alvarez, "Functionalized Carbon Nanotube Microfibers for Chronic Neural Implants," *Journal of Neuroscience Methods* 364 (2021): 109370, https://doi.org/10.1016/j.jneumeth.2021.109370.

65. P. Fattahi, G. Yang, G. Kim, and M. R. Abidian, "A Review of Organic and Inorganic Biomaterials for Neural Interfaces," *Advanced Materials* 26 (2014): 1846–1885, https://doi.org/10.1002/adma.201304496.

66. M. Nikshitha, S. M. Sudhakara, and M. S. Shetty, "Organic-inorganic Hybrids: A Comprehensive Review on Synthesis and Their Potential Applications," *Materials Chemistry and Physics* 331 (2025): 130181, https://doi.org/10.1016/j.matchemphys.2024.130181.

67. Y. Wang, Y. Zha, C. Bao, et al., "Monolithic 2D Perovskites Enabled Artificial Photonic Synapses for Neuromorphic Vision Sensors," *Advanced Materials* 36 (2024): e2311524, https://doi.org/10.1002/adma.202311524.

68. A. Batool, T. A. Sherazi, and S. A. R. Naqvi, "Organic–Inorganic Nanohybrid-Based Electrochemical Biosensors," in *Hybrid Nanomaterials: Biomedical, Environmental and Energy Applications*, eds. K. Rizwan, M. Bilal, T. Rasheed, and T. A. Nguyen, (Springer Nature, 2022), 151–173, https://doi.org/10.1007/978-981-19-4538-0_8.

69. A. Lobosco, C. Lubrano, D. Rana, et al., "Enzyme-Mediated Organic Neurohybrid Synapses," *Advanced Materials* 36 (2024): 2409614, https://doi.org/10.1002/adma.202409614.

70. C. Moraldo, E. Vuille-dit-Bille, B. Shkodra, T. Kloter, and N. Nakatsuka, "Aptamer-modified Biosensors to Visualize Neurotransmitter Flux," *Journal of Neuroscience Methods* 365 (2022): 109386, https://doi.org/10.1016/j.jneumeth.2021.109386.

71. J. Blackmore, S. Shrivastava, J. Sallet, C. R. Butler, and R. O. Cleveland, "Ultrasound Neuromodulation: A Review of Results, Mechanisms and Safety," *Ultrasound in Medicine & Biology* 45 (2019): 1509–1536, https://doi.org/10.1016/j.ultrasmedbio.2018.12.015.

72. Y. Zhang, N. Jiang, and A. K. Yetisen, "Brain Neurochemical Monitoring," *Biosensors and Bioelectronics* 189 (2021): 113351, https://doi.org/10.1016/j.bios.2021.113351.

73. H. Juárez Olguín, D. Calderón Guzmán, E. Hernández García, and G. Barragán Mejía, "The Role of Dopamine and Its Dysfunction as a Consequence of Oxidative Stress," *Oxidative Medicine and Cellular Longevity* 2016 (2016): 9730467, https://doi.org/10.1155/2016/9730467.

74. B. J. Venton and Q. Cao, "Fundamentals of Fast-Scan Cyclic Voltammetry for Dopamine Detection," *The Analyst* 145 (2020): 1158–1168, https://doi.org/10.1039/C9AN01586H.

75. M. H. Khajehpour and A. Ghaffarinejad, "Dopamine Neurotransmitter Determination using Graphite Sheet–Graphene Nano-Sensor," *Graphene 2D Mater* 9 (2024): 125–135.

76. K.-Y. Tsai, H.-F. Peng, and J.-J. Huang, "Nafion Modified Electrochemical Sensor Integrated With a Feedback-loop Indium-gallium-zinc Oxide Thin-film Transistor for Enhancing Dopamine Detection Limit," *Sensors and Actuators A: Physical* 354 (2023): 114287, https://doi.org/10.1016/j.sna.2023.114287.

77. B. N. Chandrashekar, B. E. K. Swamy, M. Pandurangachar, et al., "Electrochemical Oxidation of Dopamine at Polyethylene Glycol Modified Carbon Paste Electrode: A Cyclic Voltammetric Study," *International Journal of Electrochemical Science* 5 (2010): 578–592, https://doi.org/10.1016/S1452-3981(23)15307-7.

78. M. Kanova and P. Kohout, "Serotonin—Its Synthesis and Roles in the Healthy and the Critically Ill," *International Journal of Molecular Sciences* 22 (2021): 4837, https://doi.org/10.3390/ijms22094837.

79. L. F. Mohammad-Zadeh, L. Moses, and S. M. Gwaltney-Brant, "Serotonin: A Review," *Journal of Veterinary Pharmacology and Therapeutics* 31 (2008): 187–199, https://doi.org/10.1111/j.1365-2885.2008.00944.x.

80. F. Crespi, K. F. Martin, and C. A. Marsden, "Measurement of Extracellular Basal Levels of Serotonin in Vivo Using Nafion-coated Carbon Fibre Electrodes Combined With Differential Pulse Voltammetry," *Neuroscience* 27 (1988): 885–896, https://doi.org/10.1016/0306-4522(88)90191-1.

81. N. Ezati, M. Abdouss, M. Rouhani, P. G. Kerr, and E. Kowsari, "Novel Serotonin Decorated Molecularly Imprinted Polymer Nanoparticles Based on Biodegradable Materials; a Potential Self-targeted Delivery System for Irinotecan," *Reactive and Functional Polymers* 181 (2022): 105437, https://doi.org/10.1016/j.reactfunctpolym.2022.105437.

82. N. Nakatsuka, K. J. Heard, A. Faillétaz, et al., "Sensing Serotonin Secreted From human Serotonergic Neurons Using aptamer-modified Nanopipettes," *Molecular Psychiatry* 26 (2021): 2753–2763, https://doi.org/10.1038/s41380-021-01066-5.

83. C. A. Croushore and J. V. Sweedler, "Microfluidic Systems for Studying Neurotransmitters and Neurotransmission," *Lab on a Chip* 13 (2013): 1666–1676, https://doi.org/10.1039/c3lc41334a.

84. B. S. Meldrum, "Glutamate as a Neurotransmitter in the Brain: Review of Physiology and Pathology," *The Journal of Nutrition* 130 (2000): 1007S–1015S, https://doi.org/10.1093/jn/130.4.1007S.

85. H. Atilgan, B. Unal, E. E. Yalcinkaya, et al., "Development of an Enzymatic Biosensor Using Glutamate Oxidase on Organic–Inorganic-Structured, Electrospun Nanofiber-Modified Electrodes for Monosodium Glutamate Detection," *Biosensors* 13 (2023): 430, https://doi.org/10.3390/bios13040430.

86. M. Jamal, J. Xu, and K. M. Razeeb, "Disposable Biosensor Based on Immobilisation of Glutamate Oxidase on Pt Nanoparticles Modified Au Nanowire Array Electrode," *Biosensors and Bioelectronics* 26 (2010): 1420–1424, https://doi.org/10.1016/j.bios.2010.07.071.

87. J. Xia, H. Yang, M. Mu, et al., "Imaging in Vivo Acetylcholine Release in the Peripheral Nervous System With a Fluorescent Nanosensor," *Proceedings of the National Academy of Sciences* 118 (2021): e2023807118, https://doi.org/10.1073/pnas.2023807118.

88. M. R. Picciotto, M. J. Higley, and Y. S. Mineur, "Acetylcholine as a Neuromodulator: Cholinergic Signaling Shapes Nervous System Function and Behavior," *Neuron* 76 (2012): 116–129, https://doi.org/10.1016/j.neuron.2012.08.036.

89. S. Shakil, D. Yuan, and M. Li, "Review—Electrochemical Sensors for Acetylcholine Detection," *Journal of The Electrochemical Society* 171 (2024): 067512, https://doi.org/10.1149/1945-7111/ad546e.

90. P. M. Jahani, R. Zaimbashi, M. R. Aflatoonian, S. Tajik, and H. Beitollahi, "Electrochemical sensor for acetylcholine detection based on WO3 nanorods-modified glassy carbon electrode," *Journal of Electrochemical Science and Engineering* 14 (2024): 631–641, https://doi.org/10.5599/jese.2462.

91. J. Chen, K.-C. Lin, S. Prasad, and D. W. Schmidtke, "Label Free Impedance Based Acetylcholinesterase Enzymatic Biosensors for the Detection of Acetylcholine," *Biosensors and Bioelectronics* 235 (2023): 115340, https://doi.org/10.1016/j.bios.2023.115340.

92. M. Rothaug, C. Becker-Pauly, and S. Rose-John, "The Role of Interleukin-6 Signaling in Nervous Tissue," *Biochimica et Biophysica Acta (BBA) - Molecular Cell Research* 1863 (2016): 1218–1227.

93. G. A. Prieto and C. W. Cotman, "Cytokines and Cytokine Networks Target Neurons to Modulate Long-term Potentiation," *Cytokine & Growth Factor Reviews* 34 (2017): 27–33, https://doi.org/10.1016/j.cytogfr.2017.03.005.

94. J. C. Felger and F. E. Lotrich, "Inflammatory Cytokines in Depression: Neurobiological Mechanisms and Therapeutic Implications," *Neuroscience* 246 (2013): 199–229.

95. L. Bellingacci, J. Canonichesi, A. Mancini, L. Parnetti, and M. Di Filippo, "Cytokines, Synaptic Plasticity and Network Dynamics: A Matter of Balance," *Neural Regeneration Research* 18 (2023): 2569–2572, https://doi.org/10.4103/1673-5374.371344.

96. G.-F. Chen, T.-H. Xu, Y. Yan, et al., "Amyloid Beta: Structure, Biology and Structure-based Therapeutic Development," *Acta Pharmacologica Sinica* 38 (2017): 1205–1235, https://doi.org/10.1038/aps.2017.28.

97. C.-X. Gong and K. Iqbal, "Hyperphosphorylation of Microtubule-Associated Protein Tau: A Promising Therapeutic Target for Alzheimer Disease," *Current Medicinal Chemistry* 15 (2008): 2321–2328, https://doi.org/10.2174/092986708785909111.

98. P. G. Le, S. H. Choi, and S. Cho, "Alzheimer's Disease Biomarker Detection Using Field Effect Transistor-Based Biosensor," *Biosensors* 13 (2023): 987, https://doi.org/10.3390/bios13110987.

99. S. Murugan, P. Jakka, S. Namani, V. Mujumdar, and G. Radhakrishnan, "The Neurosteroid Pregnenolone Promotes Degradation of Key Proteins in the Innate Immune Signaling to Suppress Inflammation," *Journal of Biological Chemistry* 294 (2019): 4596–4607, https://doi.org/10.1074/jbc.RA118.005543.

100. L. Stárka, M. Dušková, and M. Hill, "Dehydroepiandrosterone: A Neuroactive Steroid," *The Journal of Steroid Biochemistry and Molecular Biology* 145 (2015): 254–260, https://doi.org/10.1016/j.jsbmb.2014.03.008.

101. S. Diviccaro, L. Cioffi, E. Falvo, S. Giatti, and R. C. Melcangi, "Allopregnanolone: An Overview on Its Synthesis and Effects," *Journal of Neuroendocrinology* 34 (2022): e12996, https://doi.org/10.1111/jne.12996.

102. S. M. Paul, G. Pinna, and A. Guidotti, "Allopregnanolone: From Molecular Pathophysiology to Therapeutics. A historical perspective," *Neurobiology of Stress* 12 (2020): 100215.

103. N. Maninger, O. M. Wolkowitz, V. I. Reus, E. S. Epel, and S. H. Mellon, "Neurobiological and Neuropsychiatric Effects of Dehydroepiandrosterone (DHEA) and DHEA Sulfate (DHEAS)," *Frontiers in Neuroendocrinology* 30 (2009): 65–91, https://doi.org/10.1016/j.yfrne.2008.11.002.

104. M. Schumacher, P. Liere, Y. Akwa, et al., "Pregnenolone Sulfate in the Brain: A Controversial Neurosteroid," *Neurochemistry International* 52 (2008): 522–540, https://doi.org/10.1016/j.neuint.2007.08.022.

105. C. C. Smith, T. T. Gibbs, and D. H. Farb, "Pregnenolone Sulfate as a Modulator of Synaptic Plasticity," *Psychopharmacology* 231 (2014): 3537–3556, https://doi.org/10.1007/s00213-014-3643-x.

106. N. Alaaraj, A. Soliman, N. Hamed, S. Ahmed, and F. Alyafei, "Comprehensive Review on the Mechanisms of Thyroxine Action on Growth and Brain Development. in," *ESPE Abstracts* vol 98 (2024).

107. J. Bernal, "Thyroid Hormones in Brain Development and Function," in *Endotext*, eds. K. R. Feingold, R. A. Adler, and S. F. Ahmed, (MDText.com, Inc., 2000).

108. A. C. Schroeder and M. L. Privalsky, "Thyroid Hormones, T3 and T4, in the Brain," *Frontiers in Endocrinology* 5 (2014): 40.

109. S. Salisbury, "Cretinism: The Past, Present and Future of Diagnosis and Cure," *Paediatrics & Child Health* 8 (2003): 105–106, https://doi.org/10.1093/pch/8.2.105.

110. S. Y. Lee and E. N. Pearce, "Hyperthyroidism *A Review*," *JAMA* 330 (2023): 1472–1483.

111. E. Knezevic, K. Nenic, V. Milanovic, and N. N. Knezevic, "The Role of Cortisol in Chronic Stress, Neurodegenerative Diseases, and Psychological Disorders," *Cells* 12 (2023): 2726, https://doi.org/10.3390/cells12232726.

112. D.-N. Pan, V. L. Jentsch, K. Langer, et al., "What a Difference Timing Makes: Cortisol Effects on Neural Underpinnings of Emotion Regulation," *Neurobiology of Stress* 25 (2023): 100544, https://doi.org/10.1016/j.ynstr.2023.100544.

113. B. S. Alghamdi, "The Neuroprotective Role of Melatonin in Neurological Disorders," *Journal of Neuroscience Research* 96 (2018): 1136–1149, https://doi.org/10.1002/jnr.24220.

114. J. G. Lee, Y. S. Woo, S. W. Park, D.-H. Seog, M. K. Seo, and W.-M. Bahk, "The Neuroprotective Effects of Melatonin: Possible Role in the Pathophysiology of Neuropsychiatric Disease," *Brain Sciences* 9 (2019): 285, https://doi.org/10.3390/brainsci9100285.

115. C. Vasey, J. McBride, and K. Penta, "Circadian Rhythm Dysregulation and Restoration: The Role of Melatonin," *Nutrients* 13 (2021): 3480, https://doi.org/10.3390/nu13103480.

116. J. Hornung, C. A. Lewis, and B. Derntl, "Chapter 12 – Sex Hormones and human Brain function," in *Handbook of Clinical Neurology*, eds. R. Lanzenberger, G. S. Kranz, and I. Savic (Elsevier, 2020), 195–207.

117. Y. Hara, E. M. Waters, B. S. McEwen, and J. H. Morrison, "Estrogen Effects on Cognitive and Synaptic Health over the Lifecourse," *Physiological Reviews* 95 (2015): 785–807, https://doi.org/10.1152/physrev.00036.2014.

118. P. Celec, D. Ostatníková, and J. Hodosy, "On the Effects of Testosterone on Brain Behavioral Functions," *Frontiers in Neuroscience* 9 (2015): 12, https://doi.org/10.3389/fnins.2015.00012.

119. S. Schiavone and L. Trabace, "Small Molecules: Therapeutic Application in Neuropsychiatric and Neurodegenerative Disorders," *Mol J Synth Chem Nat Prod Chem* 23 (2018): 411.

120. P. Kumar, D. Kumar, S. K. Jha, N. K. Jha, and R. K. Ambasta, "Chapter Three—Ion Channels in Neurological Disorders," in *Advances in Protein Chemistry and Structural Biology*, ed. R. Donev (Academic Press, 2016), 97–136.

121. W. A. Banks and N. H. Greig, "Small Molecules as Central Nervous System Therapeutics: Old Challenges, New Directions, and a Philosophic Divide," *Future Medicinal Chemistry* 11 (2019): 489–493, https://doi.org/10.4155/fmc-2018-0436.

122. A. K. Locke, A. K. Means, P. Dong, T. J. Nichols, G. L. Coté, and M. A. Grunlan, "A Layer-by-Layer Approach To Retain a Fluorescent Glucose Sensing Assay Within the Cavity of a Hydrogel Membrane," *ACS Applied Bio Materials* 1 (2018): 1319–1327, https://doi.org/10.1021/acsabm.8b00267.

123. X. Jin, G. Li, T. Xu, L. Su, D. Yan, and X. Zhang, "Fully Integrated Flexible Biosensor for Wearable Continuous Glucose Monitoring," *Biosensors and Bioelectronics* 196 (2022): 113760, https://doi.org/10.1016/j.bios.2021.113760.

124. J. P. Lowry, M. Miele, R. D. O'Neill, M. G. Boutelle, and M. Fillenz, "An Amperometric Glucose-Oxidase/Poly(*o*-phenylenediamine) Biosensor for Monitoring Brain Extracellular Glucose: In Vivo Characterisation in the Striatum of Freely-moving Rats," *Journal of Neuroscience Methods* 79 (1998): 65–74, https://doi.org/10.1016/S0165-0270(97)00171-4.

125. A. Enrico, S. Buchmann, F. De Ferrari, et al., "Cleanroom-Free Direct Laser Micropatterning of Polymers for Organic Electrochemical Transistors in Logic Circuits and Glucose Biosensors," *Advanced Science* 11 (2024): 2307042, https://doi.org/10.1002/advs.202307042.

126. N. German, A. Kausaite-Minkstimiene, A. Ramanavicius, T. Semashko, R. Mikhailova, and A. Ramanaviciene, "The Use of Different Glucose Oxidases for the Development of an Amperometric Reagentless Glucose Biosensor Based on Gold Nanoparticles Covered by Polypyrrole," *Electrochimica Acta* 169 (2015): 326–333, https://doi.org/10.1016/j.electacta.2015.04.072.

127. K. R. Choi, B. K. Troudt, and P. Bühlmann, "Ion-Selective Electrodes With Sensing Membranes Covalently Attached to Both the Inert Polymer Substrate and Conductive Carbon Contact," *Angewandte Chemie International Edition* 62 (2023): e202304674, https://doi.org/10.1002/anie.202304674.

128. C. Yang, R.-Y. Pan, F. Guan, and Z. Yuan, "Lactate Metabolism in Neurodegenerative Diseases," *Neural Regeneration Research* 19 (2023): 69–74, https://doi.org/10.4103/1673-5374.374142.

129. K. Dagar, V. Narwal, and C. S. Pundir, "An Enhanced L-lactate Biosensor Based on Nanohybrid of Chitosan, Iron-nanoparticles and Carboxylated Multiwalled Carbon Nanotubes," *Sensors International* 4 (2023): 100245, https://doi.org/10.1016/j.sintl.2023.100245.

130. J.-L. Lafuente, S. González, C. Aibar, D. Rivera, E. Avilés, and J.-J. Beunza, "Continuous and Non-Invasive Lactate Monitoring Techniques in Critical Care Patients," *Biosensors* 14 (2024): 148, https://doi.org/10.3390/bios14030148.

131. M. A. Abrar, Y. Dong, P. K. Lee, and W. S. Kim, "Bendable Electrochemical Lactate Sensor Printed With Silver Nano-particles," *Scientific Reports* 6 (2016): 30565, https://doi.org/10.1038/srep30565.

132. O. Alijevic, Z. Peng, and S. Kellenberger, "Changes in H+, K+, and Ca2+ Concentrations, as Observed in Seizures, Induce Action Potential Signaling in Cortical Neurons by a Mechanism That Depends Partially on Acid-Sensing Ion Channels," *Frontiers in Cellular Neuroscience* 15 (2021), https://doi.org/10.3389/fncel.2021.732869.

133. M. A. Booth, S. A. N. Gowers, M. Hersey, et al., "Fiber-Based Electrochemical Biosensors for Monitoring pH and Transient Neurometabolic Lactate," *Analytical Chemistry* 93 (2021): 6646–6655, https://doi.org/10.1021/acs.analchem.0c05108.

134. Y. Chen, X. Li, D. Li, C. Batchelor-McAuley, and R. G. Compton, "A Simplified Methodology: pH Sensing Using an in Situ Fabricated Ir Electrode Under Neutral Conditions," *Journal of Solid State Electrochemistry* 25 (2021): 2821–2833, https://doi.org/10.1007/s10008-021-05017-6.

135. Y. Liu, Y. Diao, G. Hu, et al., "Renewable Antimony-based pH Sensor," *Journal of Electroanalytical Chemistry* 928 (2023): 117085, https://doi.org/10.1016/j.jelechem.2022.117085.

136. H. Ren, K. Liang, D. Li, et al., "Field-Effect Transistor-Based Biosensor for pH Sensing and Mapping," *Advanced Sensor Research* 2 (2023): 2200098, https://doi.org/10.1002/adsr.202200098.

137. J. Zou, H. Bai, L. Zhang, et al., "Ion-sensitive Field Effect Transistor Biosensors for Biomarker Detection: Current Progress and Challenges," *Journal of Materials Chemistry B* 12 (2024): 8523–8542, https://doi.org/10.1039/D4TB00719K.

138. D. Angelis, R. Savani, and L. Chalak, "Nitric Oxide and the Brain. Part 1: Mechanisms of Regulation, Transport and Effects on the Developing Brain," *Pediatric Research* 89 (2021): 738–745, https://doi.org/10.1038/s41390-020-1017-0.

139. D. Angelis, R. Savani, and L. Chalak, "Nitric Oxide and The Brain. Part 2: Effects Following Neonatal Brain Injury—Friend or Foe?," *Pediatric Research* 89 (2021): 746–752, https://doi.org/10.1038/s41390-020-1021-4.

140. K. P. Dobmeier, G. W. Charville, and M. H. Schoenfisch, "Nitric Oxide-Releasing Xerogel-Based Fiber-Optic pH Sensors," *Analytical Chemistry* 78 (2006): 7461–7466, https://doi.org/10.1021/ac060995p.

141. B. K. Oh, M. E. Robbins, and M. H. Schoenfisch, "Planar Nitric Oxide (NO)-selective Ultramicroelectrode Sensor for Measuring Localized NO Surface Concentrations at xerogel Microarrays," *The Analyst* 131 (2006): 48–54, https://doi.org/10.1039/B507981K.

142. P. Luo, M. Xie, J. Luo, H. Kan, and Q. Wei, "Nitric Oxide Sensors Using Nanospiral ZnO Thin Film Deposited by GLAD for Application to Exhaled human Breath," *RSC Advances* 10 (2020): 14877–14884.

143. Y. Hu, X. Hu, J. Qiu, et al., "Nitric Oxide Detector Based on WO_3-1wt%In_2O_3-1wt%Nb_2O_5 With State-of-the-Art Selectivity and Ppb-Level Sensitivity," *ACS Applied Materials & Interfaces* 10 (2018): 42583–42592, https://doi.org/10.1021/acsami.8b14243.

144. A. V. Mokrushina, M. Heim, E. E. Karyakina, A. Kuhn, and A. A. Karyakin, "Enhanced Hydrogen Peroxide Sensing Based on Prussian Blue Modified Macroporous Microelectrodes," *Electrochemistry Communications* 29 (2013): 78–80, https://doi.org/10.1016/j.elecom.2013.01.004.

145. C. Liu, Y. Zhao, X. Cai, et al., "A Wireless, Implantable Optoelectrochemical Probe for Optogenetic Stimulation and Dopamine Detection," *Microsystems & Nanoengineering* 6 (2020): 64, https://doi.org/10.1038/s41378-020-0176-9.

146. O. A. Bamalan, M. J. Moore, and Y. Al Khalili, "Physiology, Serotonin," in *StatPearls* (StatPearls Publishing, 2025).

147. A. Carvajal-Oliveros and J. M. Campusano, "Studying the Contribution of Serotonin to Neurodevelopmental Disorders. Can This Fly?," *Frontiers in Behavioral Neuroscience* 14 (2021), https://doi.org/10.3389/fnbeh.2020.601449.

148. "Institute of Medicine (US) Forum on Neuroscience and Nervous System Disorders.Washington (DC)," in *Glutamate-Related Biomarkers in Drug Development for Disorders of the Nervous System: Workshop Summary* (National Academies Press, 2011).

149. M. M. G. Pal, "The Master Neurotransmitter and Its Implications in Chronic Stress and Mood Disorders," *Frontiers in Human Neuroscience* 15 (2021): 722323.

150. J. D. Braga, M. Thongngam, and T. Kumrungsee, "Gamma-Aminobutyric Acid as A Potential Postbiotic Mediator in the Gut–Brain Axis," *npj Science of Food* 8 (2024): 16, https://doi.org/10.1038/s41538-024-00253-2.

151. G. A. R. Johnston and P. M. Beart, "Milestone Review: GABA, From Chemistry, Conformations, Ionotropic Receptors, Modulators, Epilepsy, Flavonoids, and Stress to Neuro-Nutraceuticals," *Journal of Neurochemistry* 168 (2024): 1179–1192, https://doi.org/10.1111/jnc.16087.

152. A. Slezia, C. M. Proctor, A. Kaszas, G. G. Malliaras, and A. Williamson, "Electrophoretic Delivery of γ-aminobutyric Acid (GABA) Into Epileptic Focus Prevents Seizures in Mice," *JOVE-Journal Of Visualized Experiments* (2019): e59268, https://doi.org/10.3791/59268.

153. Q. Huang, C. Liao, F. Ge, J. Ao, and T. Liu, "Acetylcholine Bidirectionally Regulates Learning and Memory," *Journal of Neurorestoratology* 10 (2022): 100002, https://doi.org/10.1016/j.jnrt.2022.100002.

154. R. Webster, *Acetylcholine (ACh). in Neurotransmitters, Drugs and Brain Function* (John Wiley & Sons, 2001), 117–136, https://doi.org/10.1002/0470846577.ch6.

155. L. Froese, J. Dian, A. Gomez, B. Unger, and F. A. Zeiler, "The Cerebrovascular Response to Norepinephrine: A Scoping Systematic Review of the Animal and human Literature," *Pharmacology Research & Perspectives* 8 (2020): e00655, https://doi.org/10.1002/prp2.655.

156. J. O'Donnell, D. Zeppenfeld, E. McConnell, S. Pena, and M. Nedergaard, "Norepinephrine: A Neuromodulator That Boosts the Function of Multiple Cell Types to Optimize CNS Performance," *Neurochemical Research* 37 (2012): 2496–2512.

157. E. Saboory, M. Ghasemi, and N. Mehranfard, "Norepinephrine, Neurodevelopment and Behavior," *Neurochemistry International* 135 (2020): 104706, https://doi.org/10.1016/j.neuint.2020.104706.

158. M. Erta, A. Quintana, and J. Hidalgo, "Interleukin-6, a Major Cytokine in the Central Nervous System," *International Journal of Biological Sciences* 8 (2012): 1254–1266, https://doi.org/10.7150/ijbs.4679.

159. N. Gonzalez Caldito, "Role of Tumor Necrosis Factor-Alpha in the Central Nervous System: A Focus on Autoimmune Disorders," *Frontiers in Immunology* 14 (2023): 1213448, https://doi.org/10.3389/fimmu.2023.1213448.

160. L. Leung and C. M. Cahill, "TNF-α and Neuropathic Pain—A Review," *Journal of Neuroinflammation* 7 (2010): 27, https://doi.org/10.1186/1742-2094-7-27.

161. H. Hampel, J. Hardy, K. Blennow, et al., "The Amyloid-β Pathway in Alzheimer's Disease," *Molecular Psychiatry* 26 (2021): 5481–5503, https://doi.org/10.1038/s41380-021-01249-0.

162. M. Goedert, "Tau Protein and Neurodegeneration," *Seminars in Cell & Developmental Biology* 15 (2004): 45–49, https://doi.org/10.1016/j.semcdb.2003.12.015.

163. J. Lantero-Rodriguez, E. Camporesi, L. Montoliu-Gaya, et al., "Tau Protein Profiling in Tauopathies: A Human Brain Study," *Molecular Neurodegeneration* 19 (2024): 54, https://doi.org/10.1186/s13024-024-00741-9.

164. A. Michalicova, P. Majerova, and A. Kovac, "Tau Protein and Its Role in Blood–Brain Barrier Dysfunction," *Frontiers in Molecular Neuroscience* 13 (2020), https://doi.org/10.3389/fnmol.2020.570045.

165. C.-J. Liou, C.-M. Yang, T.-H. Lee, P.-S. Liu, and H.-L. Hsieh, "Neuroprotective Effects of Dehydroepiandrosterone Sulfate through Inhibiting Expression of Matrix Metalloproteinase-9 From Bradykinin-Challenged Astroglia," *Molecular Neurobiology* 56 (2019): 736–747, https://doi.org/10.1007/s12035-018-1125-6.

166. J. Bernal, "Thyroid Hormone Receptors in Brain Development and Function," *Nature Clinical Practice Endocrinology & Metabolism* 3 (2007): 249–259, https://doi.org/10.1038/ncpendmet0424.

167. H. Huang, P. Liu, D. Ma, et al., "Triiodothyronine Attenuates Neurocognitive Dysfunction Induced by Sevoflurane in the Developing Brain of Neonatal Rats," *Journal of Affective Disorders* 297 (2022): 455–462, https://doi.org/10.1016/j.jad.2021.10.086.

168. D. Ullrich, D. Führer, H. Heuer, et al., "Triiodothyronine Treatment in Mice Improves Stroke Outcome and Reduces Blood–Brain Barrier Damage," *European Thyroid Journal* 14 (2025), https://doi.org/10.1530/ETJ-24-0143.

169. K. L. Brunson, N. Khan, M. Eghbal-Ahmadi, and T. Z. Baram, "Corticotropin (ACTH) Acts Directly on Amygdala Neurons to Down-Regulate Corticotropin-Releasing Hormone Gene Expression," *Annals of Neurology* 49 (2001): 304–312, https://doi.org/10.1002/ana.66.

170. A. J. Dunn and W. Hendrik Gispen, "How ACTH Acts on the Brain," *Biobehavioral Reviews* 1 (1977): 15–23, https://doi.org/10.1016/0147-7552(77)90037-7.

171. K. D. Ketchesin, G. S. Stinnett, and A. F. Seasholtz, "Corticotropin-Releasing Hormone-Binding Protein and Stress: From Invertebrates to Humans," *Stress Amst Neth* 20 (2017): 449–464.

172. A. Slominski, "On the Role of the Corticotropin-releasing Hormone Signalling System in the Aetiology of Inflammatory Skin Disorders," *British Journal of Dermatology* 160 (2009): 229–232, https://doi.org/10.1111/j.1365-2133.2008.08958.x.

173. T. Scherer, K. Sakamoto, and C. Buettner, "Brain Insulin Signalling in Metabolic Homeostasis and Disease," *Nature Reviews Endocrinology* 17 (2021): 468–483, https://doi.org/10.1038/s41574-021-00498-x.

174. M. Shaughness, D. Acs, F. Brabazon, N. Hockenbury, and K. R. Byrnes, "Role of Insulin in Neurotrauma and Neurodegeneration: A Review," *Frontiers in Neuroscience* 14 (2020): 547175, https://doi.org/10.3389/fnins.2020.547175.

175. A. H. Dyer, C. Vahdatpour, A. Sanfeliu, and D. Tropea, "The Role of Insulin-Like Growth Factor 1 (IGF-1) in Brain Development, Maturation

and Neuroplasticity," *Neuroscience* 325 (2016): 89–99, https://doi.org/10.1016/j.neuroscience.2016.03.056.

176. A. Nuñez, J. Zegarra-Valdivia, D. Fernandez de Sevilla, J. Pignatelli, and I. Torres Aleman, "The Neurobiology of Insulin-Like Growth Factor I: From Neuroprotection to Modulation of Brain States," *Molecular Psychiatry* 28 (2023): 3220–3230.

177. F. Ferrini, C. Salio, L. Lossi, and A. Merighi, "Ghrelin in Central Neurons," *Current Neuropharmacology* 7 (2009): 37–49, https://doi.org/10.2174/157015909787602779.

178. Q. Jiao, X. Du, Y. Li, et al., "The Neurological Effects of ghrelin in Brain Diseases: Beyond Metabolic Functions," *Neuroscience & Biobehavioral Reviews* 73 (2017): 98–111, https://doi.org/10.1016/j.neubiorev.2016.12.010.

179. D. Serrenho, S. D. Santos, and A. L. Carvalho, "The Role of Ghrelin in Regulating Synaptic Function and Plasticity of Feeding-Associated Circuits," *Frontiers in Cellular Neuroscience* 13 (2019), https://doi.org/10.3389/fncel.2019.00205.

180. A. Caron, S. Lee, J. K. Elmquist, and L. Gautron, "Leptin and Brain–Adipose Crosstalks," *Nature Reviews Neuroscience* 19 (2018): 153–165, https://doi.org/10.1038/nrn.2018.7.

181. Y. Fujita and T. Yamashita, "The Effects of Leptin on Glial Cells in Neurological Diseases," *Frontiers in Neuroscience* 13 (2019): 828, https://doi.org/10.3389/fnins.2019.00828.

182. X. Zou, L. Zhong, C. Zhu, et al., "Role of Leptin in Mood Disorder and Neurodegenerative Disease," *Frontiers in Neuroscience* 13 (2019), https://doi.org/10.3389/fnins.2019.00378.

183. M. A. Bentsen, Z. Mirzadeh, and M. W. Schwartz, "Revisiting How the Brain Senses Glucose—And Why," *Cell Metabolism* 29 (2019): 11–17, https://doi.org/10.1016/j.cmet.2018.11.001.

184. S. Ritter, "Monitoring and Maintenance of Brain Glucose Supply: Importance of Hindbrain Catecholamine Neurons in this Multifaceted Task," in *Appetite and Food Intake: Central Control*, ed. R. B. S. Harris (CRC Press/Taylor & Francis, 2017), https://doi.org/10.1201/9781315120171.

185. P. Mergenthaler, U. Lindauer, G. A. Dienel, and A. Meisel, "Sugar for the Brain: The Role of Glucose in Physiological and Pathological Brain Function," *Trends in Neurosciences* 36 (2013): 587–597, https://doi.org/10.1016/j.tins.2013.07.001.

186. D. R. Tomlinson and N. J. Gardiner, "Glucose Neurotoxicity," *Nature Reviews Neuroscience* 9 (2008): 36–45, https://doi.org/10.1038/nrn2294.

187. C. R. Figley, "Lactate Transport and Metabolism in the Human Brain: Implications for the Astrocyte-Neuron Lactate Shuttle Hypothesis," *The Journal of Neuroscience* 31 (2011): 4768–4770, https://doi.org/10.1523/JNEUROSCI.6612-10.2011.

188. P. J. Magistretti and I. Allaman, "Lactate in the Brain: From Metabolic End-Product to Signalling Molecule," *Nature Reviews Neuroscience* 19 (2018): 235–249, https://doi.org/10.1038/nrn.2018.19.

189. V. Calabrese, C. Mancuso, M. Calvani, E. Rizzarelli, D. A. Butterfield, and A. M. Giuffrida Stella, "Nitric Oxide in the central Nervous System: Neuroprotection versus Neurotoxicity," *Nature Reviews Neuroscience* 8 (2007): 766–775, https://doi.org/10.1038/nrn2214.

190. A. Covarrubias-Pinto, A. I. Acuña, F. A. Beltrán, L. Torres-Díaz, and M. A. Castro, "Old Things New View: Ascorbic Acid Protects the Brain in Neurodegenerative Disorders," *International Journal of Molecular Sciences* 16 (2015): 28194–28217, https://doi.org/10.3390/ijms161226095.

191. M. Moretti and A. L. S. Rodrigues, "Functional Role of Ascorbic Acid in the Central Nervous System: A Focus on Neurogenic and Synaptogenic Processes," *Nutritional Neuroscience* 25 (2022): 2431–2441, https://doi.org/10.1080/1028415X.2021.1956848.

192. P. Fang, X. Li, J. J. Luo, H. Wang, and X. Yang, "A Double-edged Sword: Uric Acid and Neurological Disorders," *Brain Disorders & Therapy* 2 (2013): 109.

193. N. Otani, E. Hoshiyama, M. Ouchi, H. Takekawa, and K. Suzuki, "Uric Acid and Neurological Disease: A Narrative Review," *Frontiers in Neurology* 14 (2023): 1164756, https://doi.org/10.3389/fneur.2023.1164756.

194. C. A. Shaji, B. D. Robinson, A. Yeager, M. R. Beeram, and M. L. Davis, "The Tri-phasic Role of Hydrogen Peroxide in Blood-Brain Barrier Endothelial cells," *Scientific Reports* 9 (2019): 133.

195. D. Bailey and E. B. Rizk, "Origin and Use of Hydrogen Peroxide in Neurosurgery," *Neurosurgery* 89 (2021): E3–E7, https://doi.org/10.1093/neuros/nyab107.

196. R. Nisticò, S. Piccirilli, M. L. Cucchiaroni, et al., "Neuroprotective Effect of Hydrogen Peroxide on an in Vitro Model of Brain Ischaemia," *British Journal of Pharmacology* 153 (2008): 1022–1029, https://doi.org/10.1038/sj.bjp.0707587.

197. A. Sathe, Y. Yang, K. G. Schilling, et al., "Free-water: A Promising Structural Biomarker for Cognitive Decline in Aging and Mild Cognitive Impairment," *Imaging Neuroscience* 2 (2024): 1–16, https://doi.org/10.1162/imag_a_00293.

198. Y. Cao, Y. Xu, M. Cao, et al., "Fluid-based Biomarkers for Neurodegenerative Diseases," *Ageing Research Reviews* 108 (2025): 102739, https://doi.org/10.1016/j.arr.2025.102739.

199. F. Ji, O. Pasternak, Y. L. Chai, et al., "Brain free-water increases mediate the association of blood cardiovascular biomarkers With longitudinal cognitive decline in prodromal and clinical dementia," *Alzheimer's & Dementia* 16 (2020): e044477, https://doi.org/10.1002/alz.044477.

200. X.-Z. Jing, G.-Y. Li, Y.-P. Wu, et al., "Free water imaging as a novel biomarker in Wilson's disease: A cross-sectional study," *Parkinsonism & Related Disorders* 106 (2023): 105234, https://doi.org/10.1016/j.parkreldis.2022.105234.

201. Y. Fukuda and H. H. Loeschcke, "Effect of H+ on Spontaneous Neuronal Activity in the Surface Layer of the Rat Medulla Oblongata in Vitro," *Pflugers Archiv European Journal of Physiology* 371 (1977): 125–134, https://doi.org/10.1007/BF00580780.

202. J. A. Neubauer and J. Sunderram, "Oxygen-sensing Neurons in the central Nervous System," *Journal of Applied Physiology* 96 (2004): 367–374, https://doi.org/10.1152/japplphysiol.00831.2003.

203. D. André-Lévigne, R. Pignel, S. Boet, V. Jaquet, D. F. Kalbermatten, and S. Madduri, "Role of Oxygen and Its Radicals in Peripheral Nerve Regeneration: From Hypoxia to Physoxia to Hyperoxia," *International Journal of Molecular Sciences* 25 (2024): 2030, https://doi.org/10.3390/ijms25042030.

204. T. Akaishi, E. Onishi, M. Abe, et al., "The human central Nervous System Discharges Carbon Dioxide and Lactic Acid Into the Cerebrospinal Fluid," *Fluids and Barriers of the CNS* 16 (2019): 8, https://doi.org/10.1186/s12987-019-0128-7.

205. R.-M. Deng, Y.-C. Liu, J.-Q. Li, J.-G. Xu, and G. Chen, "The Role of Carbon Dioxide in Acute Brain Injury," *Medical Gas Research* 10 (2020): 81–84.

206. Q. Qiu, M. Yang, D. Gong, H. Liang, and T. Chen, "Potassium and Calcium Channels in Different Nerve Cells Act as Therapeutic Targets in Neurological Disorders," *Neural Regeneration Research* 20 (2025): 1258–1276, https://doi.org/10.4103/NRR.NRR-D-23-01766.

207. K. A. Alam, P. Svalastoga, A. Martinez, J. C. Glennon, and J. Haavik, "Potassium Channels in Behavioral Brain Disorders. Molecular Mechanisms and Therapeutic Potential: A Narrative Review," *Neuroscience & Biobehavioral Reviews* 152 (2023): 105301, https://doi.org/10.1016/j.neubiorev.2023.105301.

208. T. Glaser, V. F. Arnaud Sampaio, C. Lameu, and H. Ulrich, "Calcium Signalling: A Common Target in Neurological Disorders and Neurogenesis," *Seminars in Cell & Developmental Biology* 95 (2019): 25–33, https://doi.org/10.1016/j.semcdb.2018.12.002.

209. E. Pchitskaya, E. Popugaeva, and I. Bezprozvanny, "Calcium Signaling and Molecular Mechanisms Underlying Neurodegenerative Dis-

eases," *Cell Calcium* 70 (2018): 87–94, https://doi.org/10.1016/j.ceca.2017.06.008.

210. G. Zündorf and G. Reiser, "Calcium Dysregulation and Homeostasis of Neural Calcium in the Molecular Mechanisms of Neurodegenerative Diseases Provide Multiple Targets for Neuroprotection," *Antioxidants & Redox Signaling* 14 (2011): 1275–1288.

211. Y.-G. Fan, T.-Y. Wu, L.-X. Zhao, et al., "From Zinc Homeostasis to Disease Progression: Unveiling the Neurodegenerative Puzzle," *Pharmacological Research* 199 (2024): 107039, https://doi.org/10.1016/j.phrs.2023.107039.

212. Z. Li, Y. Liu, R. Wei, V. W. Yong, and M. Xue, "The Important Role of Zinc in Neurological Diseases," *Biomolecules* 13 (2022): 28, https://doi.org/10.3390/biom13010028.

213. J. Wang, T. He, and C. Lee, "Development of Neural Interfaces and Energy Harvesters towards Self-powered Implantable Systems for Healthcare Monitoring and Rehabilitation Purposes," *Nano Energy* 65 (2019): 104039, https://doi.org/10.1016/j.nanoen.2019.104039.

214. W. Ouyang, W. Lu, Y. Zhang, and Y. Liu, "A Wireless and Batteryless Implant for Multimodal Closed-loop Neuromodulation in Small Animals," *Nature Biomedical Engineering* 7 (2023): 1252–1269, https://doi.org/10.1038/s41551-023-01029-x.

215. S. Oh, J. Jekal, J. Liu, et al., "Bioelectronic Implantable Devices for Physiological Signal Recording and Closed-Loop Neuromodulation," *Advanced Functional Materials* 34 (2024): 2403562, https://doi.org/10.1002/adfm.202403562.

216. S. Park, H. Yuk, R. Zhao, et al., "Adaptive and Multifunctional Hydrogel Hybrid Probes for Long-term Sensing and Modulation of Neural Activity," *Nature Communications* 12 (2021): 3435, https://doi.org/10.1038/s41467-021-23802-9.

217. G. Gong, Y. Zhou, Q. Li, and W. Zhao, "Bioinspired Adaptive Sensors: A Review on Current Developments in Theory and Application," *Advanced Materials* (2025): 2505420.

218. N. Mintz Hemed, F.-J. Hwang, E. T. Zhao, J. B. Ding, and N. A. Melosh, "Multiplexed neurochemical sensing With sub-nM sensitivity Across 2.25 mm2 area," *Biosensors and Bioelectronics* 261 (2024): 116474, https://doi.org/10.1016/j.bios.2024.116474.

219. B. Gil Rosa, O. E. Akingbade, and X. Guo, "Multiplexed Immunosensors for Point-of-care Diagnostic Applications," *Biosensors and Bioelectronics* 203 (2022): 114050, https://doi.org/10.1016/j.bios.2022.114050.

220. G. Korbakis and P. M. Vespa, "Multimodal Neurologic Monitoring," *Handb Clin Neurol* 140 (2017): 91–105.

221. L. Li, B. Zhang, W. Zhao, et al., "Multimodal Technologies for Closed-Loop Neural Modulation and Sensing," *Advanced Healthcare Materials* 13 (2024): 2303289, https://doi.org/10.1002/adhm.202303289.

222. M. E. E. Alahi, A. Nag, and S. C. Mukhopadhyay, "Self-Powered Implantable Energy Harvesters for Medical Electronics," in *Flexible Sensors for Energy-Harvesting Applications*, eds. A. Nag and S. C. Mukhopadhyay (Springer International Publishing, 2022), 169–184, https://doi.org/10.1007/978-3-030-99600-0_8.

223. Z. L. Wang, "Self-Powered Nanosensors and Nanosystems," *Advanced Materials* 24 (2012): 280–285, https://doi.org/10.1002/adma.201102958.

224. Z. Wu, T. Cheng, and Z. L. Wang, "Self-Powered Sensors and Systems Based on Nanogenerators," *Sensors* 20 (2020): 2925.

225. M. Mariello, "Recent Advances on Hybrid Piezo-Triboelectric Bio-Nanogenerators: Materials, Architectures and Circuitry," *Nanoenergy Advances* 2 (2022): 64–109, https://doi.org/10.3390/nanoenergyadv2010004.

226. NeuroPace, RNS® System Responsive Thalamic Stimulation for Primary Generalized Seizures (NAUTILUS) Study, https://clinicaltrials.gov/study/NCT05147571 (2024).

227. K. L. Montgomery, A. J. Yeh, J. S. Ho, et al., "Wirelessly Powered, Fully Internal Optogenetics for Brain, Spinal and Peripheral Circuits in Mice," *Nature Methods* 12 (2015): 969–974, https://doi.org/10.1038/nmeth.3536.

228. H. Zhang, P. Gutruf, K. Meacham, et al., "Wireless, Battery-free Optoelectronic Systems as Subdermal Implants for Local Tissue Oximetry," *Science Advances* 5 (2019): eaaw0873, https://doi.org/10.1126/sciadv.aaw0873.

229. T. Stuart, W. J. Jeang, R. A. Slivicki, et al., "Wireless, Battery-Free Implants for Electrochemical Catecholamine Sensing and Optogenetic Stimulation," *ACS Nano* 17 (2023): 561–574, https://doi.org/10.1021/acsnano.2c09475.

230. D. Maity, P. Guha Ray, P. Buchmann, M. Mansouri, and M. Fussenegger, "Blood-Glucose-Powered Metabolic Fuel Cell for Self-Sufficient Bioelectronics," *Advanced Materials* 35 (2023): 2300890.

231. H. Zhao, S. Xue, M.-D. Hussherr, A. P. Teixeira, and M. Fussenegger, "Autonomous Push Button–Controlled Rapid Insulin Release From a Piezoelectrically Activated Subcutaneous Cell Implant," *Science Advances* 8 (2022): eabm4389, https://doi.org/10.1126/sciadv.abm4389.

232. L. Dong, C. Jin, A. B. Closson, et al., "Cardiac Energy Harvesting and Sensing Based on Piezoelectric and Triboelectric Designs," *Nano Energy* 76 (2020): 105076, https://doi.org/10.1016/j.nanoen.2020.105076.

233. J. E. Fleming, E. Dunn, and M. M. Lowery, "Simulation of Closed-Loop Deep Brain Stimulation Control Schemes for Suppression of Pathological Beta Oscillations in Parkinson's Disease," *Frontiers in Neuroscience* 14 (2020), https://doi.org/10.3389/fnins.2020.00166.

234. S. Wang, G. Zhu, L. Shi, and C. Zhang, "Closed-Loop Adaptive Deep Brain Stimulation in Parkinson's Disease: Procedures to Achieve It and Future Perspectives," *J Park Dis* 13 (2023): 453–471.

235. L. A. Johnson, S. D. Nebeck, A. Muralidharan, M. D. Johnson, K. B. Baker, and J. L. Vitek, "Closed-Loop Deep Brain Stimulation Effects on Parkinsonian Motor Symptoms in a Non-Human Primate—Is Beta Enough?," *Brain Stimulation* 9 (2016): 892–896, https://doi.org/10.1016/j.brs.2016.06.051.

236. N. Dale, S. Hatz, F. Tian, and E. Llaudet, "Listening to the Brain: Microelectrode Biosensors for Neurochemicals," *Trends in Biotechnology* 23 (2005): 420–428, https://doi.org/10.1016/j.tibtech.2005.05.010.

237. L.-E. Cheran, P. Benvenuto, and M. Thompson, "Coupling of Neurons With Biosensor Devices for Detection of the Properties of Neuronal Populations," *Chemical Society Reviews* 37 (2008): 1229–1242, https://doi.org/10.1039/b712830b.

238. M. Mirzaei and M. Sawan, "Microelectronics-Based Biosensors Dedicated to the Detection of Neurotransmitters: A Review," *Sensors* 14 (2014): 17981–18008, https://doi.org/10.3390/s141017981.

239. X. Fan, W. Nie, H. Tsai, and N. Wang, "PEDOT:PSS for Flexible and Stretchable Electronics: Modifications, Strategies, and Applications," *Advanced Science* 6 (2019): 1900813.

240. K. V. Ratnam, H. Manjunatha, S. Janardan, K. C. Babu Naidu, and S. Ramesh, "Nonenzymatic Electrochemical Sensor Based on Metal Oxide, MO (M = Cu, Ni, Zn, and Fe) Nanomaterials for Neurotransmitters: An Abridged Review," *Sensors International* 1 (2020): 100047, https://doi.org/10.1016/j.sintl.2020.100047.

241. B. M. Blaschke, N. Tort-Colet, and A. Guimerà-Brunet, "Mapping Brain Activity with Flexible Graphene Micro-Transistors," *2D Mater* 4 (2017): 025040.

242. A. M. Baracu and L. A. Dinu Gugoasa, "Review—Recent Advances in Microfabrication, Design and Applications of Amperometric Sensors and Biosensors," *Journal of The Electrochemical Society* 168 (2021): 037503, https://doi.org/10.1149/1945-7111/abe8b6.

243. R. Thull and D. Grant, "Physical and Chemical Vapor Deposition and Plasma-assisted Techniques for Coating Titanium," in *Titanium in Medicine: Material Science, Surface Science, Engineering, Biological Responses and Medical Applications*, eds. D. M. Brunette, P. Tengvall, M.

Textor, and P. Thomsen (Springer, 2001), 283–341, https://doi.org/10.1007/978-3-642-56486-4_10.

244. W. Huang, X. Wang, M. Sheng, et al., "Low Temperature PECVD SiNx Films Applied in OLED Packaging," *Materials Science and Engineering: B* 98 (2003): 248–254, https://doi.org/10.1016/S0921-5107(03)00045-X.

245. D. Framil, M. Van Gompel, F. Bourgeois, I. Furno, and Y. Leterrier, "The Influence of Microstructure on Nanomechanical and Diffusion Barrier Properties of Thin PECVD SiOx Films Deposited on Parylene C Substrates," *Frontiers in Materials* 6 (2019): 319, https://doi.org/10.3389/fmats.2019.00319.

246. S. Majee, D. Barshilia, S. Kumar, P. Mishra, and J. Akhtar, "Signature of Growth Deposition Technique on the Properties of PECVD and Thermal SiO2," in *AIP Conf. Proc* (2018), 020023.

247. J. Bian, L. Zhou, X. Wan, and C. Zhu, "Laser Transfer, Printing, and Assembly Techniques for Flexible Electronics," *Advanced Electronic Materials* 5 (2019): 1800900.

248. B. Derby, "Inkjet Printing of Functional and Structural Materials: Fluid Property Requirements, Feature Stability, and Resolution," *Annual Review of Materials Research* 40 (2010): 395–414, https://doi.org/10.1146/annurev-matsci-070909-104502.

249. A. Negro, T. Cherbuin, and M. P. Lutolf, "3D Inkjet Printing of Complex, Cell-Laden Hydrogel Structures," *Scientific Reports* 8 (2018): 17099.

250. M. Singh, H. M. Haverinen, P. Dhagat, and G. E. Jabbour, "Inkjet Printing—Process and Its Applications," *Advanced Materials* 22 (2010): 673–685, https://doi.org/10.1002/adma.200901141.

251. R. Sharan, S. Prabhakaran, and R. Mohan, "Screen-printed Electrodes for Detection of Neurotransmitters," in *Future Approaches to Electrochemical Sensing of Neurotransmitters*, eds. K. S. Shalini Devi and S. Tsujimura (Royal Society of Chemistry, 2025), https://doi.org/10.1039/9781837675593.

252. A. García-Miranda Ferrari, S. J. Rowley-Neale, and C. E. Banks, "Screen-printed Electrodes: Transitioning the Laboratory in-to-the Field," *Talanta Open* 3 (2021): 100032, https://doi.org/10.1016/j.talo.2021.100032.

253. E. Cantù, S. Tonello, G. Abate, and D. Uberti, "Aerosol Jet Printed 3D Electrochemical Sensors for Protein Detection," *Sensors* 18 (2018): 3719.

254. E. W. C. Phuah, W. L. Hart, H. Sumer, and P. R. Stoddart, "Patterning of Biomaterials by Aerosol Jet Printing: A Parametric Study," *Bioprinting* 18 (2020): e00081, https://doi.org/10.1016/j.bprint.2020.e00081.

255. S. Fruncillo, X. Su, H. Liu, and L. S. Wong, "Lithographic Processes for the Scalable Fabrication of Micro- and Nanostructures for Biochips and Biosensors," *ACS Sensors* 6 (2021): 2002–2024.

256. B. Della Ventura, R. Funari, K. K. Anoop, and S. Amoruso, "Nano-machining of Biosensor Electrodes Through Gold Nanoparticles Deposition Produced by Femtosecond Laser Ablation," *Applied Physics B* 119 (2015): 497–501, https://doi.org/10.1007/s00340-015-6091-3.

257. M. A. A. Rehmani, K. Lal, A. Shaukat, and K. M. Arif, "Laser Ablation Assisted Micropattern Screen Printed Transduction Electrodes for Sensing Applications," *Scientific Reports* 12 (2022): 6928, https://doi.org/10.1038/s41598-022-10878-6.

258. E. T. Athira and J. Satija, "Plasmonic Nanoparticle Etching-based Optical Sensors: Current Status and Future Prospects," *The Analyst* 148 (2023): 6188–6200, https://doi.org/10.1039/D3AN01244A.

259. C. Jiang, F. Yan, Y. Qin, et al., "A Sensitive Acetylcholinesterase Biosensor Based on NaOH Etching Glassy Carbon Electrode for Electrochemical Determination of 3-nitropropionic Acid," *Journal of Electroanalytical Chemistry* 893 (2021): 115329, https://doi.org/10.1016/j.jelechem.2021.115329.

260. R. Guider, D. Gandolfi, T. Chalyan, et al., "Sensitivity and Limit of Detection of Biosensors Based on Ring Resonators," *Sensing and Bio-Sensing Research* 6 (2015): 99–102, https://doi.org/10.1016/j.sbsr.2015.08.002.

261. Á. Lavín, J. D. Vicente, M. Holgado, and M. F. Laguna, "On the Determination of Uncertainty and Limit of Detection in Label-Free Biosensors," *Sensors* 18 (2018): 2038.

262. Í. Molina-Fernández, J. Leuermann, A. Ortega-Moñux, J. G. Wangüemert-Pérez, and R. Halir, "Biosensors With Coherent Phase Readout," *Optics Express* 27 (2019): 12616–12629, https://doi.org/10.1364/OE.27.012616.

263. D. Badocco, I. Lavagnini, A. Mondin, G. Favaro, and P. Pastore, "Definition of the limit of quantification in the presence of instrumental and non-instrumental errors. Comparison Among various definitions applied to the calibration of zinc by inductively coupled plasma–mass spectrometry," *Spectrochimica Acta Part B: Atomic Spectroscopy* 114 (2015): 81–86, https://doi.org/10.1016/j.sab.2015.10.004.

264. D. A. Armbruster and T. Pry, "Limit of Blank, Limit of Detection and Limit of Quantitation," *Clinical Biochemist Reviews* 29 (2008): S49–S52.

265. S. Ahmed, N. Shaikh, N. Pathak, and A. Sonawane, "Chapter 3 – An Overview of Sensitivity and Selectivity of Biosensors for Environmental applications," in *Tools, Techniques and Protocols for Monitoring Environmental Contaminants*, eds. S. Kaur Brar, K. Hegde, and V. L. Pachapur (Elsevier, 2019), 53–73, https://doi.org/10.1016/B978-0-12-814679-8.00003-0.

266. N. Bhalla, P. Jolly, N. Formisano, and P. Estrela, "Introduction to Biosensors," *Essays in Biochemistry* 60 (2016): 1–8.

267. B. Bucur, C. Purcarea, S. Andreescu, and A. Vasilescu, "Addressing the Selectivity of Enzyme Biosensors: Solutions and Perspectives," *Sensors* 21 (2021): 3038, https://doi.org/10.3390/s21093038.

268. W. J. Peveler, M. Yazdani, and V. M. Rotello, "Selectivity and Specificity: Pros and Cons in Sensing," *ACS Sensors* 1 (2016): 1282–1285.

269. B. Purohit, P. R. Vernekar, N. P. Shetti, and P. Chandra, "Biosensor Nanoengineering: Design, Operation, and Implementation for Biomolecular Analysis," *Sensors International* 1 (2020): 100040, https://doi.org/10.1016/j.sintl.2020.100040.

270. Y. Ou, A. Marie Buchanan, C. E. Witt, and P. Hashemi, "Frontiers in Electrochemical Sensors for Neurotransmitter Detection: Towards Measuring Neurotransmitters as Chemical Diagnostics for Brain Disorders," *Analytical Methods* 11 (2019): 2738–2755, https://doi.org/10.1039/C9AY00055K.

271. R. Machado, N. Soltani, S. Dufour, et al., "Biofouling-Resistant Impedimetric Sensor for Array High-Resolution Extracellular Potassium Monitoring in the Brain," *Biosensors* 6 (2016): 53, https://doi.org/10.3390/bios6040053.

272. X. Xu, Y. Zuo, S. Chen, A. Hatami, and H. Gu, "Advancements in Brain Research: The In Vivo/In Vitro Electrochemical Detection of Neurochemicals," *Biosensors* 14 (2024): 125.

273. Y. Liu, Z. Liu, Y. Zhou, and Y. Tian, "Implantable Electrochemical Sensors for Brain Research," *JACS Au* 3 (2023): 1572–1582, https://doi.org/10.1021/jacsau.3c00200.

274. M. Mariello, K. Kim, K. Wu, S. P. Lacour, and Y. Leterrier, "Recent Advances in Encapsulation of Flexible Bioelectronic Implants: Materials, Technologies, and Characterization Methods," *Advanced Materials* 34 (2022): 2201129.

275. J. A. Rogers, T. Someya, and Y. Huang, "Materials and Mechanics for Stretchable Electronics," *Science* 327 (2010): 1603–1607, https://doi.org/10.1126/science.1182383.

276. B. Fan, B. Wolfrum, and J. T. Robinson, "Impedance Scaling for Gold and Platinum Microelectrodes," *Journal of Neural Engineering* 18 (2021): 056025, https://doi.org/10.1088/1741-2552/ac20e5.

277. Q. Zhang, G. Zhao, S. Wang, Y. Song, and Y. Sun, "Polymer-Based Electrochemical Sensors for the Diagnosis of Neurodegenerative Diseases," *Cellular and Molecular Neurobiology* 45 (2025): 52, https://doi.org/10.1007/s10571-025-01570-0.

278. L. Ferlauto, A. N. D'Angelo, P. Vagni, et al., "Development and Characterization of PEDOT:PSS/Alginate Soft Microelectrodes for Application

in Neuroprosthetics," *Frontiers in Neuroscience* 12 (2018), https://doi.org/10.3389/fnins.2018.00648.

279. J. Li, D. Mo, J. Hu, et al., "PEDOT:PSS-based Bioelectronics for Brain Monitoring and Modulation," *Microsystems & Nanoengineering* 11 (2025): 87, https://doi.org/10.1038/s41378-025-00948-w.

280. P. Calcagnile, L. Blasi, F. Rizzi, et al., "Parylene C Surface Functionalization and Patterning With pH-Responsive Microgels," *ACS Applied Materials & Interfaces* 6 (2014): 15708–15715, https://doi.org/10.1021/am502467y.

281. B. J. Coelho, J. V. Pinto, J. Martins, et al., "Parylene C as a Multipurpose Material for Electronics and Microfluidics," *Polymers* 15 (2023): 2277, https://doi.org/10.3390/polym15102277.

282. M. Mariello, M. von Allmen, K. Wu, M. Van Gompel, S. P. Lacour, and Y. Leterrier, "Hermetic, Hybrid Multilayer, Sub-5µm-Thick Encapsulations Prepared With Vapor-Phase Infiltration of Metal Oxides in Conformal Polymers for Flexible Bioelectronics," *Advanced Functional Materials* 34, no. 41 (2024): 2403973, https://doi.org/10.1002/adfm.202403973.

283. A. Altuna, E. Bellistri, E. Cid, et al., "SU-8 Based Microprobes for Simultaneous Neural Depth Recording and Drug Delivery in the Brain," *Lab on a Chip* 13 (2013): 1422–1430, https://doi.org/10.1039/c3lc41364k.

284. G. Márton, E. Z. Tóth, L. Wittner, et al., "The Neural Tissue Around SU-8 Implants: A Quantitative in Vivo Biocompatibility Study," *Materials Science and Engineering: C* 112 (2020): 110870, https://doi.org/10.1016/j.msec.2020.110870.

285. B. Rubehn and T. Stieglitz, "In Vitro Evaluation of the Long-term Stability of Polyimide as a Material for Neural Implants," *Biomaterials* 31 (2010): 3449–3458, https://doi.org/10.1016/j.biomaterials.2010.01.053.

286. K. C. Cheung, P. Renaud, H. Tanila, and K. Djupsund, "Flexible Polyimide Microelectrode Array for in Vivo Recordings and Current Source Density Analysis," *Biosensors and Bioelectronics* 22 (2007): 1783–1790, https://doi.org/10.1016/j.bios.2006.08.035.

287. A. B. Frazier and M. G. Allen, "Metallic Microstructures Fabricated Using Photosensitive Polyimide Electroplating Molds," *Journal of Microelectromechanical Systems* 2 (1993): 87–94, https://doi.org/10.1109/84.232605.

288. X. Hu, F. Yang, M. Guo, J. Pei, H. Zhao, and Y. Wang, "Fabrication of Polyimide Microfluidic Devices by Laser Ablation Based Additive Manufacturing," *Microsystem Technologies* 26 (2020): 1573–1583, https://doi.org/10.1007/s00542-019-04698-4.

289. J. S. Ordonez, C. Boehler, M. Schuettler, and T. Stieglitz, "Improved Polyimide Thin-film Electrodes for Neural Implants," 2012 Annual International Conference of the IEEE Engineering in Medicine and Biology Society (IEEE, 2012): 5134–5137.

290. F. Fu, J. Wang, H. Zeng, and J. Yu, "Functional Conductive Hydrogels for Bioelectronics," *ACS Materials Letters* 2 (2020): 1287–1301, https://doi.org/10.1021/acsmaterialslett.0c00309.

291. K. Sagdic, E. Fernández-Lavado, M. Mariello, O. Akouissi, and S. P. Lacour, "Hydrogels and Conductive Hydrogels for Implantable Bioelectronics," *MRS Bulletin* 48 (2023): 495–505, https://doi.org/10.1557/s43577-023-00536-1.

292. Y. Wang, J. Liu, Y. Zhu, D. Zhu, and H. Chen, "Formation and Characterization of Dendritic Interfacial Electrodes inside an Ionomer," *ACS Applied Materials & Interfaces* 9 (2017): 30258–30262, https://doi.org/10.1021/acsami.7b08012.

293. S. Nisar, G. Dastgeer, Z. M. Shazad, et al., "2D Materials in Advanced Electronic Biosensors for Point-of-Care Devices," *Advanced Science* 11 (2024): 2401386, https://doi.org/10.1002/advs.202401386.

294. B. Della Ventura, M. Banchelli, R. Funari, et al., "Biosensor Surface Functionalization by a Simple Photochemical Immobilization of Antibodies: Experimental Characterization by Mass Spectrometry and Surface Enhanced Raman Spectroscopy," *The Analyst* 144 (2019): 6871–6880, https://doi.org/10.1039/C9AN00443B.

295. A. Henriksson, P. Neubauer, and M. Birkholz, "Functionalization of Oxide-Free Silicon Surfaces for Biosensing Applications," *Advanced Materials Interfaces* 8 (2021): 2100927, https://doi.org/10.1002/admi.202100927.

296. D. Zigah, M. Pellissier, B. Fabre, F. Barrière, and P. Hapiot, "Covalent Immobilization and SECM Analysis in Feedback Mode of Glucose Oxidase on a Modified Oxidized Silicon Surface," *Journal of Electroanalytical Chemistry* 628 (2009): 144–147, https://doi.org/10.1016/j.jelechem.2009.01.013.

297. M. Patel, M. Agrawal, and A. Srivastava, "Signal Amplification Strategies in Electrochemical Biosensors via Antibody Immobilization and Nanomaterial-based Transducers," *Materials Advances* 3 (2022): 8864–8885, https://doi.org/10.1039/D2MA00427E.

298. R. J. Chen, S. Bangsaruntip, K. A. Drouvalakis, et al., "Noncovalent Functionalization of Carbon Nanotubes for Highly Specific Electronic Biosensors," *Proceedings of the National Academy of Sciences* 100 (2003): 4984–4989, https://doi.org/10.1073/pnas.0837064100.

299. W. Putzbach and N. J. Ronkainen, "Immobilization Techniques in the Fabrication of Nanomaterial-Based Electrochemical Biosensors: A Review," *Sensors* 13 (2013): 4811–4840, https://doi.org/10.3390/s130404811.

300. B. A. Snopok, A. Laroussi, T. V. Snopok, and S. Nizamov, "Electrostatic Surface Functionalization of Physical Transducers of (Bio)Chemical Sensors: Thiocyanate-Modified Gold Interface," *Engineering Proceedings* 82 (2024): 70.

301. M. Oliverio, S. Perotto, G. C. Messina, L. Lovato, and F. De Angelis, "Chemical Functionalization of Plasmonic Surface Biosensors: A Tutorial Review on Issues, Strategies, and Costs," *ACS Applied Materials & Interfaces* 9 (2017): 29394–29411, https://doi.org/10.1021/acsami.7b01583.

302. O. Seitz, P. G. Fernandes, R. Tian, et al., "Control and Stability of Self-assembled Monolayers Under Biosensing Conditions," *Journal of Materials Chemistry* 21 (2011): 4384–4392, https://doi.org/10.1039/c1jm10132c.

303. D. Blasi, L. Sarcina, A. Tricase, et al., "Enhancing the Sensitivity of Biotinylated Surfaces by Tailoring the Design of the Mixed Self-Assembled Monolayer Synthesis," *ACS Omega* 5 (2020): 16762–16771, https://doi.org/10.1021/acsomega.0c01717.

304. S. Dong and J. Li, "Self-assembled Monolayers of Thiols on Gold Electrodes for Bioelectrochemistry and Biosensors," *Bioelectrochemistry and Bioenergetics* 42 (1997): 7–13, https://doi.org/10.1016/S0302-4598(96)05172-0.

305. A. Tewari, K. Björkström, A. M. Ghafari, E. Macchia, L. Torsi, and R. Österbacka, "Stability of Thiol-based Self-assembled Monolayer Functionalized Electrodes in EG-OFET-based Applications," *FlatChem* 42 (2023): 100553, https://doi.org/10.1016/j.flatc.2023.100553.

306. L. Rouvière, N. Al-Hajj, J. Hunel, et al., "Silane-Based SAMs Deposited by Spin Coating as a Versatile Alternative Process to Solution Immersion," *Langmuir* 38 (2022): 6464–6471, https://doi.org/10.1021/acs.langmuir.2c00668.

307. G. K. Toworfe, S. Bhattacharyya, R. J. Composto, C. S. Adams, I. M. Shapiro, and P. Ducheyne, "Effect of functional end groups of silane self-assembled monolayer surfaces on apatite formation, fibronectin adsorption and osteoblast cell function," *Journal of Tissue Engineering and Regenerative Medicine* 3 (2009): 26–36, https://doi.org/10.1002/term.131.

308. M. J. Russo, M. Han, P. E. Desroches, et al., "Antifouling Strategies for Electrochemical Biosensing: Mechanisms and Performance Toward Point of Care Based Diagnostic Applications," *ACS Sensors* 6 (2021): 1482–1507, https://doi.org/10.1021/acssensors.1c00390.

309. C. Erkmen, O. Selcuk, D. N. Unal, S. Kurbanoglu, and B. Uslu, "Layer-by-layer Modification Strategies for Electrochemical Detection of Biomarkers," *Biosens Bioelectron X* 12 (2022): 100270.

310. S. Mariani, V. Robbiano, L. M. Strambini, et al., "Layer-by-layer Biofunctionalization of Nanostructured Porous Silicon for High-sensitivity

and High-selectivity Label-free Affinity Biosensing," *Nature Communications* 9 (2018): 5256, https://doi.org/10.1038/s41467-018-07723-8.

311. S. Malik, J. Singh, R. Goyat, and Y. Saharan, "Nanomaterials-Based Biosensor and Their Applications: A Review," *Heliyon* 9 (2023): e19929.

312. Z. Bérces, Á. Horvátha, A. Jádyc, and A. Pongrácz, "Neural Cell Response to Nanostructured Biosensor Surfaces," *Procedia Engineering* 87 (2014): 971–974.

313. M. Ramesh, R. Janani, C. Deepa, and L. Rajeshkumar, "Nanotechnology-Enabled Biosensors: A Review of Fundamentals, Design Principles, Materials, and Applications," *Biosensors* 13 (2022): 40.

314. R. Li, H. Qi, Y. Ma, et al., "A Flexible and Physically Transient Electrochemical Sensor for Real-time Wireless Nitric Oxide Monitoring," *Nature Communications* 11 (2020): 3207, https://doi.org/10.1038/s41467-020-17008-8.

315. Y. Zhao, K.-Q. Jin, J.-D. Li, and K.-K. Sheng, "Flexible and Stretchable Electrochemical Sensors for Biological Monitoring," *Advanced Materials* 37 (2025): 2305917.

316. Z. Ghasemi, H. Salimi Jazi, M. Kharaziha, K. Raeissi, and F. Karimzadeh, "A Freestanding Electrochemical Sensor Based on Surface Molecularly Imprinted Polydopamine for Glucose Detection," *Surfaces and Interfaces* 62 (2025): 106144, https://doi.org/10.1016/j.surfin.2025.106144.

317. O. Demkiv, W. Nogala, N. Stasyuk, H. Klepach, T. Danysh, and M. Gonchar, "Highly Sensitive Amperometric Sensors Based on Laccase-mimetic Nanozymes for the Detection of Dopamine," *RSC Advances* 14 (2024): 5472–5478, https://doi.org/10.1039/D3RA07587G.

318. X. Liu and J. Liu, "Biosensors and sensors for dopamine detection," *VIEW* 2 (2021): 20200102.

319. K. Y. Inoue, M. Matsudaira, R. Kubo, et al., "LSI-based Amperometric Sensor for Bio-imaging and Multi-point Biosensing," *Lab on a Chip* 12 (2012): 3481–3490, https://doi.org/10.1039/c2lc40323d.

320. J. C. Patel, "Voltammetry: Electrochemical Detection of Neurotransmitters in the Brain," in *Encyclopedia of Life Sciences* (John Wiley & Sons, 2016), 1–14, https://doi.org/10.1002/9780470015902.a0025817.

321. A. Navaee and A. Salimi, "Chapter 7 – Enzyme-based Electrochemical Biosensors," in *Electrochemical Biosensors*, ed. A. A. Ensafi (Elsevier, 2019), 167–211, https://doi.org/10.1016/B978-0-12-816491-4.00007-3.

322. I. S. Kucherenko, O. O. Soldatkin, D. Y. Kucherenko, O. V. Soldatkinacd, and S. V. Dzyadevych, "Advances in Nanomaterial Application in Enzyme-based Electrochemical Biosensors: A Review," *Nanoscale Advances* 1 (2019): 4560–4577, https://doi.org/10.1039/C9NA00491B.

323. J. M. Seibold, S. W. Abeykoon, A. E. Ross, and R. J. White, "Development of an Electrochemical, Aptamer-Based Sensor for Dynamic Detection of Neuropeptide Y," *ACS Sensors* 8 (2023): 4504–4511.

324. T. Cheng, N. Afshan, J. Jiao, and J. Jiao, "Current Progress in Aptamer-based Sensors for the Detection of Protein Biomarkers in Neurodegenerative Diseases," *Biosensors and Bioelectronics: X* 20 (2024): 100528.

325. Q. Liu, W. Zhang, S. Chen, et al., "SELEX Tool: A Novel and Convenient Gel-based Diffusion Method for Monitoring of Aptamer-target Binding," *Journal of Biological Engineering* 14 (2020): 1, https://doi.org/10.1186/s13036-019-0223-y.

326. K. Sefah, D. Shangguan, X. Xiong, M. B. O'Donoghue, and W. Tan, "Development of DNA Aptamers Using Cell-SELEX," *Nature Protocols* 5 (2010): 1169–1185, https://doi.org/10.1038/nprot.2010.66.

327. N. K. Navani and Y. Li, "Nucleic Acid Aptamers and Enzymes as Sensors," *Current Opinion in Chemical Biology* 10 (2006): 272–281, https://doi.org/10.1016/j.cbpa.2006.04.003.

328. M. A. Romero-Reyes, K. N. Patterson, and J. M. Heemstra, "Co-immobilization of Enzymes and Aptamers to Create Self-Regenerating Ultrafiltration Membranes for Toxin Removal," *ACS Materials Letters* 5 (2023): 1565–1569, https://doi.org/10.1021/acsmaterialslett.3c00055.

329. Y. Jia, S. Chen, Q. Wang, and J. Li, "Recent Progress in Biosensor Regeneration Techniques," *Nanoscale* 16 (2024): 2834–2846, https://doi.org/10.1039/D3NR05456J.

330. Y. Du, B. Li, H. Wei, Y. Wang, and E. Wang, "Multifunctional Label-Free Electrochemical Biosensor Based on an Integrated Aptamer," *Analytical Chemistry* 80 (2008): 5110–5117, https://doi.org/10.1021/ac800303c.

331. H. Gao, Y. Bai, B. He, and C. S. Tan, "A Simple Label-Free Aptamer-Based Electrochemical Biosensor for the Sensitive Detection of C-Reactive Proteins," *Biosensors* 12 (2022): 1180, https://doi.org/10.3390/bios12121180.

332. S. Li, Y. Coffinier, C. Lagadec, et al., "Redox-labelled Electrochemical Aptasensors With Nanosupported Cancer Cells," *Biosensors and Bioelectronics* 216 (2022): 114643, https://doi.org/10.1016/j.bios.2022.114643.

333. Y. Biniuri, G.-F. Luo, M. Fadeev, V. Wulf, and I. Willner, "Redox-Switchable Binding Properties of the ATP–Aptamer," *Journal of the American Chemical Society* 141 (2019): 15567–15576, https://doi.org/10.1021/jacs.9b06256.

334. M. D. Mayer and R. Y. Lai, "Effects of Redox Label Location on the Performance of an Electrochemical Aptamer-based Tumor Necrosis Factor-alpha Sensor," *Talanta* 189 (2018): 585–591, https://doi.org/10.1016/j.talanta.2018.07.055.

335. G. Matteoli, S. Luin, L. Bellucci, R. Nifosì, F. Beltram, and G. Signore, "Aptamer-based Gold Nanoparticle Aggregates for Ultrasensitive Amplification-free Detection of PSMA," *Scientific Reports* 13 (2023): 19926, https://doi.org/10.1038/s41598-023-46974-4.

336. T.-C. Chiu and C.-C. Huang, "Aptamer-Functionalized Nano-Biosensors," *Sensors* 9 (2009): 10356–10388.

337. S. Niazi, I. M. Khan, W. Akhtar, et al., "Aptamer Functionalized Gold Nanoclusters as an Emerging Nanoprobe in Biosensing, Diagnostic, Catalysis and Bioimaging," *Talanta* 268 (2024): 125270, https://doi.org/10.1016/j.talanta.2023.125270.

338. E. Fernandes, A. Ledo, G. A. Gerhardt, and R. M. Barbosa, "Amperometric Bio-sensing of Lactate and Oxygen Concurrently With Local Field Potentials During *Status Epilepticus*," *Talanta* 268 (2024): 125302, https://doi.org/10.1016/j.talanta.2023.125302.

339. A. Stuber, A. Cavaccini, A. Manole, et al., "Interfacing Aptamer-Modified Nanopipettes With Neuronal Media and Ex Vivo Brain Tissue," *ACS Measurement Science Au* 4 (2024): 92–103, https://doi.org/10.1021/acsmeasuresciau.3c00047.

340. R. B. Rashid, X. Ji, and J. Rivnay, "Organic Electrochemical Transistors in Bioelectronic Circuits," *Biosensors & Bioelectronics* 113461 (2021), https://doi.org/10.1016/j.bios.2021.113461.

341. M. Wu, K. Yao, N. Huang, et al., "Ultrathin, Soft, Bioresorbable Organic Electrochemical Transistors for Transient Spatiotemporal Mapping of Brain Activity," *Advanced Science* 10 (2023): 2300504, https://doi.org/10.1002/advs.202300504.

342. K. Xie, N. Wang, X. Lin, and Z. Wang, "Organic Electrochemical Transistor Arrays for Real-Time Mapping of Evoked Neurotransmitter Release In Vivo," *eLife* 9 (2020): e50345.

343. F. Hempel, J. K. Y. Law, T. C. Nguyen, et al., "PEDOT:PSS Organic Electrochemical Transistors for Electrical Cell-substrate Impedance Sensing Down to Single Cells," *Biosensors and Bioelectronics* 180 (2021): 113101, https://doi.org/10.1016/j.bios.2021.113101.

344. S. T. Keene, T. P. A. van der Pol, D. Zakhidov, et al., "Enhancement-Mode PEDOT:PSS Organic Electrochemical Transistors Using Molecular De-Doping," *Advanced Materials* 32 (2020): 2000270, https://doi.org/10.1002/adma.202000270.

345. S.-M. Kim, C.-H. Kim, Y. Kim, et al., "Influence of PEDOT:PSS Crystallinity and Composition on Electrochemical Transistor Performance and Long-term Stability," *Nature Communications* 9 (2018): 3858, https://doi.org/10.1038/s41467-018-06084-6.

346. S. Carli, M. Bianchi, M. Di Lauro, et al., "Multifunctionally-doped PEDOT for Organic Electrochemical Transistors," *Frontiers in Materials* 9 (2022), https://doi.org/10.3389/fmats.2022.1063763.

347. M. Luginieski, B. B. M. Torres, and G. C. Faria, "Guidelines on Measuring Volumetric Capacitance in Organic Electrochemical Transistors," *ACS Applied Electronic Materials* 6 (2024): 2225–2231, https://doi.org/10.1021/acsaelm.3c01673.

348. M. Skowrons, D. Dahal, P. R. Paudel, and B. Lüssem, "Depletion Type Organic Electrochemical Transistors and the Gradual Channel Approximation," *Advanced Functional Materials* 34 (2024): 2303324, https://doi.org/10.1002/adfm.202303324.

349. X. Ji, X. Lin, and J. Rivnay, "Organic Electrochemical Transistors as on-site Signal Amplifiers for Electrochemical Aptamer-based Sensing," *Nature Communications* 14 (2023): 1665, https://doi.org/10.1038/s41467-023-37402-2.

350. Z. Lu, K. Xu, K. Xiao, et al., "Biomolecule Sensors Based on Organic Electrochemical Transistors," *npj Flexible Electronics* 9 (2025): 9, https://doi.org/10.1038/s41528-025-00383-x.

351. Y. Deng, H. Qi, Y. Ma, et al., "A Flexible and Highly Sensitive Organic Electrochemical Transistor-based Biosensor for Continuous and Wireless Nitric Oxide Detection," *Proceedings of the National Academy of Sciences* 119 (2022): e2208060119, https://doi.org/10.1073/pnas.2208060119.

352. S. Wang, X. Chen, C. Zhao, et al., "An Organic Electrochemical Transistor for Multi-modal Sensing, Memory and Processing," *Nature Electronics* 6 (2023): 281–291, https://doi.org/10.1038/s41928-023-00950-y.

353. I. Gualandi, D. Tonelli, F. Mariani, and E. Scavetta, "Selective Detection of Dopamine With an all PEDOT:PSS Organic Electrochemical Transistor," *Science Reports* 6 (2016): 35419.

354. W. Li, J. Jin, T. Xiong, P. Yu, and L. Mao, "Fast-Scanning Potential-Gated Organic Electrochemical Transistors for Highly Sensitive Sensing of Dopamine in Living Rat Brain," *Angewandte Chemie International Edition* 61 (2022): e202204134, https://doi.org/10.1002/anie.202204134.

355. I. Gualandi, M. Tessarolo, F. Mariani, et al., "Layered Double Hydroxide-Modified Organic Electrochemical Transistor for Glucose and Lactate Biosensing," *Sensors* 20 (2020): 3453, https://doi.org/10.3390/s20123453.

356. B. Burtscher, P. A. Manco Urbina, C. Diacci, et al., "Sensing Inflammation Biomarkers With Electrolyte-Gated Organic Electronic Transistors," *Advanced Healthcare Materials* 10 (2021): 2100955, https://doi.org/10.1002/adhm.202100955.

357. B. Burtscher, C. Diacci, A. Makhinia, et al., "Functionalization of PEDOT:PSS for Aptamer-based Sensing of IL6 Using Organic Electrochemical Transistors," *Npj Biosensing* 1 (2024): 7, https://doi.org/10.1038/s44328-024-00007-w.

358. A. Raza, U. Farooq, K. Naseem, et al., "A Focused Review on Organic Electrochemical Transistors: A Potential Futuristic Technological Application in Microelectronics," *Microchemical Journal* 207 (2024): 111737, https://doi.org/10.1016/j.microc.2024.111737.

359. M. H. Park, J. Kim, S. C. Lee, et al., "Critical Role of Silk Fibroin Secondary Structure on the Dielectric Performances of Organic Thin-film Transistors," *RSC Advances* 6 (2016): 5907–5914, https://doi.org/10.1039/C5RA20826B.

360. C.-H. Wang, C.-Y. Hsieh, and J.-C. Hwang, "Flexible Organic Thin-Film Transistors With Silk Fibroin as the Gate Dielectric," *Advanced Materials* 23 (2011): 1630–1634, https://doi.org/10.1002/adma.201004071.

361. D.-L. Wen, D.-H. Sun, P. Huang, et al., "Recent Progress in Silk Fibroin-based Flexible Electronics," *Microsystems & Nanoengineering* 7 (2021): 1–25, https://doi.org/10.1038/s41378-021-00261-2.

362. W. Huang, J. Chen, Y. Yao, et al., "Vertical Organic Electrochemical Transistors for Complementary Circuits," *Nature* 613 (2023): 496–502, https://doi.org/10.1038/s41586-022-05592-2.

363. G. Frusconi, Z. M. Kovács-Vajna, P. W. M. Blom, P. Gkoupidenis, and F. Torricelli, "Microfabrication of Organic Electrochemical Transistors for High-Performance Integrated Bioelectronics," *Advanced Materials Technologies* 10 (2025): 2401440, https://doi.org/10.1002/admt.202401440.

364. W. Huang, Y. Zhang, M. Song, et al., "Encapsulation Strategies on 2D Materials for Field Effect Transistors and Photodetectors," *Chinese Chemical Letters* 33 (2022): 2281–2290, https://doi.org/10.1016/j.cclet.2021.08.086.

365. P. M. Bulemo, D.-H. Kim, H. Shin, and H.-J. Cho, "Selectivity in Chemiresistive Gas Sensors: Strategies and Challenges," *Chemical Reviews* 125 (2025): 4111–4183.

366. H. Zhang, Z. Zhang, Z. Li, H. Han, W. Song, and J. Yi, "A Chemiresistive-potentiometric Multivariate Sensor for Discriminative Gas Detection," *Nature Communications* 14 (2023): 3495, https://doi.org/10.1038/s41467-023-39213-x.

367. S. Dhall, J. Prakash, A. Nigam, A. K. Astakala, and K. Sood, "WO3-based Chemiresistive Sensors for NO Detection at Low Temperatures," *Microchemical Journal* 215 (2025): 114366, https://doi.org/10.1016/j.microc.2025.114366.

368. S.-X. L. Luo and T. M. Swager, "Chemiresistive Sensing With Functionalized Carbon Nanotubes," *Nature Reviews Methods Primers* 3 (2023): 73, https://doi.org/10.1038/s43586-023-00255-6.

369. R. J. Rath, S. Farajikhah, F. Oveissi, F. Dehghani, and S. Naficy, "Chemiresistive Sensor Arrays for Gas/Volatile Organic Compounds Monitoring: A Review," *Advanced Engineering Materials* 25 (2023): 2200830, https://doi.org/10.1002/adem.202200830.

370. N. Nasiri and C. Clarke, "Nanostructured Chemiresistive Gas Sensors for Medical Applications," *Sensors* 19 (2019): 462.

371. A. K. Sharma and A. Mahajan, "Chapter 8 – Potential Applications of Chemiresistive Gas sensors," in *Carbon Nanomaterials and Their Nanocomposite-Based Chemiresistive Gas Sensors*, ed. S. Dhall (Elsevier, 2023), 223–245, https://doi.org/10.1016/B978-0-12-822837-1.00002-2.

372. Y. Li, Y. Mao, C. Xiao, X. Xu, and X. Li, "Flexible pH Sensor Based on a Conductive PANI Membrane for pH Monitoring," *RSC Advances* 10 (2019): 21–28, https://doi.org/10.1039/C9RA09188B.

373. P. George, J. Muthuswamy, J. Currie, N. Thakor, and M. Paranjape, "Sensing Nitric Oxide Neuronal Messengers Using Screen-Printed Carbon Micro-Electrode Arrays," in *Transducers '01 Eurosensors XV*, ed. E. Obermeier (Springer, 2001), 378–381, https://doi.org/10.1007/978-3-642-59497-7_90.

374. E. C. Rutherford, F. Pomerleau, P. Huettl, I. Strömberg, and G. A. Gerhardt, "Chronic second-by-second measures of l -glutamate in the central nervous system of freely moving rats," *Journal of Neurochemistry* 102 (2007): 712–722, https://doi.org/10.1111/j.1471-4159.2007.04596.x.

375. O. Frey, J. Rothe, F. Heer, P. D. van der Wal, N. F. de Rooij, and A. Hierlemann, "Multisite Monitoring of Choline Using Biosensor Microprobe Arrays in Combination With CMOS Circuitry," *Biomedical Engineering / Biomedizinische Technik* 59 (2014): 305–314, https://doi.org/10.1515/bmt-2012-0098.

376. L. C. Kimble, J. S. Twiddy, J. M. Berger, and A. G. Forderhase, "Simultaneous, Real-Time Detection of Glutamate and Dopamine in Rat Striatum Using Fast-Scan Cyclic Voltammetry," *ACS Sensors* 8 (2023): 4091–4100.

377. A. Mendoza, T. Asrat, F. Liu, P. Wonnenberg, and A. G. Zestos, "Carbon Nanotube Yarn Microelectrodes Promote High Temporal Measurements of Serotonin Using Fast Scan Cyclic Voltammetry," *Sensors* 20 (2020): 1173, https://doi.org/10.3390/s20041173.

378. E. Castagnola, R. Garg, S. K. Rastogi, T. Cohen-Karni, and X. T. Cui, "3D fuzzy Graphene Microelectrode Array for Dopamine Sensing at Sub-cellular Spatial Resolution," *Biosensors and Bioelectronics* 191 (2021): 113440, https://doi.org/10.1016/j.bios.2021.113440.

379. M. K. Zachek, J. Park, P. Takmakov, R. M. Wightman, and G. S. McCarty, "Microfabricated FSCV-Compatible Microelectrode Array for Real-time Monitoring of Heterogeneous Dopamine Release," *The Analyst* 135 (2010): 1556–1563, https://doi.org/10.1039/c0an00114g.

380. A. K. Dengler and G. S. McCarty, "Microfabricated Microelectrode Sensor for Measuring Background and Slowly Changing Dopamine Concentrations," *Journal of Electroanalytical Chemistry* 693 (2013): 28–33, https://doi.org/10.1016/j.jelechem.2013.01.022.

381. O. Frey, T. Holtzman, R. M. McNamara, et al., "Enzyme-based Choline and L-glutamate Biosensor Electrodes on Silicon Microprobe Arrays," *Biosensors and Bioelectronics* 26 (2010): 477–484, https://doi.org/10.1016/j.bios.2010.07.073.

382. J. Njagi, M. M. Chernov, J. C. Leiter, and S. Andreescu, "Amperometric Detection of Dopamine in Vivo With an Enzyme Based Carbon fiber Microbiosensor," *Analytical Chemistry* 82 (2010): 989–996, https://doi.org/10.1021/ac9022605.

383. O. N. Schuvailo, S. V. Dzyadevych, A. V. El'skaya, et al., "Carbon Fibre-based Microbiosensors for in Vivo Measurements of Acetylcholine and Choline," *Biosensors and Bioelectronics* 21 (2005): 87–94, https://doi.org/10.1016/j.bios.2004.09.017.

384. C. Dias, E. Fernandes, R. M. Barbosa, and A. Ledo, "A Platinized Carbon Fiber Microelectrode-Based Oxidase Biosensor for Amperometric Monitoring of Lactate in Brain Slices," *Sensors* 22 (2022): 7011, https://doi.org/10.3390/s22187011.

385. H. Abu-Ali, C. Ozkaya, F. Davis, N. Walch, and A. Nabok, "Electrochemical Aptasensor for Detection of Dopamine," *Chemosensors* 8 (2020): 28.

386. H. M. N. Ahmad, A. Andrade, and E. Song, "Continuous Real-Time Detection of Serotonin Using an Aptamer-Based Electrochemical Biosensor," *Biosensors* 13 (2023): 983, https://doi.org/10.3390/bios13110983.

387. C. Li, Y. He, S. Ingebrandt, and X. T. Vu, "Microscale Sensor Arrays for the Detection of Dopamine Using PEDOT:PSS Organic Electrochemical Transistors," *Sensors* 24 (2024): 5244, https://doi.org/10.3390/s24165244.

388. N. Saraf, E. R. Woods, M. Peppler, and S. Seal, "Highly Selective Aptamer Based Organic Electrochemical Biosensor With Pico-level Detection," *Biosensors and Bioelectronics* 117 (2018): 40–46, https://doi.org/10.1016/j.bios.2018.05.031.

389. Y. Yao, F. Alimardani, P. Ren, et al., "Dual-Gate Organic Electrochemical Transistors Based on Laser-Scribed Graphene for Detecting Dopamine and Glutamate," *Advanced Materials Technologies* 10 (2025): 2401732, https://doi.org/10.1002/admt.202401732.

390. K. Duy Mac and J. Su, "Optical Biosensors for Diagnosing Neurodegenerative Diseases," *Npj Biosensing* 2 (2025): 20, https://doi.org/10.1038/s44328-025-00040-3.

391. S. Kumar, A. Iadicicco, S. Kim, D. Tosi, and C. Marques, "Introduction to the Feature Issue: Advances in Optical Biosensors for Biomedical Applications," *Biomedical Optics Express* 15 (2024): 3183–3190, https://doi.org/10.1364/BOE.527613.

392. S. Mostufa, B. Rezaei, S. Ciannella, et al., "Advancements and Perspectives in Optical Biosensors," *ACS Omega* 9 (2024): 24181–24202, https://doi.org/10.1021/acsomega.4c01872.

393. Y. Zhang, Y. Hu, Q. Liu, and K. Lou, "Multiplexed optical fiber sensors for dynamic brain monitoring," *Matter* 5 (2022): 3947–3976.

394. M. Chemchem, A. Chemchem, B. Aydıner, and Z. Seferoğlu, "Recent Advances in Colorimetric and Fluorometric Sensing of Neurotransmitters by Organic Scaffolds," *European Journal of Medicinal Chemistry* 244 (2022): 114820, https://doi.org/10.1016/j.ejmech.2022.114820.

395. C. Liu, F. A. Gomez, Y. Miao, P. Cui, and W. Lee, "A Colorimetric Assay System for Dopamine Using Microfluidic Paper-based Analytical Devices," *Talanta* 194 (2019): 171–176, https://doi.org/10.1016/j.talanta.2018.10.039.

396. Q. Fan, Y. Gao, F. Mazur, and R. Chandrawati, "Nanoparticle-based Colorimetric Sensors to Detect Neurodegenerative Disease Biomarkers," *Biomaterials Science* 9 (2021): 6983–7007, https://doi.org/10.1039/D1BM01226F.

397. Z. Wang, Y. Dong, X. Sui, et al., "An Artificial Intelligence-assisted Microfluidic Colorimetric Wearable Sensor System for Monitoring of Key Tear Biomarkers," *npj Flexible Electronics* 8 (2024): 35, https://doi.org/10.1038/s41528-024-00321-3.

398. H. Wang, T. Zhang, X. Chen, J. Gu, and X. Ren, "Colorimetric-Assisted Photoelectrochemical Sensing for Dual-Mode Detection of Neuron-Specific Enolase via the Photoanode-Photocathode System," *Analytical Chemistry* 97, no. 28 (2025): 15350–15357, https://doi.org/10.1021/acs.analchem.5c02247.

399. X. Li, L. Gao, and Z. Chen, "Highly Sensitive Colorimetric Detection of Glucose Through Glucose Oxidase and Cu2+-catalyzed 3,3′,5,5′-tetramethylbenzidine Oxidation," *Spectrochimica Acta Part A: Molecular and Biomolecular Spectroscopy* 213 (2019): 37–41, https://doi.org/10.1016/j.saa.2019.01.050.

400. H. Chen, S. Cai, J. Luo, et al., "Colorimetric Biosensing Assays Based on Gold Nanoparticles Functionalized/Combined With Non-antibody Recognition Elements," *TrAC Trends in Analytical Chemistry* 173 (2024): 117654, https://doi.org/10.1016/j.trac.2024.117654.

401. C. Liu, X. Lin, J. Liao, et al., "Carbon Dots-based Dopamine Sensors: Recent Advances and Challenges," *Chinese Chemical Letters* 35 (2024): 109598, https://doi.org/10.1016/j.cclet.2024.109598.

402. J. P. Leite, F. Figueira, R. F. Mendes, F. A. Almeida Paz, and L. Gales, "Metal–Organic Frameworks as Sensors for Human Amyloid Diseases," *ACS Sens* 8 (2023): 1033–1053.

403. R. Govindaraju, S. Govindaraju, and K. K. Yun, "J Fluorescent-Based Neurotransmitter Sensors: Present and Future Perspectives," *Biosensors* 13 (2023): 1008.

404. J. Day-Cooney, R. Dalangin, H. Zhong, and T. Mao, "Genetically Encoded Fluorescent Sensors for Imaging Neuronal Dynamics in Vivo," *Journal of Neurochemistry* 164 (2023): 284–308, https://doi.org/10.1111/jnc.15608.

405. F. Sun, J. Zhou, B. Dai, et al., "Next-generation GRAB Sensors for Monitoring Dopaminergic Activity in Vivo," *Nature Methods* 17 (2020): 1156–1166, https://doi.org/10.1038/s41592-020-00981-9.

406. X. Xia and Y. Li, "A High-performance GRAB Sensor Reveals Differences in the Dynamics and Molecular Regulation Between Neuropeptide and Neurotransmitter Release," *Nature Communications* 16 (2025): 819, https://doi.org/10.1038/s41467-025-56129-w.

407. F. Sun, J. Zeng, M. Jing, et al., "A Genetically Encoded Fluorescent Sensor Enables Rapid and Specific Detection of Dopamine in Flies, Fish, and Mice," *Cell* 174 (2018): 481–496.e19, https://doi.org/10.1016/j.cell.2018.06.042.

408. X. Zhou, K. J. Belavek, and E. W. Miller, "Origins of Ca2+ Imaging With Fluorescent Indicators," *Biochemistry* 60 (2021): 3547–3554, https://doi.org/10.1021/acs.biochem.1c00350.

409. N. A. Smith, B. T. Kress, Y. Lu, D. Chandler-Militello, A. Benraiss, and M. Nedergaard, "Fluorescent Ca2+ Indicators Directly Inhibit the Na,K-ATPase and Disrupt Cellular Functions," *Science Signaling* 11 (2018): eaal2039, https://doi.org/10.1126/scisignal.aal2039.

410. Y. Zhang, M. Rózsa, Y. Liang, et al., "Fast and Sensitive GCaMP Calcium Indicators for Imaging Neural Populations," *Nature* 615 (2023): 884–891, https://doi.org/10.1038/s41586-023-05828-9.

411. A. Badura, X. R. Sun, A. Giovannucci, L. A. Lynch, and S. S.-H. Wang, "Fast Calcium Sensor Proteins for Monitoring Neural Activity," *Neurophotonics* 1 (2014): 025008, https://doi.org/10.1117/1.NPh.1.2.025008.

412. J. Langer and C. R. Rose, "Synaptically Induced Sodium Signals in Hippocampal Astrocytes in Situ," *The Journal of Physiology* 587 (2009): 5859–5877, https://doi.org/10.1113/jphysiol.2009.182279.

413. L. C. Daniell, "Determination of the Intravesicular Ionized Sodium Concentration in a Cell-free Brain Membrane Vesicle Preparation Using the Fluorescent Indicator,SBFI," *Analytical Biochemistry* 202 (1992): 239–244.

414. S. Dufour, P. Dufour, O. Chever, R. Vallée, and F. Amzica, "*In Vivo* Simultaneous Intra- and Extracellular Potassium Recordings Using

a Micro-optrode," *Journal of Neuroscience Methods* 194 (2011): 206–217, https://doi.org/10.1016/j.jneumeth.2010.10.004.

415. S.-Y. Wu, Y. Shen, I. Shkolnikov, and R. E. Campbell, "Fluorescent Indicators for Biological Imaging of Monatomic Ions," *Frontiers in Cell and Developmental Biology* 10 (2022): 885440, https://doi.org/10.3389/fcell.2022.885440.

416. J. Wellbourne-Wood, T. S. Rimmele, and J.-Y. Chatton, "Imaging Extracellular Potassium Dynamics in Brain Tissue Using a Potassium-sensitive Nanosensor," *Neurophotonics* 4 (2017): 015002, https://doi.org/10.1117/1.NPh.4.1.015002.

417. H. Wang, M. Jing, and Y. Li, "Lighting up the Brain: Genetically Encoded Fluorescent Sensors for Imaging Neurotransmitters and Neuromodulators," *Current Opinion in Neurobiology* 50 (2018): 171–178, https://doi.org/10.1016/j.conb.2018.03.010.

418. N. Byron and S. Sakata, "Fiber Photometry-based Investigation of Brain Function and Dysfunction," *Neurophotonics* 11 (2024): S11502.

419. E. H. Simpson, T. Akam, T. Patriarchi, et al., "Lights, Fiber, Action! A Primer on In Vivo Fiber Photometry," *Neuron* 112 (2024): 718–739, https://doi.org/10.1016/j.neuron.2023.11.016.

420. M. Kielbinski and J. Bernacka, "Fiber Photometry in Neuroscience Research: Principles, Applications, and Future Directions," *Pharmacological Reports* 76 (2024): 1242–1255.

421. A. Formozov, A. Dieter, and J. S. Wiegert, "A Flexible and Versatile System for Multi-color fiber Photometry and Optogenetic Manipulation," *Cell Reports Methods* 3 (2023): 100418, https://doi.org/10.1016/j.crmeth.2023.100418.

422. F. Pisano, M. Pisanello, S. J. Lee, et al., "Depth-resolved fiber Photometry With a Single Tapered Optical fiber Implant," *Nature Methods* 16 (2019): 1185–1192, https://doi.org/10.1038/s41592-019-0581-x.

423. R. Weissleder, "A Clearer Vision for in Vivo Imaging," *Nature Biotechnology* 19 (2001): 316–317, https://doi.org/10.1038/86684.

424. L. Gu, D. J. Hall, Z. Qin, et al., "In Vivo Time-gated Fluorescence Imaging With Biodegradable Luminescent Porous Silicon Nanoparticles," *Nature Communications* 4 (2013): 2326, https://doi.org/10.1038/ncomms3326.

425. J. Choi, A. J. Taal, W. L. Meng, et al., "Fully Integrated Time-Gated 3D Fluorescence Imager for Deep Neural Imaging," *IEEE Transactions on Biomedical Circuits and Systems* 14 (2020): 636–645, https://doi.org/10.1109/TBCAS.2020.3008513.

426. G. Hong, A. L. Antaris, and H. Dai, "Near-infrared Fluorophores for Biomedical Imaging," *Nature Biomedical Engineering* 1 (2017): 0010, https://doi.org/10.1038/s41551-016-0010.

427. Z.-Q. Liu, B. Vázquez-Rodríguez, R. N. Spreng, B. C. Bernhardt, R. F. Betzel, and B. Misic, "Time-resolved Structure-function Coupling in Brain Networks," *Communications Biology* 5 (2022): 532, https://doi.org/10.1038/s42003-022-03466-x.

428. B. Crouch, L. Sommerlade, P. Veselcic, G. Riedel, B. Schelter, and B. Platt, "Detection of Time-, Frequency- and Direction-resolved Communication Within Brain Networks," *Scientific Reports* 8 (2018): 1825, https://doi.org/10.1038/s41598-018-19707-1.

429. W. Ling, X. Shang, C. Yu, et al., "Miniaturized Implantable Fluorescence Probes Integrated With Metal–Organic Frameworks for Deep Brain Dopamine Sensing," *ACS Nano* 18 (2024): 10596–10608, https://doi.org/10.1021/acsnano.4c00632.

430. H. Ahn, S. Kim, Y. Kim, S. Kim, J.-R. Choi, and K. Kim, "Plasmonic Sensing, Imaging, and Stimulation Techniques for Neuron Studies," *Biosensors and Bioelectronics* 182 (2021): 113150, https://doi.org/10.1016/j.bios.2021.113150.

431. N. S. S. Mousavi, K. B. Ramadi, Y.-A. Song, and S. Kumar, "Plasmonics for Neuroengineering," *Communications Materials* 4 (2023): 1–16.

432. D. Zheng, F. Pisano, L. Collard, et al., "Toward Plasmonic Neural Probes: SERS Detection of Neurotransmitters Through Gold-Nanoislands-Decorated Tapered Optical Fibers With Sub-10 nm Gaps," *Advanced Materials* 35 (2023): 2200902, https://doi.org/10.1002/adma.202200902.

433. N. J. Wittenberg, B. Wootla, L. R. Jordan, et al., "Applications of SPR for the characterization of molecules important in the pathogenesis and treatment of neurodegenerative diseases," *Expert Review of Neurotherapeutics* 14 (2014): 449–463, https://doi.org/10.1586/14737175.2014.896199.

434. Y. Zeng, X. Wang, J. Zhou, et al., "Phase Interrogation SPR Sensing Based on White Light Polarized Interference for Wide Dynamic Detection Range," *Optics Express* 28 (2020): 3442–3450, https://doi.org/10.1364/OE.382242.

435. X. Liu, D. Song, Q. Zhang, Y. Tian, L. Ding, and H. Zhang, "Wavelength-modulation Surface Plasmon Resonance Sensor," *TrAC Trends in Analytical Chemistry* 24 (2005): 887–893, https://doi.org/10.1016/j.trac.2005.05.010.

436. X. Ma, X. Xu, Z. Zheng, et al., "Dynamically Modulated Intensity Interrogation Scheme Using Waveguide Coupled Surface Plasmon Resonance Sensors," *Sensors and Actuators A: Physical* 157 (2010): 9–14, https://doi.org/10.1016/j.sna.2009.11.004.

437. D. Harpaz, B. Koh, R. S. Marks, R. C. S. Seet, I. Abdulhalim, and A. I. Y. Tok, "Point-of-Care Surface Plasmon Resonance Biosensor for Stroke Biomarkers NT-proBNP and S100β Using a Functionalized Gold Chip With Specific Antibody," *Sensors* 19 (2019): 2533, https://doi.org/10.3390/s19112533.

438. A. Rezabakhsh, R. Rahbarghazi, and F. Fathi, "Surface plasmon resonance biosensors for detection of Alzheimer's biomarkers; an effective step in early and accurate diagnosis," *Biosensors and Bioelectronics* 167 (2020): 112511, https://doi.org/10.1016/j.bios.2020.112511.

439. R. Kant and B. D. Gupta, "Fiber-Optic SPR Based Acetylcholine Biosensor Using Enzyme Functionalized Ta 2 O 5 Nanoflakes for Alzheimer's Disease Diagnosis," *Journal of Lightwave Technology* 36 (2018): 4018–4024, https://doi.org/10.1109/JLT.2018.2856924.

440. X. Li, R. Tong, Y. Wang, and L. Wang, "ssDNA-Functionalized Optical Fiber SPR Sensor for Trace Dopamine Detection," *Microwave and Optical Technology Letters* 67 (2025): e70278, https://doi.org/10.1002/mop.70278.

441. J. Zhao, X. Zhang, C. R. Yonzon, A. J. Hoes, and R. P. Van Duyne, "Localized Surface Plasmon Resonance Biosensors," *Nanomed* 1 (2006): 219–228.

442. J.-S. Chen, P.-F. Chen, H. T.-H. Lin, and N.-T. Huang, "A Localized Surface Plasmon Resonance (LSPR) Sensor Integrated Automated Microfluidic System for Multiplex Inflammatory Biomarker Detection," *The Analyst* 145 (2020): 7654–7661, https://doi.org/10.1039/D0AN01201G.

443. H. Zhang, X. Zhou, X. Li, P. Gong, Y. Zhang, and Y. Zhao, "Recent Advancements of LSPR Fiber-Optic Biosensing: Combination Methods, Structure, and Prospects," *Biosensors* 13 (2023): 405.

444. T. Xu and Z. Geng, "Strategies to Improve Performances of LSPR Biosensing: Structure, Materials, and Interface Modification," *Biosensors and Bioelectronics* 174 (2021): 112850, https://doi.org/10.1016/j.bios.2020.112850.

445. X. Lin, Y. Luo, D. Li, et al., "Recent Advances in Localized Surface Plasmon Resonance (LSPR) Sensing Technologies," *Nanotechnology* 36 (2025): 202001, https://doi.org/10.1088/1361-6528/adb6a4.

446. V. Pellas, H. David, Y. Mazouzi, et al., "Gold Nanorods for LSPR Biosensing: Synthesis, Coating by Silica, and Bioanalytical Applications," *Biosensors* 10 (2020): 146.

447. N. Li, Y. Lu, S. Li, et al., "Monitoring the Electrochemical Responses of Neurotransmitters Through Localized Surface Plasmon Resonance Using Nanohole Array," *Biosensors and Bioelectronics* 93 (2017): 241–249, https://doi.org/10.1016/j.bios.2016.08.105.

448. C. L. Haynes and R. P. Van Duyne, "Nanosphere Lithography: a Versatile Nanofabrication Tool for Studies of Size-Dependent Nanoparticle Optics," *The Journal of Physical Chemistry B* 105 (2001): 5599–5611, https://doi.org/10.1021/jp010657m.

449. F. S. Alfonso, Y. Zhou, E. Liu, et al., "Label-free Optical Detection of Bioelectric Potentials Using Electrochromic Thin Films," *Proceedings of the National Academy of Sciences* 117 (2020): 17260–17268, https://doi.org/10.1073/pnas.2002352117.

450. F. Amouyan, A. R. Sadrolhosseini, S. M. Hamidi, M. Kazemzad, and M. Hamzehzadeh, "Tamm Plasmon-based Dopamine Detection by Using a Chitosan-polyaniline-gold Nanostructure," *Optical Materials Express* 13 (2023): 783–795, https://doi.org/10.1364/OME.479666.

451. J. L. Chávez, J. A. Hagen, and N. Kelley-Loughnane, "Fast and Selective Plasmonic Serotonin Detection With Aptamer-Gold Nanoparticle Conjugates," *Sensors* 17 (2017): 681, https://doi.org/10.3390/s17040681.

452. M. Singh, J. Truong, W. B. Reeves, and J. Hahm, "Emerging Cytokine Biosensors With Optical Detection Modalities and Nanomaterial-Enabled Signal Enhancement," *Sensors* 17 (2017): 428, https://doi.org/10.3390/s17020428.

453. J. Lee, J. Park, J.-Y. Lee, and J.-S. Yeo, "Contact Transfer Printing of Side Edge Prefunctionalized Nanoplasmonic Arrays for Flexible microRNA Biosensor," *Advanced Science* 2 (2015): 1500121, https://doi.org/10.1002/advs.201500121.

454. P. Ramirez-Priego, E. Mauriz, J. F. Giarola, and L. M. Lechuga, "Overcoming Challenges in Plasmonic Biosensors Deployment for Clinical and Biomedical Applications: A Systematic Review and Meta-analysis," *Sensing and Bio-Sensing Research* 46 (2024): 100717, https://doi.org/10.1016/j.sbsr.2024.100717.

455. Y. Zhang, H. Wu, H. Wang, et al., "Ultraminiature Optical Fiber-Tip Directly-Printed Plasmonic Biosensors for Label-Free Biodetection," *Biosensors and Bioelectronics* 218 (2022): 114761, https://doi.org/10.1016/j.bios.2022.114761.

456. M. Mariello, et al., "Magnesium-based Optrodes for Real-time Optical Monitoring of Water Transport in Ultrathin Encapsulations for Soft Implantable Bioelectronics (to be submitted)," *Advanced Functional Materials* (2024): 2412995.

457. A. Biswas, S. Lee, P. Cencillo-Abad, et al., "Nanoplasmonic Aptasensor for Sensitive, Selective, and Real-time Detection of Dopamine From Unprocessed Whole Blood," *Science Advances* 10 (2024): eadp7460, https://doi.org/10.1126/sciadv.adp7460.

458. L. Liu, D. Wang, Y. Luo, et al., "Intraoperative Assessment of Microimplantation-induced Acute Brain Inflammation With Titanium Oxynitride-based Plasmonic Biosensor," *Biosensors and Bioelectronics* 264 (2024): 116664, https://doi.org/10.1016/j.bios.2024.116664.

459. K. F. Kastl, C. R. Lowe, and C. E. Norman, "Encoded and Multiplexed Surface Plasmon Resonance Sensor Platform," *Analytical Chemistry* 80 (2008): 7862–7869, https://doi.org/10.1021/ac8011818.

460. T. Allsop and R. A. R. Neal, "A Review: Evolution and Diversity of Optical Fibre Plasmonic Sensors," *Sensors* 19 (2019): 4874, https://doi.org/10.3390/s19224874.

461. Y. Esfahani Monfared, "Overview of Recent Advances in the Design of Plasmonic Fiber-Optic Biosensors," *Biosensors* 10 (2020): 77, https://doi.org/10.3390/bios10070077.

462. M. Lu, C. Wang, R. Fan, M. Lin, J. Guang, and W. Peng, "Review of Fiber-Optic Localized Surface Plasmon Resonance Sensors: Geometries, Fabrication Technologies, and Bio-Applications," *Photonic Sensors* 14 (2024): 240202.

463. S. C. Piantadosi, M.-K. Lee, M. Wu, et al., "An Integrated Microfluidic and Fluorescence Platform for Probing in Vivo Neuropharmacology," *Neuron* 113 (2025): 1491–1506.e6, https://doi.org/10.1016/j.neuron.2025.03.017.

464. J. C. Ranasinghe, Z. Wang, and S. Huang, "Raman Spectroscopy on Brain Disorders: Transition From Fundamental Research to Clinical Applications," *Biosensors* 13 (2022): 27, https://doi.org/10.3390/bios13010027.

465. L. Li, Y. Lu, Z. Qian, et al., "Ultra-sensitive Surface Enhanced Raman Spectroscopy Sensor for In-Situ Monitoring of Dopamine Release Using Zipper-Like Ortho-nanodimers," *Biosensors and Bioelectronics* 180 (2021): 113100, https://doi.org/10.1016/j.bios.2021.113100.

466. D. DePaoli, É. Lemoine, K. Ember, et al., "Rise of Raman Spectroscopy in Neurosurgery: A Review," *Journal of Biomedical Optics* 25 (2020): 1–36, https://doi.org/10.1117/1.JBO.25.5.050901.

467. R. Pilot, R. Signorini, C. Durante, L. Orian, M. Bhamidipati, and L. Fabri, "A Review on Surface-Enhanced Raman Scattering," *Biosensors* 9 (2019): 57.

468. X. X. Han, R. S. Rodriguez, C. L. Haynes, Y. Ozaki, and B. Zhao, "Surface-enhanced Raman Spectroscopy," *Nature Reviews Methods Primers* 1 (2022): 87, https://doi.org/10.1038/s43586-021-00083-6.

469. G. C. Schatz, M. A. Young, and R. P. Van Duyne, "Electromagnetic Mechanism of SERS," in *Surface-Enhanced Raman Scattering: Physics and Applications*, eds. K. Kneipp, M. Moskovits, and H. Kneipp (Springer Berlin Heidelberg, 2006), 19–45, https://doi.org/10.1007/3-540-33567-6_2.

470. F. Gao, F. Li, J. Wang, et al., "SERS-Based Optical Nanobiosensors for the Detection of Alzheimer's Disease," *Biosensors* 13 (2023): 880, https://doi.org/10.3390/bios13090880.

471. M. Kim, S. Huh, H. J. Park, et al., "Surface-Functionalized SERS Platform for Deep Learning-Assisted Diagnosis of Alzheimer's Disease," *Biosensors and Bioelectronics* 251 (2024): 116128, https://doi.org/10.1016/j.bios.2024.116128.

472. R. Boudries, H. Williams, S. Paquereau-Gaboreau, et al., "Surface-Enhanced Raman Scattering Nanosensing and Imaging in Neuroscience," *ACS Nano* 18 (2024): 22620–22647, https://doi.org/10.1021/acsnano.4c05200.

473. S. Bock, Y.-S. Choi, M. Kim, et al., "Highly Sensitive Near-Infrared SERS Nanoprobes for In Vivo Imaging Using Gold-Assembled Silica Nanoparticles With Controllable Nanogaps," *Journal of Nanobiotechnology* 20 (2022): 130, https://doi.org/10.1186/s12951-022-01327-7.

474. M. N. R. Naim, J. T. Upoma, A. H. M. I. Ferdous, K. Khandakar, M. G. Sadeque, and M. S. Rana, "Terahertz Spectrum-based Refractive Index Sensor for Brain Lesion Detection Using Photonic Crystal Fibers," *PLoS ONE* 20 (2025): e0320355, https://doi.org/10.1371/journal.pone.0320355.

475. W. M. Nouman, S. E.-S. Abd El-Ghany, S. M. Sallam, A.-F. B. Dawood, and A. H. Aly, "Biophotonic Sensor for Rapid Detection of Brain Lesions Using 1D Photonic Crystal," *Optical and Quantum Electronics* 52 (2020): 287, https://doi.org/10.1007/s11082-020-02409-2.

476. C. Malek, S. A. O. Abdallah, S. K. Awasthi, M. A. Ismail, W. Sabra, and A. H. Aly, "Biophotonic Sensor for Swift Detection of Malignant Brain Tissues by Using Nanocomposite YBa2Cu3O7/Dielectric Material as a 1D Defective Photonic Crystal," *Scientific Reports* 13 (2023): 8115, https://doi.org/10.1038/s41598-023-34601-1.

477. R. Jha, P. Gorai, A. Shrivastav, and A. Pathak, "Label-Free Biochemical Sensing Using Processed Optical Fiber Interferometry: A Review," *ACS Omega* 9 (2024): 3037–3069.

478. M. Hosseinzadeh, S. Salmani, and M. H. M. Ara, "Interferometric Optical Testing to Discriminate Benign and Malignant Brain Tumors," *Journal of Photochemistry and Photobiology B: Biology* 199 (2019): 111590, https://doi.org/10.1016/j.jphotobiol.2019.111590.

479. M. Kim, H. Yoon, S. Choi, et al., "Miniaturized and Wireless Optical Neurotransmitter Sensor for Real-Time Monitoring of Dopamine in the Brain," *Sensors* 16 (2016): 1894, https://doi.org/10.3390/s16111894.

480. M. O. Correia, P. Sousa, R. O. Rodrigues, and G. Minas, "A Proof-of-Concept Study Aiming for the Integration of an Optical Biosensor in Advanced Microfluidic Devices for Alzheimer's Disease Studies," *Applies Science* 15 (2025): 3837.

481. B. Zhou, K. Fan, and L. Kong, "A Biocompatible Hydrogel-coated fiber-optic Probe for Monitoring pH Dynamics in Brains of Freely Moving

Mice," in *27th International Conference on Optical Fiber Sensors (2022), paper W4.69 W4.69* (Optica Publishing Group, 2022), https://doi.org/10.1364/OFS.2022.W4.69.

482. F. B. Kamal Eddin, Y. W. Fen, N. A. S. Omar, J. Y. C. Liew, and W. M. E. M. M. Daniyal, "Femtomolar Detection of Dopamine Using Surface Plasmon Resonance Sensor Based on Chitosan/Graphene Quantum Dots Thin Film," *Spectrochimica Acta Part A: Molecular and Biomolecular Spectroscopy* 263 (2021): 120202, https://doi.org/10.1016/j.saa.2021.120202.

483. W. Hu, Y. Huang, C. Chen, Y. Liu, T. Guo, and B.-O. Guan, "Highly Sensitive Detection of Dopamine Using a Graphene Functionalized Plasmonic fiber-optic Sensor With Aptamer Conformational Amplification," *Sensors and Actuators B: Chemical* 264 (2018): 440–447, https://doi.org/10.1016/j.snb.2018.03.005.

484. Y. Choi, C. S. Jeon, K. B. Kim, H.-J. Kim, S. H. Pyun, and Y. M. Park, "Quantitative Detection of Dopamine in human Serum With Surface-enhanced Raman Scattering (SERS) of Constrained Vibrational Mode," *Talanta* 260 (2023): 124590, https://doi.org/10.1016/j.talanta.2023.124590.

485. W.-H. Chen, W. Wang, Q. Lin, et al., "Plasmonic Sensing Assay for Long-Term Monitoring (PSALM) of Neurotransmitters in Urine," *ACS Nanoscience Au* 3 (2023): 161–171, https://doi.org/10.1021/acsnanoscienceau.2c00048.

486. L. Wu, X. Liu, S. Zong, Z. Wang, and Y. Cui, "A SERS Composite Hydrogel Device for Point-of-Care Analysis of Neurotransmitter in Whole Blood," *Biosensors* 13 (2023): 611, https://doi.org/10.3390/bios13060611.

487. S. Kasera, L. O. Herrmann, J. Barrio, J. J. Baumberg, and O. A. Scherman, "Quantitative Multiplexing With Nano-self-assemblies in SERS," *Scientific Reports* 4 (2014): 6785, https://doi.org/10.1038/srep06785.

488. R. Kou, Y. Kobayashi, S. Inoue, et al., "Dopamine Detection on Activated Reaction Field Consisting of Graphene-integrated Silicon Photonic Cavity," *Optics Express* 27 (2019): 32058–32068, https://doi.org/10.1364/OE.27.032058.

489. M. Ding, Y. Huang, T. Guo, L.-P. Sun, and B.-O. Guan, "Mesoporous Nanospheres Functionalized Optical Microfiber Biosensor for Low Concentration Neurotransmitter Detection," *Optics Express* 24 (2016): 27152–27159, https://doi.org/10.1364/OE.24.027152.

490. D. Huang, J. Wang, C. Song, and Y. Zhao, "Ultrasound-Responsive Matters for Biomedical Applications," *The Innovation* 4 (2023): 100421, https://doi.org/10.1016/j.xinn.2023.100421.

491. C. M. I. Quarato, D. Lacedonia, M. Salvemini, et al., "A Review on Biological Effects of Ultrasounds: Key Messages for Clinicians," *Diagnostics* 13 (2023): 855.

492. B. Han, Y. Liu, Q. Zhou, et al., "The Advance of Ultrasound-enabled Diagnostics and Therapeutics," *Journal of Controlled Release* 375 (2024): 1–19, https://doi.org/10.1016/j.jconrel.2024.08.039.

493. C. Tian, J. Xia, and X. Wang, "Editorial: Optics and Ultrasound in Biomedicine: Sensing, Imaging, and Therapy," *Frontiers in Physics* 9 (2021).

494. E. K. Akdogan, M. Allahverdi, and A. Safari, "Piezoelectric Composites for Sensor and Actuator Applications," *IEEE Transactions on Ultrasonics, Ferroelectrics and Frequency Control* 52 (2005): 746–775, https://doi.org/10.1109/TUFFC.2005.1503962.

495. Z. Chen, L. Yang, Z. Yang, Z. Wang, W. He, and W. Zhang, "Ultrasonic-responsive Piezoelectric Stimulation Enhances Sonodynamic Therapy for HER2-positive Breast Cancer," *Journal of Nanobiotechnology* 22 (2024): 369, https://doi.org/10.1186/s12951-024-02639-6.

496. G. Andreoni, M. Mazzola, S. Matteoli, S. D'Onofrio, and L. Forzoni, "Ultrasound System Typologies, User Interfaces and Probes Design: A Review," *Procedia Manufacturing* 3 (2015): 112–119, https://doi.org/10.1016/j.promfg.2015.07.115.

497. N. A. Kamel, "Bio-piezoelectricity: Fundamentals and Applications in Tissue Engineering and Regenerative Medicine," *Biophysical Reviews* 14 (2022): 717–733, https://doi.org/10.1007/s12551-022-00969-z.

498. J. Owen, C. Crake, J. Y. Lee, et al., "A Versatile Method for the Preparation of Particle-loaded Microbubbles for Multimodality Imaging and Targeted Drug Delivery," *Drug Delivery and Translational Research* 8 (2018): 342–356, https://doi.org/10.1007/s13346-017-0366-7.

499. F. Xi, Y. Feng, Q. Chen, L. Chen, and J. Liu, "Microbubbles Ultrasonic Cavitation Regulates Tumor Interstitial Fluid Pressure and Enhances Sonodynamic Therapy," *Frontiers in Oncology* 12 (2022): 852454, https://doi.org/10.3389/fonc.2022.852454.

500. C.-H. Wang, Y.-F. Huang, and C.-K. Yeh, "Aptamer-Conjugated Nanobubbles for Targeted Ultrasound Molecular Imaging," *Langmuir* 27 (2011): 6971–6976, https://doi.org/10.1021/la2011259.

501. S. Nikazar, "Chapter 29 – Ultrasound-assisted biosensors," in *Materials and Components of Biosensors in Healthcare*, eds. M. S. Hasnain, A. K. Nayak, and T. M. Aminabhavi (Academic Press, 2025), 671–689, https://doi.org/10.1016/B978-0-443-21676-3.00013-3.

502. B. Gil, S. Anastasova, and G.-Z. Yang, "Low-powered Implantable Devices Activated by Ultrasonic Energy Transfer for Physiological Monitoring in Soft Tissue *via* Functionalized Electrochemical Electrodes," *Biosensors and Bioelectronics* 182 (2021): 113175, https://doi.org/10.1016/j.bios.2021.113175.

503. Z. Liu, H. Zhang, K. Lu, et al., "Low-intensity Pulsed Ultrasound Modulates Disease Progression in the SOD1G93A Mouse Model of Amyotrophic Lateral Sclerosis," *Cell Reports* 43 (2024): 114660, https://doi.org/10.1016/j.celrep.2024.114660.

504. I. Udroiu, F. Todaro, A. Vitaliti, et al., "Low-intensity Pulsed Ultrasound Induces Multifaced Alterations in Chromosome Segregation, Cytoskeletal filaments and Cell Junctions," *Scientific Reports* 15 (2025): 4964, https://doi.org/10.1038/s41598-025-88569-1.

505. W. Jiang, Y. Wang, J. Tang, et al., "Low-intensity Pulsed Ultrasound Treatment Improved the Rate of Autograft Peripheral Nerve Regeneration in Rat," *Scientific Reports* 6 (2016): 22773, https://doi.org/10.1038/srep22773.

506. T. Xu, X. Lu, D. Peng, et al., "Ultrasonic Stimulation of the Brain to Enhance the Release of Dopamine—A Potential Novel Treatment for Parkinson's Disease," *Ultrasonics Sonochemistry* 63 (2020): 104955, https://doi.org/10.1016/j.ultsonch.2019.104955.

507. M. Kaisti, "Detection Principles of Biological and Chemical FET Sensors," *Biosensors and Bioelectronics* 98 (2017): 437–448, https://doi.org/10.1016/j.bios.2017.07.010.

508. T.-H. Hyun and W.-J. Cho, "High-Performance FET-Based Dopamine-Sensitive Biosensor Platform Based on SOI Substrate," *Biosensors* 13 (2023): 516, https://doi.org/10.3390/bios13050516.

509. N. Liu, X. Xiang, L. Fu, et al., "Regenerative Field Effect Transistor Biosensor for In Vivo Monitoring of Dopamine in Fish Brains," *Biosensors and Bioelectronics* 188 (2021): 113340, https://doi.org/10.1016/j.bios.2021.113340.

510. C. Zhao, T. Man, Y. Cao, P. S. Weiss, H. G. Monbouquette, and A. M. Andrews, "Flexible and Implantable Polyimide Aptamer-Field-Effect Transistor Biosensors," *ACS Sensors* 7 (2022): 3644–3653, https://doi.org/10.1021/acssensors.2c01909.

511. Y. Niu, Z. Qin, Y. Zhang, C. Chen, S. Liu, and H. Chen, "Expanding the Potential of Biosensors: A Review on Organic Field Effect Transistor (OFET) and Organic Electrochemical Transistor (OECT) Biosensors," *Materials Futures* 2 (2023): 042401, https://doi.org/10.1088/2752-5724/ace3dd.

512. E. Stern, J. F. Klemic, D. A. Routenberg, et al., "Label-free Immunodetection With CMOS-compatible Semiconducting Nanowires," *Nature* 445 (2007): 519–522, https://doi.org/10.1038/nature05498.

513. A. Poghossian and M. J. Schöning, "Label-Free Sensing of Biomolecules With Field-Effect Devices for Clinical Applications," *Electroanalysis* 26 (2014): 1197–1213, https://doi.org/10.1002/elan.201400073.

514. J. B. Schlenoff, "Zwitteration: Coating Surfaces With Zwitterionic Functionality to Reduce Nonspecific Adsorption," *Langmuir* 30 (2014): 9625–9636, https://doi.org/10.1021/la500057j.

515. T. W. Navaraj, W. Navaraj, D. Shakthivel, et al., "Nanowire FET Based Neural Element for Robotic Tactile Sensing Skin," *Frontiers in Neuroscience* 11 (2017).

516. C. Delacour, F. Veliev, T. Crozes, et al., "Neuron-Gated Silicon Nanowire Field Effect Transistors to Follow Single Spike Propagation Within Neuronal Network," *Advanced Engineering Materials* 23 (2021): 2001226, https://doi.org/10.1002/adem.202001226.

517. K. Hongki, K. Jee-Yeon, C. Yang-Kyu, and N. Yoonkey, "In-depth Characterization of Silicon Nanowire Field-Effect Transistor (SiNW-FET) for Neural Recording and Direct Performance Comparison With Passive MEA," *Frontiers in Neuroscience* 10 (2016), https://doi.org/10.3389/conf.fnins.2016.93.00062.

518. J. I. Abdul Rashid, J. Abdullah, N. A. Yusof, and R. Hajian, "The Development of Silicon Nanowire as Sensing Material and Its Applications," *Journal of Nanomaterials* 2013 (2013): 328093, https://doi.org/10.1155/2013/328093.

519. V. Sessi, B. Ibarlucea, F. Seichepine, et al., "Multisite Dopamine Sensing with Femtomolar Resolution Using a CMOS Enabled Aptasensor Chip," *Frontiers in Neuroscience* 16 (2022), https://doi.org/10.3389/fnins.2022.875656.

520. C.-H. Lee, W.-P. Hu, and W.-Y. Chen, "Electric-field Assisted Silicon Nanowire Field Effect Transistor for the Ultra-low Concentration Nucleic Acid Detection," *Biosensors and Bioelectronics* 268 (2025): 116909, https://doi.org/10.1016/j.bios.2024.116909.

521. C.-A. Vu, W.-P. Hu, Y.-S. Yang, H. W.-H. Chan, and W.-Y. Chen, "Signal Enhancement of Silicon Nanowire Field-Effect Transistor Immunosensors by RNA Aptamer," *ACS Omega* 4 (2019): 14765–14771, https://doi.org/10.1021/acsomega.9b01264.

522. S. K. Krishnan, N. Nataraj, M. Meyyappan, and U. Pal, "Graphene-Based Field-Effect Transistors in Biosensing and Neural Interfacing Applications: Recent Advances and Prospects," *Analytical Chemistry* 95 (2023): 2590–2622, https://doi.org/10.1021/acs.analchem.2c03399.

523. Z. Ji, J. Wei, F. Luo, et al., "Investigating on Sensing Mechanism of MoS2-FET Biosensors in Response to Proteins," *Nanotechnology* 34 (2023): 435503, https://doi.org/10.1088/1361-6528/aceb6a.

524. N. Lee, M.-H. Shin, E. Lee, et al., "Three-Dimensional Tungsten Disulfide Raman Biosensor for Dopamine Detection," *ACS Applied Bio Materials* 3 (2020): 7687–7695, https://doi.org/10.1021/acsabm.0c00876.

525. S.-E. Lee, Y. Choi, Y. Oh, D. Lee, J. Kim, and S. Hong, "Black Phosphorus-Based Reusable Biosensor Platforms for the Ultrasensitive Detection of Cortisol in Saliva," *ACS Applied Materials & Interfaces* 16 (2024): 11305–11314, https://doi.org/10.1021/acsami.3c18605.

526. G. Hu, J. Wu, C. Ma, et al., "Controlling the Dirac Point Voltage of Graphene by Mechanically Bending the Ferroelectric Gate of a Graphene Field Effect Transistor," *Materials Horizons* 6 (2019): 302–310, https://doi.org/10.1039/C8MH01499J.

527. Z. Wang, W. Dai, Z. Zhang, and H. Wang, "Aptamer-Based Graphene Field-Effect Transistor Biosensor for Cytokine Detection in Undiluted Physiological Media for Cervical Carcinoma Diagnosis," *Biosensors* 15 (2025): 138, https://doi.org/10.3390/bios15030138.

528. K. S. Novoselov, V. I. Fal'ko, L. Colombo, P. R. Gellert, M. G. Schwab, and K. Kim, "A Roadmap for Graphene," *Nature* 490 (2012): 192–200, https://doi.org/10.1038/nature11458.

529. S. Jiang and Z. Cao, "Ultralow-Fouling, Functionalizable, and Hydrolyzable Zwitterionic Materials and Their Derivatives for Biological Applications," *Advanced Materials* 22 (2010): 920–932, https://doi.org/10.1002/adma.200901407.

530. A. Teixeira do Nascimento, P. R. Stoddart, T. Goris, et al., "Stimuli-Responsive Materials for Biomedical Applications," *Advanced Materials* 37 (2025): e07559, https://doi.org/10.1002/adma.202507559.

531. B. M. Manzi, M. Werner, E. P. Ivanova, R. J. Crawford, and V. A. Baulin, "Simulations of Protein Adsorption on Nanostructured Surfaces," *Scientific Reports* 9 (2019): 4694.

532. N. Fourati, M. Seydou, C. Zerrouki, et al., "Ultrasensitive and Selective Detection of Dopamine Using Cobalt-Phthalocyanine Nanopillar-Based Surface Acoustic Wave Sensor," *ACS Applied Materials & Interfaces* 6 (2014): 22378–22386, https://doi.org/10.1021/am506403f.

533. C. Zhao, K. M. Cheung, I.-W. Huang, et al., "Implantable aptamer–field-effect transistor neuroprobes for in vivo neurotransmitter monitoring," *Science Advances* 7 (2021): eabj7422, https://doi.org/10.1126/sciadv.abj7422.

534. M. Grabka, K. Jasek, and Z. Witkiewicz, "Surface Acoustic Wave Immunosensor for Detection of Botulinum Neurotoxin," *Sensors* 23 (2023): 7688, https://doi.org/10.3390/s23187688.

535. J. O. Park, Y. Choi, H. M. Ahn, et al., "Aggregation of Ag Nanoparticle Based on Surface Acoustic Wave for Surface-enhanced Raman Spectroscopy Detection of Dopamine," *Analytica Chimica Acta* 1285 (2024): 342036, https://doi.org/10.1016/j.aca.2023.342036.

536. M. Abrantes, D. Rodrigues, T. Domingues, et al., "Ultrasensitive Dopamine Detection With Graphene Aptasensor Multitransistor Arrays," *Journal of Nanobiotechnology* 20 (2022): 495, https://doi.org/10.1186/s12951-022-01695-0.

537. C.-H. Lin, C.-Y. Hsiao, C.-H. Hung, et al., "Ultrasensitive Detection of Dopamine Using a Polysilicon Nanowire Field-effect Transistor," *Chemical Communications* (2008): 5749–5751, https://doi.org/10.1039/b812968a.

538. Y. Lee, J. Buchheim, B. Hellenkamp, et al., "Carbon-nanotube field-effect transistors for resolving single-molecule aptamer–ligand binding kinetics," *Nature Nanotechnology* 19 (2024): 660–667, https://doi.org/10.1038/s41565-023-01591-0.

539. J. Amaral, J. Gaspar, V. Pinto, et al., "Measuring Brain Activity With Magnetoresistive Sensors Integrated in Micromachined Probe Needles," *Applied Physics A* 111 (2013): 407–412, https://doi.org/10.1007/s00339-013-7621-7.

540. N. Sergeeva-Chollet, H. Dyvorne, H. Polovy, M. Pannetier-Lecoeur, and C. Fermon, "Magnetoresistive Hybrid Sensors for Simultaneous Low-Field MRI and Biomagnetic Measurements," in *17th International Conference on Biomagnetism Advances in Biomagnetism—Biomag2010*, eds. S. Supek and A. Sušac (Springer, 2010), 70–73, https://doi.org/10.1007/978-3-642-12197-5_12.

541. R. Qiao, C. Fu, H. Forgham, et al., "Magnetic Iron Oxide Nanoparticles for Brain Imaging and Drug Delivery," *Advanced Drug Delivery Reviews* 197 (2023): 114822, https://doi.org/10.1016/j.addr.2023.114822.

542. L. Kaub, S. Milz, N. Barapatre, et al., "Magnetic Iron-oxide Nanoparticles in the Brain Connected to Alcohol-associated Liver Disease," *Scientific Reports* 15 (2025): 24505, https://doi.org/10.1038/s41598-025-09756-8.

543. M. Wang, L. Jin, X. Zhao, and H. Liu, "Advancements in Magnetic Nanoparticle-based Biosensors for Point-of-care Testing," *Frontiers in Bioengineering and Biotechnology* 12 (2024).

544. H. Fan, J. Wang, Q. Feng, et al., "Detection Techniques of Biological and Chemical Hall Sensors," *RSC Advances* 11: 7257–7270, https://doi.org/10.1039/D0RA10027G.

545. K. Wu, D. Tonini, S. Liang, R. Saha, V. K. Chugh, and J.-P. Wang, "Giant Magnetoresistance Biosensors in Biomedical Applications," *ACS Applied Materials & Interfaces* 14 (2022): 9945–9969, https://doi.org/10.1021/acsami.1c20141.

546. K. Wu, D. Su, R. Saha, and J.-P. Wang, "Giant Magnetoresistance (GMR) Materials and Devices for Biomedical and Industrial Applications," in *Spintronics* (John Wiley & Sons, 2022), 3–49, https://doi.org/10.1002/9781119698968.ch2.

547. T. Nakano, K. Fujiwara, and M. Oogane, "Tunnel-Magnetoresistance Sensors With Sub-pT Detectivity for Detecting Bio-magnetic Fields," *Applied Physics Letters* 126 (2025): 160503, https://doi.org/10.1063/5.0263879.

548. N. Maciel, E. Marques, L. Naviner, Y. Zhou, and H. Cai, "Magnetic Tunnel Junction Applications," *Sensors* 20 (2019): 121, https://doi.org/10.3390/s20010121.

549. J. Luo, Z. Xu, Z. Jin, M. Wang, X. Cai, and J. Chen, "Development and Comprehensive Evaluation of TMR Sensor-Based Magnetrodes," *ACS Applied Materials & Interfaces* 16 (2024): 31677–31686, https://doi.org/10.1021/acsami.4c01148.

550. A. Kanno, N. Nakasato, M. Oogane, et al., "Scalp Attached Tangential Magnetoencephalography Using Tunnel Magneto-resistive Sensors," *Scientific Reports* 12 (2022): 6106, https://doi.org/10.1038/s41598-022-10155-6.

551. Z.-X. Luo, L. Fox, M. Cummings, T. J. Lowery, and E. Daviso, "New Frontiers in *in Vitro* Medical Diagnostics by Low Field *T*2 Magnetic Resonance Relaxometry," *TrAC Trends in Analytical Chemistry* 83 (2016): 94–102, https://doi.org/10.1016/j.trac.2016.02.025.

552. S. D. Oberdick, K. V. Jordanova, J. T. Lundstrom, et al., "Iron oxide nanoparticles as positive T1 contrast agents for low-field magnetic resonance imaging at 64 mT," *Scientific Reports* 13 (2023): 11520, https://doi.org/10.1038/s41598-023-38222-6.

553. P. Khandelwal, C. E. Beyer, Q. Lin, P. McGonigle, L. E. Schechter, and A. C. Bach, "Nanoprobe NMR Spectroscopy and in Vivo Microdialysis: New Analytical Methods to Study Brain Neurochemistry," *Journal of Neuroscience Methods* 133 (2004): 181–189, https://doi.org/10.1016/j.jneumeth.2003.10.012.

554. E. Holmes, T. M. Tsang, and S. J. Tabrizi, "The Application of NMR-based Metabonomics in Neurological Disorders," *NeuroRx* 3 (2006): 358–372, https://doi.org/10.1016/j.nurx.2006.05.004.

555. J. H. Walton, J. S. Ropp, M. V. Shutov, et al., "A Micromachined Double-Tuned NMR Microprobe," *Analytical Chemistry* 75 (2003): 5030–5036.

556. H. Shao, C. Min, D. Issadore, et al., "Magnetic Nanoparticles and microNMR for Diagnostic Applications," *Theranostics* 2 (2012): 55–65, https://doi.org/10.7150/thno.3465.

557. D. Issadore, C. Min, M. Liong, J. Chung, R. Weissleder, and H. Lee, "Miniature Magnetic Resonance System for Point-of-care Diagnostics," *Lab on a Chip* 11 (2011): 2282–2287, https://doi.org/10.1039/c1lc20177h.

558. M. Mariello, L. Fachechi, F. Guido, and M. De Vittorio, "Multifunctional sub-100 μm thickness flexible piezo/triboelectric hybrid water energy harvester based on biocompatible AlN and soft parylene C-PDMS-Ecoflex™," *Nano Energy* 83 (2021): 105811, https://doi.org/10.1016/j.nanoen.2021.105811.

559. M. Mariello, L. Fachechi, F. Guido, and M. C. Vittorio, "Ultra-thin Skin-Contact-Actuated Hybrid Piezo/Triboelectric Wearable Sensor Based on AlN and Parylene-Encapsulated Elastomeric Blend," *Advanced Functional Materials* 2101047 (2021), https://doi.org/10.1002/adfm.202101047.

560. A. T. Le, M. Ahmadipour, and S.-Y. Pung, "A Review on ZnO-based Piezoelectric Nanogenerators: Synthesis, Characterization Techniques, Performance Enhancement and Applications," *Journal of Alloys and Compounds* 844 (2020): 156172, https://doi.org/10.1016/j.jallcom.2020.156172.

561. J.-H. Bae and S.-H. Chang, "PVDF-based Ferroelectric Polymers and Dielectric Elastomers for Sensor and Actuator Applications: A Review," *Functional Composites and Structures* 1 (2019): 012003, https://doi.org/10.1088/2631-6331/ab0f48.

562. B. Lu, Y. Chen, D. Ou, et al., "Ultra-flexible Piezoelectric Devices Integrated With Heart to Harvest the Biomechanical Energy," *Scientific Reports* 5 (2015): 16065.

563. C. K. Jeong, "Toward Bioimplantable and Biocompatible Flexible Energy Harvesters Using Piezoelectric Ceramic Materials," *MRS Communications* 10 (2020): 365–378, https://doi.org/10.1557/mrc.2020.48.

564. C. Fang, T. Tong, T. Bu, et al., "Overview of Power Management for Triboelectric Nanogenerators," *Advanced Intelligent Systems* 2 (2020): 1900129, https://doi.org/10.1002/aisy.201900129.

565. J. Luo and Z. L. Wang, "Recent Progress of Triboelectric Nanogenerators: From Fundamental Theory to Practical Applications," *EcoMat* 2 (2020): e12059.

566. G. Jian, S. Zhu, X. Yuan, et al., "Biodegradable Triboelectric Nanogenerator as a Implantable Power Source for Embedded Medicine Devices," *NPG Asia Materials* 16 (2024): 1–11, https://doi.org/10.1038/s41427-023-00528-2.

567. Z. Liu, H. Li, B. Shi, Y. Fan, Z. L. Wang, and Z. Li, "Wearable and Implantable Triboelectric Nanogenerators," *Advanced Functional Materials* 29 (2019): 1808820, https://doi.org/10.1002/adfm.201808820.

568. Q. Zheng, H. Zhang, B. Shi, et al., "In Vivo Self-Powered Wireless Cardiac Monitoring via Implantable Triboelectric Nanogenerator," *ACS Nano* 10 (2016): 6510–6518, https://doi.org/10.1021/acsnano.6b02693.

569. Y. Ma, Q. Zheng, Y. Liu, et al., "Self-Powered, One-Stop, and Multifunctional Implantable Triboelectric Active Sensor for Real-Time Biomedical Monitoring," *Nano Letters* 16 (2016): 6042–6051, https://doi.org/10.1021/acs.nanolett.6b01968.

570. F. Dell'Anna, T. Dong, P. Li, et al., "State-of-the-Art Power Management Circuits for Piezoelectric Energy Harvesters," *IEEE Circuits and Systems Magazine* 18 (2018): 27–48.

571. F. Xi, Y. Pang, W. Li, T. Jiang, L. Zhang, and T. Guo, "Universal Power Management Strategy for Triboelectric Nanogenerator," *Nano Energy Complete* (2017): 168–176.

572. W. Wang, J. Pang, J. Su, et al., "Applications of nanogenerators for biomedical engineering and healthcare systems," *InfoMat* 4 (2022): e12262.

573. Y. Meng, G. Gao, and J. Zhu, "Self-powered Bifunctional Sensor Based on Tribotronic Planar Graphene Transistors," *Scientific Reports* 11 (2021): 21483, https://doi.org/10.1038/s41598-021-01011-0.

574. G. Ding, S.-T. Han, V. A. L. Roy, C.-C. Kuo, and Y. Zhou, "Triboelectric Nanogenerator for Neuromorphic Electronics," *Energy Reviews* 2 (2023): 100014, https://doi.org/10.1016/j.enrev.2023.100014.

575. M. Mariello, F. Guido, V. M. Mastronardi, M. T. Todaro, D. Desmaële, and M. De Vittorio, "Nanogenerators for Harvesting Mechanical Energy Conveyed by Liquids," *Nano Energy* 57 (2019): 141–156, https://doi.org/10.1016/j.nanoen.2018.12.027.

576. K. Agarwal, R. Jegadeesan, Y.-X. Guo, and N. V. Thakor, "Wireless Power Transfer Strategies for Implantable Bioelectronics," *IEEE Reviews in Biomedical Engineering* 10 (2017): 136–161, https://doi.org/10.1109/RBME.2017.2683520.

577. R. A. Bullen, T. C. Arnot, J. B. Lakeman, and F. C. Walsh, "Biofuel Cells and Their Development," *Biosensors and Bioelectronics* 21 (2006): 2015–2045, https://doi.org/10.1016/j.bios.2006.01.030.

578. S. Cosnier, A. Le Goff, and M. Holzinger, "Towards Glucose Biofuel Cells Implanted in human Body for Powering Artificial Organs: Review," *Electrochemistry Communications* 38 (2014): 19–23, https://doi.org/10.1016/j.elecom.2013.09.021.

579. G. Liu, Y. Lu, F. Zhang, and Q. Liu, "Electronically Powered Drug Delivery Devices: Considerations and Challenges," *Expert Opinion on Drug Delivery* 19 (2022): 1636–1649, https://doi.org/10.1080/17425247.2022.2141709.

580. Z. Gao, Y. Zhou, J. Zhang, et al., "Advanced Energy Harvesters and Energy Storage for Powering Wearable and Implantable Medical Devices," *Advanced Materials* 36 (2024): 2404492, https://doi.org/10.1002/adma.202404492.

581. H. Stapf, F. Selbmann, Y. Joseph, and P. Rahimi, "Membrane-Based NEMS/MEMS Biosensors," *ACS Applied Electronic Materials* 6 (2024): 2120–2133.

582. J. P. Seymour, F. Wu, K. D. Wise, and E. Yoon, "State-of-the-art MEMS and Microsystem Tools for Brain Research," *Microsystems & Nanoengineering* 3 (2017): 16066, https://doi.org/10.1038/micronano.2016.66.

583. X. Li, H. Yu, X. Gan, et al., "Integrated MEMS/NEMS Resonant Cantilevers for Ultrasensitive Biological Detection," *Journal of Sensors* 2009 (2009): 1–10, https://doi.org/10.1155/2009/637874.

584. S. Forouzanfar, N. Pala, M. Madou, and C. Wang, "Perspectives on C-MEMS and C-NEMS Biotech Applications," *Biosensors and Bioelectronics* 180 (2021): 113119, https://doi.org/10.1016/j.bios.2021.113119.

585. T. P. J. Knowles, W. Shu, F. Huber, et al., "Label-free Detection of Amyloid Growth With Microcantilever Sensors," *Nanotechnology* 19 (2008): 384007, https://doi.org/10.1088/0957-4484/19/38/384007.

586. K. Takahashi, H. Oyama, N. Misawa, K. Okumura, M. Ishida, and K. Sawada, "Surface stress sensor using MEMS-based Fabry–Perot interferometer for label-free biosensing," *Sensors and Actuators B: Chemical* 188 (2013): 393–399, https://doi.org/10.1016/j.snb.2013.06.106.

587. H. J. Lee, N. Choi, E.-S. Yoon, and I.-J. Cho, "MEMS devices for drug delivery," *Advanced Drug Delivery Reviews* 128 (2018): 132–147, https://doi.org/10.1016/j.addr.2017.11.003.

588. E. Castagnola, E. M. Robbins, D. D. Krahe, et al., "Stable *in-vivo* Electrochemical Sensing of Tonic Serotonin Levels Using PEDOT/CNT-coated Glassy Carbon Flexible Microelectrode Arrays," *Biosensors and Bioelectronics* 230 (2023): 115242, https://doi.org/10.1016/j.bios.2023.115242.

589. M. Xia, B. N. Agca, T. Yoshida, et al., "Scalable, Flexible Carbon fiber Electrode Thread Arrays for Three-dimensional Probing of Neurochemical Activity in Deep Brain Structures of Rodents," *Biosensors and Bioelectronics* 241 (2023): 115625, https://doi.org/10.1016/j.bios.2023.115625.

590. W. F. Gillis, C. A. Lissandrello, J. Shen, et al., "Carbon Fiber on Polyimide Ultra-Microelectrodes," *Journal of Neural Engineering* 15 (2018): 016010, https://doi.org/10.1088/1741-2552/aa8c88.

591. S. Li, J. Liu, Y. Lu, et al., "Mutual Promotion of Electrochemical-localized Surface Plasmon Resonance on nanochip for Sensitive Sialic Acid Detection," *Biosensors and Bioelectronics* 117 (2018): 32–39, https://doi.org/10.1016/j.bios.2018.05.062.

592. B. Aghajanloo, S. Nazarnezhad, F. Arshadi, A. G. Prakash Kottapalli, C. Pastras, and M. Asadnia, "Emerging Trends in Biosensor and Microfluidics Integration for Inner Ear Theragnostics," *Biosensors and Bioelectronics* 286 (2025): 117588, https://doi.org/10.1016/j.bios.2025.117588.

593. U. Chae, H. Shin, H. J. Lee, J. Lee, and N. Choi, "A New MEMS Neural Probe System Integrated With Push-pull Microfluidic Channels and Biosensors for Real-time Monitoring of Neurochemicals," in *2016 IEEE 29th International Conference on Micro Electro Mechanical Systems (MEMS)* (IEEE, 2016), 329–332, https://doi.org/10.1109/MEMSYS.2016.7421627.

594. Y. Q. Fu, J. K. Luo, N. T. Nguyen, et al., "Advances in Piezoelectric Thin Films for Acoustic Biosensors, Acoustofluidics and Lab-on-chip Applications," *Progress in Materials Science* 89 (2017): 31–91, https://doi.org/10.1016/j.pmatsci.2017.04.006.

595. J. Schulte, D. Ashouri, and T. Stieglitz, "The Longevity of Neural Interfaces—Mechanical Oscillation of Thin Film Metal-Based Neural Electrodes Determine Stability During Electrical Stimulation," *Advanced Functional Materials* 34 (2024): 2310130, https://doi.org/10.1002/adfm.202310130.

596. P. Oldroyd, J. Gurke, and G. G. Malliaras, "Stability of Thin Film Neuromodulation Electrodes Under Accelerated Aging Conditions," *Advanced Functional Materials* 33 (2023): 2208881, https://doi.org/10.1002/adfm.202208881.

597. A. Carnicer-Lombarte, S.-T. Chen, G. G. Malliaras, and D. G. Barone, "Foreign Body Reaction to Implanted Biomaterials and Its Impact in Nerve Neuroprosthetics," *Frontiers in Bioengineering and Biotechnology* 9 (2021): 622524.

598. V. S. Polikov, P. A. Tresco, and W. M. Reichert, "Response of Brain Tissue to Chronically Implanted Neural Electrodes," *Journal of Neuroscience Methods* 148 (2005): 1–18, https://doi.org/10.1016/j.jneumeth.2005.08.015.

599. G. A. Katirtsidis, X. Illa, N. Ria, E. del Corro, E. Masvidal Codina, and J. A. Garrido, "Long-Term Stable Neural Interfaces With Nanoporous Graphene Electrodes and Hybrid Polyimide-Aluminium Oxide Encapsulation," *Small Methods* 9 (2025): e01720, https://doi.org/10.1002/smtd.202501720.